ORIGINAL ARTICLE

Allantofuranone, a new antifungal antibiotic from *Allantophomopsis lycopodina* IBWF58B-05A

Anja Schüffler[1], Daniela Kautz[1], Johannes C Liermann[2], Till Opatz[2] and Timm Anke[3]

In a screening for new bioactive compounds, the extract of *Allantophomopsis lycopodina* strain IBWF58B-05A, an imperfect ascomycete, was found to exhibit strong but rather selective antibiotic activity against *Paecilomyces variotii*. The bioactivity-guided isolation yielded allantofuranone, a new and uncommon γ-lactone. This compound showed antifungal activity against *P. variotii* and *Penicillium* species. This paper describes the isolation, structure elucidation and biological characteristics of allantofuranone.
The Journal of Antibiotics (2009) **62**, 119–121; doi:10.1038/ja.2008.21; published online 30 January 2009

INTRODUCTION

Fungi associated with plants have to adapt to environments differing greatly in their chemical composition and varying substantially during the host's development. They have to cope both with the plants defense and competing microorganisms and have therefore developed a rich and diverse secondary metabolism as part of their survival strategy. *Allantophomopsis lycopodina* is a plant pathogen responsible for leaf lesions on lingonberry, *Vaccinium vitis-idaea*[1] and a fruit-rot pathogen (black rot) on cranberries, *V. macrocarpon*.[2] To our knowledge, no secondary metabolites have been reported from this species. A closer look into the compounds produced during fermentations of our strain, however, revealed the presence of an antifungal antibiotic. In the following, we describe the production, isolation, structure elucidation and biological activities of allantofuranone (**1**), a new and unusual γ-lactone.

RESULTS AND DISCUSSION

Structure elucidation

The isolation of allantofuranone (**1**) was guided by its inhibitory activity against *Paecilomyces variotii* as described in the Experimental section. Allantofuranone had a nominal molecular weight of 324 Da and an elemental composition determined by HR-MS of $C_{19}H_{16}O_5$, requiring 12 unsaturations. The presence of two mono-substituted phenyl residues could be deduced by their characteristic pattern in the ^{1}H-NMR spectrum. Their ortho protons were shifted downfield, and two of them showed a heteronuclear multiple bond correlation (HMBC) to a ketone carbonyl with a typical shift of 193.97 p.p.m. The carbonyl group itself exhibited intense correlations with two diastereotopic methylene protons forming an AB spin system. The neighboring quaternary center resonated at δ_C 107.61 and showed an HMBC correlation with a methoxy group at δ_H 3.28. The chemical shift of the quaternary carbon gave evidence for the presence of an acetal. The methylene protons showed a ^3J C,H correlation to a further quaternary carbon at 122.92 p.p.m., which is bound to the second phenyl residue. Only one of the two remaining carbon atoms showed a weak ^4J correlation to one of the methylene protons. Their chemical shifts (167.46 and 140.19 p.p.m.) were in good agreement with those of C-2 and C-3 in a 3-hydroxyfuran-2(5H)-one ring.[3] This hypothesis could later be confirmed by X-ray crystallography. Remarkably, allantofuranone crystallized in the centrosymmetric space group $P\bar{1}$, thus the natural product was racemic (Figures 1 and 2).

Biological activities

Up to $50\,\mu g\,ml^{-1}$, no antibiotic activity was observed in the serial dilution assay against: *Micrococcus luteus*, *Bacillus brevis*, *B. subtilis*, *Mycobacterium phlei*, *Pseudomonas aeruginosa*, *Athrobacter citreus*, *Corynebacterium insidiosum*, *Escherichia coli*, *Enterobacter dissolvens*, *Absidia glauca* (+), *A. glauca* (−), *Ascochyta pisi*, *Aspergillus ochraceus*, *Fusarium oxysporum*, *F. fujikuroi*, *Nematospora coryli*, *Zygorhynchus moelleri* and *Mucor miehei*. Compound **1** exhibited antifungal activity against *P. islandicum* and *P. notatum* at $25\,\mu g\,ml^{-1}$ and against *P. variotii* starting from $10\,\mu g\,ml^{-1}$.

In the agar diffusion assay, the antifungal activity of **1** against *P. notatum*, *P. islandicum* and *P. variotii* was more pronounced (Table 1). Activity was observed against *Magnaporthe grisea* (15 μg per disc) and *P. lilacinus* (30 μg per disc), whereas *P. farinosa* was not inhibited. Interestingly, *P. lilacinus* started forming reddish pigments beginning

[1]Department of Biotechnology, University of Kaiserslautern, Kaiserslautern, Germany; [2]Institut für Organische Chemie, Department Chemie, Universität Hamburg, Hamburg, Germany and [3]Institute of Biotechnology and Drug Research, Kaiserslautern, Germany
Correspondence: Dr T Anke, Institute of Biotechnology and Drug Research, Erwin-Schrödinger-Strasse 56, D-67663 Kaiserslautern, Germany.
E-mail: timm.anke@ibwf.uni-kl.de

at 5.0 μg per disc of **1**. The germination of *P. infestans* and *M. grisea* spores was inhibited at an IC_{100} value of 50 μg ml^{-1}. The spore germination of the other fungal species was not inhibited (up to 100 μg ml^{-1}). No interference with respiration (*P. notatum* and *P. variotii*) and no phytotoxic, cytotoxic and nematicidal effects were observed at concentrations of up to 100 μg ml^{-1}.

Compounds such as xenofuranones A and B (**2**, **3**),[3] butyrolactone II (**4**)[4] or WF-3681 (**5**)[5] show structural similarities to **1**. It was reported that they exhibited no antibacterial and only weak cytotoxic activity. This corresponds to our findings. The xenofuranones and WF-3681

showed no activity against yeasts, which also matches our results. Unfortunately, there was no information about their activity against filamentous fungi.

EXPERIMENTAL SECTION

General

Melting points were determined with a Dr Tottoli apparatus and are uncorrected. Optical rotations were measured with a Krüss P8000 polarimeter at 589 nm. UV and IR spectra were measured with a Perkin-Elmer Lambda-16 spectrophotometer and a Bruker IFS48 FTIR spectrometer, respectively. NMR spectra were recorded with a Bruker Avance-II or with a Bruker DRX-500 spectrometer. The spectra were measured in CDCl$_3$ and the chemical shifts were referenced to the residual solvent signal (CDCl$_3$: δ_H=7.26 p.p.m. and δ_C=77.16 p.p.m.).[6] APCIMS spectra were measured with a Hewlett Packard MSD1100. FD-MS spectra were recorded on a Finnigan MAT 95 spectrometer. ESI-HR-MS spectra were recorded on a MicroMass/Waters Q-TOF Ultra 3 spectrometer equipped with a LockSpray interface using NaI/CsI or trialkylamines as external reference.
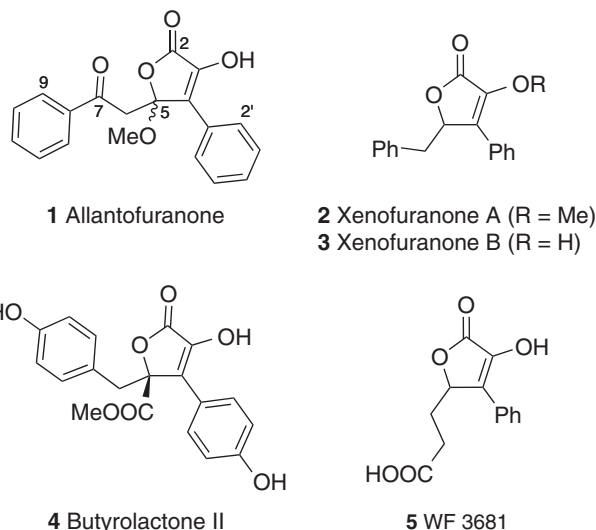

Figure 1 Allantofuranone and related compounds.

1 Allantofuranone

2 Xenofuranone A (R = Me)
3 Xenofuranone B (R = H)

4 Butyrolactone II

5 WF 3681

Table 1 Antifungal activity of allantofuranone (1) in the agar plate diffusion assay

Organism	Diameter inhibition zone (mm) μg per disc[a]								
	0.5	1	2.5	5.0	10	15	20	30	40
Penicillium notatum	—	—	10i	13i	17i	20i	21i	22i	24i
P. islandicum	—	—	—	12i	23i	27d	29d	35d	44d
Paecilomyces variotii	—	12i	27d	29d	38d	42d	45d	47d	47d
P. lilacinus	—	—	—	—	—	—	—	12i	14i
Magnaporthe grisea	—	—	—	—	—	12i	15i	20i	23i

Abbreviations: d, inhibition zone diffuse; i, inhibition zone incomplete.
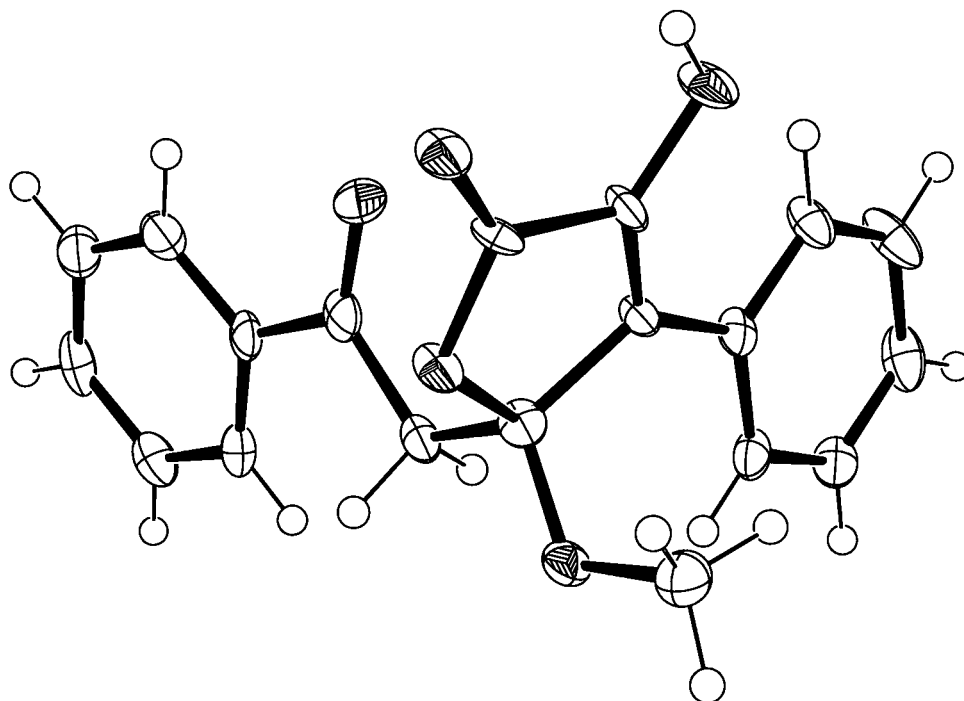[a]Diameter 6 mm.

Figure 2 Crystal structure of **1** (ORTEP, ellipsoids drawn at 50% probability).

Producing organism

The filamentous ascomycete IBWF58B-05A was isolated from a strongly rotten piece of wood from a deciduous tree collected in France. It was identified by microscopy and sequencing of its internal transcribed spacer (ITS). The ITS sequence shows homologies of 99.8% to *A. lycopodina* IFO 32908 (GenBank accession no. AB041243). The microscopic characteristics fit the description by Carris.[7] The spores are inequilateral/light lunate shaped, $2.5–3\,\mu m \times 10–13\,\mu m$ and are produced in conidiomata (diameter $100–300\,\mu m$ in YMG agar culture). The agar culture is dark grey-brown to black. Strain IBWF58B-05A has been deposited in the culture collection of the Institute of Biotechnology and Drug Research (IBWF e.V.), Kaiserslautern, Germany. For maintenance, the fungus was grown on agar slants on YMG agar (yeast extract $4.0\,g\,l^{-1}$, malt extract $10\,g\,l^{-1}$, glucose $10\,g\,l^{-1}$, the pH value was adjusted to 5.5 before autoclaving). Solid media contained 2.0% of agar.

Fermentation and isolation

The fungus was grown in YMG medium in a 20-l fermenter (Biolafitte C6) at $22–24\,^\circ C$ with agitation (130 r.p.m.) and aeration ($3\,l\,min^{-1}$). For inoculation, a well-grown shake culture (500 ml) in the same medium was used. When the carbon source was depleted after 7 days, the fermentation was stopped. The culture fluid (16.5 l) was separated from the mycelia by filtration and extracted twice with an equal volume of EtOAc. After evaporation of the solvent, the oily crude extract (4.5 g) was applied onto a column with silica gel (Merck 60, 0.063–0.2 mm, 150 g). Elution with cyclohexane/EtOAc (3:1) yielded 693 mg of an intermediate product. Pure **1** was obtained by preparative HPLC (Merck, Lichrosorb RP 18, $7\,\mu m$, column $250\,mm \times 25\,mm$) with a MeCN/H_2O gradient (50–62% MeCN in 12 min, flow: $20\,ml\,min^{-1}$; yield: 191.3 mg (Rt 10.5–12.0 min).

Allantofuranone (1)

Yellow crystals, m.p. 147–149 $^\circ C$; no significant optical rotation was detected; UV λ_{max}^{MeOH} (nm) (log ε) 227 (4.08), 246 (4.21), 289 (4.26); λ_{min}^{MeOH} (nm) (log ε)=219 (4.04), 231 (4.06), 262 (4.03); IR ν_{max} (KBr) (cm^{-1}) 3304, 1755, 1695, 1394, 1304, 1216, 1177, 1152, 1122, 989, 766, 689; FD-MS *m/z* 324.1 (M)$^+$, 648.6 (2M)$^+$; ESI-HRMS *m/z* 347.0891 (calcd for $C_{19}H_{16}O_5+Na^+$ 347.0890). ^1H- and ^{13}C-NMR data are presented in Table 2.

X-ray crystallographic data of 1

Crystals of **1** were grown by slow evaporation of a methanolic solution of **1**. Data were obtained at 100 K on a Bruker APEX diffractometer with graphite-monochromated Mo-K_α radiation. Formula $C_{19}H_{16}O_5$, crystal size $0.02 \times 0.10 \times 0.38\,mm^3$, triclinic, space group $P\bar{1}$, a=8.779(4) Å, b=9.672(4) Å, c=10.765(5) Å, α=75.886(8)$^\circ$, β=76.808(7)$^\circ$, γ=79.356(7)$^\circ$, V=816.4(6) Å^3, Z=2, D=1.319 $g\,cm^{-3}$, R=0.0638, R_w=0.1417. CCDC-717550 contains the supplementary crystallographic data for this paper. These data can be obtained free of charge at www.ccdc.cam.ac.uk/conts/retrieving.html (or from the Cambridge Crystallographic Data Centre, 12 Union Road, Cambridge CB2 1EZ, UK; Fax: +44-1223/336-033; E-mail: deposit@ccdc.cam.ac.uk).

Biological assays

Antimicrobial activities against bacteria and fungi were determined in the agar plate diffusion or serial dilution assay as described previously.[8] Cytotoxicity was assayed as described previously.[9] The cell lines Jurkat (ATCC TIB 152), Colo-320 (DSMZ ACC 144) and L-1210 (DSMZ ACC 123) were grown in RPMI 1640 medium (Invitrogen, Karlsruhe, Germany). Neuro-2A (DSMZ ACC 148) and SH-SY5Y (DSMZ ACC209) were grown in DMEM medium (Invitrogen). All media were supplemented with 10% heat-inactivated fetal calf serum (Invitrogen), $65\,\mu g\,ml^{-1}$ of penicillin G and $100\,\mu g\,ml^{-1}$ of streptomycin sulfate. The viability was measured photometrically with XTT (suspension cell lines) or with Giemsa staining (monolayer cells). The influence of **1** on the oxygen uptake by *P. variotii* and *Penicillium notatum* was tested as described previously.[10] Phytotoxicity was tested with *Setaria italica* and *Lepidium sativum*.[11] The spore germination was tested with *M. grisea* as described

previously.[12] This method was adapted for the spore germination assay with *Phytophthora infestans*, *Botrytis cinerea* and *Fusarium graminearum*. The nematicidal activity was tested with *Meloidogyne incognita* and *Caenorhabditis elegans* as described earlier.[13]

Table 2 ^1H- (400 MHz) and ^{13}C-NMR (101 MHz) of 1 in CDCl$_3$

Position	δ_H	δ_C
2	—	167.46 (s)
3	—	140.19 (s)
4	—	122.92 (s)
5	—	107.61 (s)
6	3.90, (d, J=16.5 Hz)	43.97 (t)
	3.67, (d, J=16.5 Hz)	
7	—	193.97 (s)
8	—	136.99 (s)
9/13	7.83 (m)	128.33 (d)
10/12	7.40 (m)	128.71 (d)
11	7.52 (m)	133.54 (d)
1′	—	129.17 (s)
2′/6′	7.89 (m)	127.72 (d)
3′/5′	7.45 (m)	129.20 (d)
4′	7.37 (m)	129.45 (d)
5-OCH$_3$	3.28 (s)	50.16 (q)

1 Putnam, M. L. *Allantophomopsis lycopodina*—a new aerial pathogen of lingonberry (*Vaccinium vitis-idaea*). *Plant Pathol.* **54,** 248 (2005).

2 Olatinwo, R. O., Hanson, E. J. & Schilder, A. M. C. A first assessment of the cranberry fruit rot complex in Michigan. *Plant Dis.* **87,** 550–556 (2003).

3 Brachmann, A. O., Forst, S., Furgani, G. M., Fodor, A. & Bode, H. B. Xenofuranones A and B: phenylpyruvate dimers from *Xenorhabdus szentirmaii*. *J. Nat. Prod.* **69,** 1830–1832 (2006).

4 Rao, K. V. *et al.* Butyrolactones from *Aspergillus terreus*. *Chem. Pharm. Bull.* **48,** 559–562 (2000).

5 Nishikawa, M., Tsurumi, Y, Namiki, T., Yoshida, K. & Okuhara, M. Studies on WF-3681, a novel aldose reductase inhibitor. I. Taxonomy, fermentation, isolation and characterization. *J. Antibiot.* **40,** 1394–1399 (1987).

6 Gottlieb, H. E., Kotlyar, V. & Nudelman, A. NMR chemical shifts of common laboratory solvents as trace impurities. *J. Org. Chem.* **62,** 7512–7515 (1997).

7 Carris, L. M. Cranberry black rot fungi: *Allantophomopsis cytisporea* and *Allantophomopsis lycopodina*. *Can. J. Bot.* **68,** 2283–2291 (1990).

8 Anke, H., Bergendorff, O. & Sterner, O. Assays of the biological activities of guaiane sesquiterpenoids isolated from the fruit bodies of edible *Lactarius* species. *Food Chem. Toxicol.* **27,** 393–397 (1989).

9 Schöttler, S., Bascope, M., Sterner, O. & Anke, T. Isolation and characterization of two verrucarins from *Myrothecium roridum*. *Z. Naturforsch. C. J. Biosci.* **61,** 309–314 (2006).

10 Weber, W., Anke, T., Steffan, B. & Steglich, W. Antibiotics from Basidiomycetes. XXXII. Strobilurin E: a new cytostatic and antifungal (E)-beta-methoxyacrylate antibiotic from *Crepidotus fulvotomentosus* Peck. *J. Antibiot.* **43,** 207–212 (1990).

11 Stärk, A., Anke, T., Mocek, U. & Steglich, W. Antibiotics from Basidiomycetes. XLII. Omphalone, an antibiotically active benzoquinone derivative from fermentations of *Lentinellus omphalodes*. *Z Naturforsch. C. J. Biosci.* **46,** 989–992 (1991).

12 Kettering, M., Valdivia, C., Sterner, O., Anke, H. & Thines, E. Heptemerones A~G, seven novel diterpenoids from *Coprinus heptemerus*: producing organism, fermentation, isolation and biological activities. *J. Antibiot.* **58,** 390–396 (2005).

13 Stadler, M., Mayer, A., Anke, H. & Sterner, O. Fatty acids and other compounds with nematocidal activity from cultures of Basidiomycetes. *Planta Med.* **60,** 128–132 (1994).

ORIGINAL ARTICLE

Ammocidins B, C and D, new cytotoxic 20-membered macrolides from *Saccharothrix* sp. AJ9571

Ryo Murakami[1], Junko Shinozaki[2], Takayuki Kajiura[2], Ikuko Kozone[3], Motoki Takagi[3], Kazuo Shin-Ya[4], Haruo Seto[5] and Yoichi Hayakawa[6]

Ammocidins B, C and D were isolated from the culture broth of *Saccharothrix* sp. AJ9571, an ammocidin A-producing strain. Their structures were determined by a detailed spectroscopic analysis and by a comparison of their NMR data with those of ammocidin A. Ammocidins A and B showed potent anti-proliferative activities against human cancer cell lines.
The Journal of Antibiotics (2009) **62**, 123–127; doi:10.1038/ja.2008.23; published online 30 January 2009

INTRODUCTION

In the course of our screening for apoptosis inducers in Ras-dependent Ba/F3-V12 cells, we isolated ammocidin A (formerly named ammocidin) from the culture broth of *Saccharothrix* sp. AJ9571.[1,2] Ammocidin A induced apoptotic cell death in Ras-dependent Ba/F3-V12 cells with an IC_{50} of $66 \, \mathrm{ng \, ml^{-1}}$, and no cell death was observed in IL-3-dependent Ba/F3-V12 cells at less than $100 \, \mathrm{\mu g \, ml^{-1}}$ of ammocidin A. Further searching for congeners from the ammocidin-producing strain resulted in the isolation of ammocidins B, C and D (Figure 1). In this paper, we report the isolation, structure elucidation and cytotoxic activities of the ammocidins.

RESULTS

Production and isolation

The seed medium was composed of yeast extract 0.1%, beef extract 0.1%, N-Z amine type A 0.2% and glucose 1.0% (pH 7.3). *Saccharothrix* sp. AJ9571 was cultured in flasks containing the seed medium on a rotary shaker at 30 °C for 4 days. The resultant seed culture at 2.0% was transferred into 500-ml Erlenmeyer flasks containing 100 ml of a production medium consisting of glycerol 2.0%, starch 1.0%, rape seed meal 2.0%, soytone 0.3% and calcium carbonate 0.3% (pH 7.0). The fermentation was carried out on a rotary shaker at 30 °C for 7 days. The culture filtrate (10 l) was extracted with ethyl acetate and the extract was subjected to silica gel column chromatography with chloroform–methanol (8:1). The active eluate was chromatographed on a Sephadex LH-20 column with methanol. The active fraction was purified by HPLC using a Senshu Pak PEGASIL ODS column with 70% methanol. Further purification was carried out on the same column with 33% acetonitrile to give ammocidins A (387 mg), B (24 mg), C (15 mg) and D (24 mg).

Physico-chemical properties

The physico-chemical properties of ammocidins B, C and D are summarized in Table 1. The molecular formulae of ammocidins B, C and D were determined by high-resolution electrospray ionization mass spectra to be $C_{60}H_{98}O_{22}$, $C_{53}H_{86}O_{18}$ and $C_{46}H_{74}O_{16}$, respectively. The IR spectra indicated the presence of hydroxyl ($3430 \, \mathrm{cm^{-1}}$) and conjugated carbonyl groups (1670–$1720 \, \mathrm{cm^{-1}}$). The UV spectra of ammocidins B, C and D are characterized by a maximum absorption around 320 nm.

Structure elucidation

The structures of ammocidins B, C and D were established by ^{1}H- and ^{13}C-NMR and two-dimensional NMR experiments (Correlation Spectroscopy (COSY), Heteronuclear multiple quantum coherence (HMQC), heteronuclear multiple-bond correlation (HMBC)) on a 600-MHz spectrometer. The ^{1}H and ^{13}C-NMR assignments of ammocidins B, C and D in CD$_3$OD are listed in Table 2.

The ^{1}H-NMR spectrum of ammocidin B showed the presence of 12 methyl groups between 1.10 and 2.08 p.p.m. and four methoxy groups between 3.24 and 3.53 p.p.m. The ^{13}C-NMR spectrum confirmed the presence of 60 carbons. ^{1}H spin networks from 7-H to 9-H, from 15-H to 20-H, from 22-H to 23-H and from 25-H to 28-H, and ^{1}H–^{13}C long-range correlations as shown in Figure 2 revealed the aglycone structure of ammocidin B, which is the same as ammocidin A. Moreover, a ^{1}H spin network from an anomeric proton (1′-H) to 6′-H and an heteronuclear multiple-bond correlation between 1′-H and C-5′ revealed the presence of 6-deoxyglucose, which is the same component as that of ammocidin A. Two 2,6-dideoxy-3-methyl-pyranose moieties were constructed by ^{1}H spin networks from an anomeric proton 1″-H (1‴-H) to 2″-H (2‴-H) and from H-4″

Ammocidins B, C and D from *Saccharothrix* sp. AJ9571
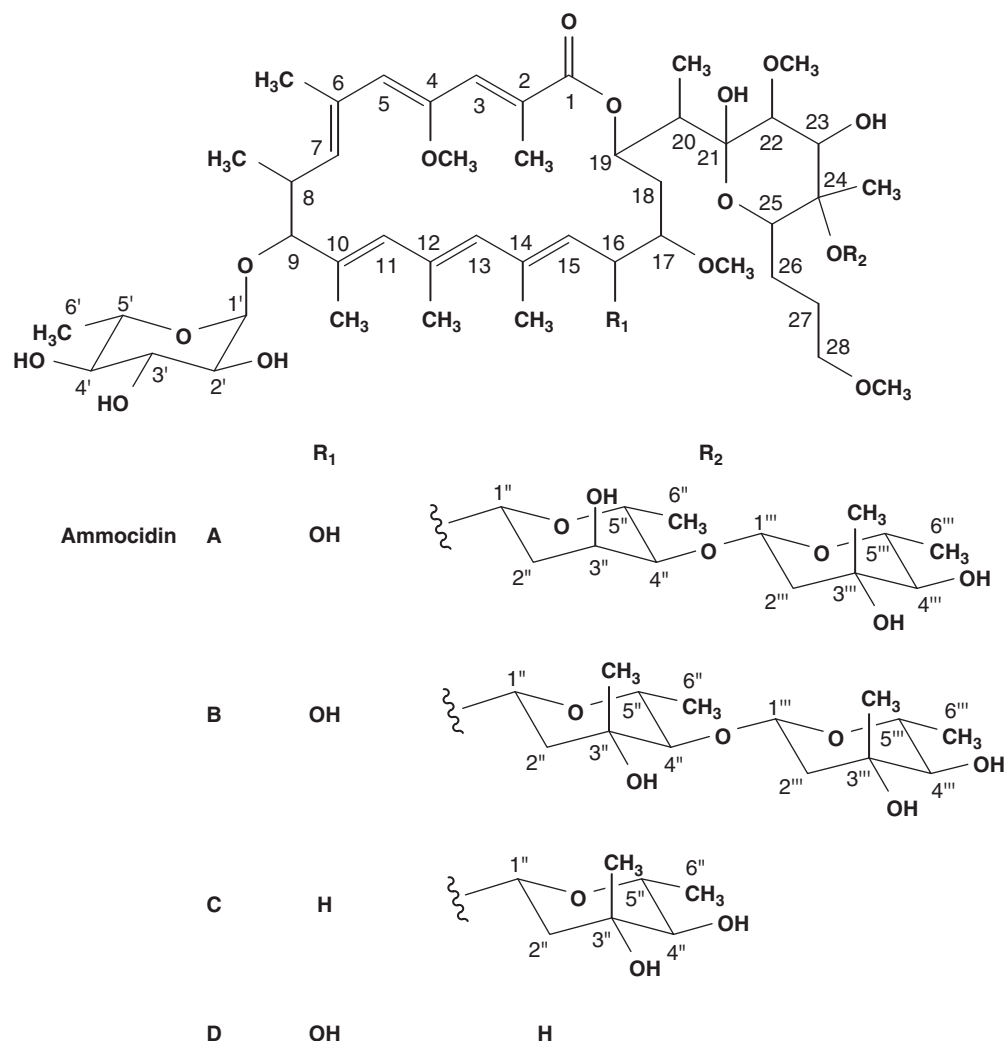R Murakami *et al*

124

Figure 1 Structures of ammocidin A, B, C and D.

Table 1 Physico-chemical properties of ammocidin B, C, and D

	Ammocidin B	Ammocidin C	Ammocidin D
Appearance	Colorless powder	Colorless powder	Colorless powder
MP	140–143 °C	111–115 °C	116–119 °C
$[\alpha]_D^{25}$ (MeOH)	+32.9 (*c* 1.06)	+3.2 (*c* 0.66)	−12.5 (*c* 1.17)
Molecular formula	$C_{60}H_{98}O_{22}$	$C_{53}H_{86}O_{18}$	$C_{46}H_{74}O_{16}$
HR-ESI-MS			
Found	1193.6415 $[M+Na]^+$	1009.5773 $[M-H]^-$	881.4944 $[M-H]^-$
Calculated	1193.6447	1009.5736	881.4899
UV λ_{max} nm (ε) in MeOH	266 (14 782), 323 (16 255)	208 (9127), 320 (6126)	203 (8752), 224 (8911), 322 (6063)
IR ν_{max} (KBr) cm^{-1}	3430, 1670, 1630	3430, 1720, 1640	3430, 1720, 1630

Abbreviations: HR-ESI-MS, High-resolution electrospray ionization mass spectra; KBr, potassium bromide; MP, melting point.

(H-4‴) to 6″-CH₃ (6‴-CH₃), and heteronuclear multiple-bond correlation from 3″-CH₃ (3‴-CH₃) to C-2″ (C-2‴), C-3″ (C-3‴) and C-4″ (C-4‴). Vicinal proton coupling constants (Table 2) and an NOE between 1″-H (1‴-H) and 3″-CH₃ (3‴-CH₃) identified these sugars as β-olivomycose. The three glycoside linkages were formed on the basis of long-range couplings between 1′-H and C-9, between 1″-H and C-24, and between 1‴-H and C-4″. These data indicate that

ammocidin B is an ammocidin A derivative containing the second β-olivomycose residue in place of the β-digitoxose residue (Figure 1).

The ¹H- and ¹³C-NMR spectra of ammocidin C were similar to those of ammocidin B, although signals due to the terminal olivomycose residue (C-1‴–C-6‴) were absent in ammocidin C. In the aglycone, signals indicative of a methylene group (δ_C 32.2, δ_H 2.58, 1.98) appeared in place of those for the oxymethine (C-16) in

Ammocidins B, C and D from *Saccharothrix* sp. AJ9571
R Murakami *et al*

125

Table 2 ^{13}C- and ^{1}H-NMR data for ammocidin B, C and D in methanol-d_4

No.	Ammocidin B		Ammocidin C		Ammocidin D	
	δ_C	δ_H	δ_C	δ_H	δ_C	δ_H
1	171.2		171.4		171.4	
2	125.3		125.5		125.3	
3	138.2	6.96 (1H, s)	138.5	7.01(1H, s)	138.3	6.97 (1H, s)
4	153.6		154.0		153.6	
5	134.2	5.76 (1H, s)	133.9	5.77 (1H, s)	134.2	5.76 (1H, s)
6	131.8		132.0		131.8	
7	142.0	5.32 (1H, d, 10.0)	141.7	5.35 (1H, d, 10.0)	142.1	5.32 (1H, d, 10.0)
8	36.8	2.85 (1H, m)	36.8	2.84 (1H, m)	36.8	2.85 (1H, m)
9	87.7	3.81 (1H, d, 9.0)	88.2	3.81 (1H, d, 9.0)	87.8	3.81 (1H, d, 9.0)
10	134.7		134.2		134.8	
11	136.2	5.90 (1H, s)	137.6	5.92 (1H, s)	136.3	5.90 (1H, s)
12	134.2		133.0		134.2	
13	133.5	5.56 (1H, s)	135.1	5.71 (1H, s)	133.5	5.57 (1H, s)
14	136.1		137.1		136.1	
15	129.4	5.21 (1H, d, 7.0)	127.4	5.05 (1H, t, 7.0)	129.4	5.21 (1H, d, 7.0)
16	67.8	4.83 (1H, dd, 7.2, 1.0)	32.2	2.58, 1.98 (2H, m)	67.8	4.82 (1H, dd, 7.2, 1.0)
17	82.8	2.66 (1H, m)	80.2	2.76 (1H, m)	82.9	2.67 (1H, m)
18	36.8	1.89, 1.61 (2H, m)	41.2	1.97, 1.37 (2H, m)	35.8	1.90, 1.62 (2H, m)
19	72.2	5.50 (1H, m)	72.5	5.50 (1H, m)	72.3	5.50 (1H, m)
20	44.9	2.01 (1H, m)	44.5	2.00 (1H, m)	44.8	2.03 (1H, m)
21	99.9		100.0		100.3	
22	82.2	3.02 (1H, d, 9.5)	82.1	3.04 (1H, d, 9.5)	82.3	3.01 (1H, d, 9.5)
23	76.0	3.96 (1H, d, 9.5)	76.4	3.88 (1H, d, 9.5)	78.3	3.78 (1H, d, 9.5)
24	82.2		82.3		75.0	
25	73.8	3.66 (1H, t. 9.0)	73.9	3.65 (1H, t. 9.0)	75.5	3.54 (1H, t, 9.0)
26	25.7	1.59, 1.21 (2H, m)	25.8	1.57, 1.19 (2H, m)	25.7	1.52, 1.33 (2H, m)
27	27.8	1.50, 1.30 (2H, m)	27.9	1.48, 1.32 (2H, m)	27.9	1.63, 1.25 (2H, m)
28	73.9	3.27 (2H, m)	74.0	3.26 (2H, m)	74.0	3.28 (2H, m)
2-Me	13.1	2.08 (3H, s)	13.1	2.09 (3H, s)	13.1	2.16 (3H, s)
6-Me	13.7	2.06 (3H, s)	13.7	2.05 (3H, s)	13.8	2.08 (3H, s)
8-Me	18.4	1.16 (3H, d, 6.5)	18.6	1.16 (3H, d, 6.5)	18.5	1.16 (3H, d, 6.5)
10-Me	12.0	1.58 (3H, s)	12.0	1.57 (3H, s)	12.0	1.58 (3H, s)
12-Me	18.1	1.88 (3H, s)	18.5	1.90 (3H, s)	18.2	1.88 (3H, s)
14-Me	17.6	1.71 (3H, s)	17.0	1.82 (3H, s)	17.7	1.72 (3H, s)
20-Me	9.2	1.10 (3H, d, 7.0)	9.2	1.07 (3H, d, 7.0)	9.2	1.10 (3H, d, 7.0)
24-Me	11.3	1.11 (3H, s)	11.1	1.12 (3H, s)	13.8	1.03 (3H, s)
4-OMe	61.3	3.51 (3H, s)	61.4	3.53 (3H, s)	61.4	3.51(3H, s)
17-OMe	57.6	3.34 (3H, s)	57.4	3.29 (3H, s)	57.6	3.34 (3H, s)
22-OMe	61.5	3.53 (3H, s)	61.5	3.53 (3H, s)	61.6	3.54 (3H, s)
28-OMe	58.7	3.24 (3H, s)	58.7	3.24 (3H, s)	58.7	3.23 (3H, s)
1′	96.1	4.65 (1H, d, 3.5)	96.0	4.67 (1H, d, 3.5)	96.1	4.65 (1H, d, 3.5)
2′	73.6	3.39 (1H, dd, 9.5, 3.5)	73.6	3.38 (1H, dd, 9.5, 3.5)	73.6	3.39 (1H, dd, 9.5, 3.5)
3′	74.8	3.66 (1H, t, 9.5, 9.5)	74.9	3.65 (1H, t, 9.5, 9.5)	74.8	3.66(1H, t, 9.5, 9.5)
4′	77.5	2.97 (1H, t, 9.5, 9.5)	77.6	2.99 (1H, t, 9.5, 9.5)	77.6	2.99 (1H, t, 9.5, 9.5)
5′	69.1	3.75 (1H, dd, 9.5, 6.5)	69.1	3.75 (1H, dd, 9.5, 6.5)	69.1	3.74 (1H, dd, 9.5, 6.5)
6′	18.1	1.24 (3H, d, 6.5)	18.1	1.22 (3H, d, 6.5)	18.1	1.23 (3H, d, 6.5)
1″	94.0	4.85 (1H, dd, 10.0, 1.5)	94.1	4.84 (1H, dd, 10.0, 1.5)		
2″	45.9	1.88 (1H, dd, 13.0, 1.5) 1.63 (1H, dd, 13.0, 10.0)	47.1	1.83 (1H, dd, 13.0, 1.5) 1.63 (1H, dd, 13.0, 10.0)		
3″	71.5		72.5			
4″	90.3	3.15 (1H, d, 10.0)	80.1	3.09 (1H, d, 10.0)		
5″	71.5	3.49 (1H, dd, 10.0, 6.5)	72.5	3.40 (1H, dd, 10.0, 6.5)		
6″	18.4	1.26 (3H, d, 6.5)	18.8	1.27 (3H, d, 6.5)		
3″-Me	22.5	1.24 (3H, s)	20.4	1.23 (3H, s)		
1‴	102.0	4.63 (1H, dd, 10.0, 2.0)				
2‴	46.3	1.98 (1H, dd, 13.0, 2.0) 1.68 (1H, dd, 13.0, 10.0)				

Ammocidins B, C and D from *Saccharothrix* sp. AJ9571
R Murakami *et al*

126

Table 2 Continued

No.	Ammocidin B		Ammocidin C		Ammocidin D	
	δ_C	δ_H	δ_C	δ_H	δ_C	δ_H
3‴	72.2					
4‴	79.8	3.12 (1H, d, 10.0)				
5‴	72.8	3.45 (1H, dd, 10.0, 6.5)				
6‴	18.4	1.26 (3H, d, 6.5)				
3‴-Me	20.3	1.24 (3H, s)				
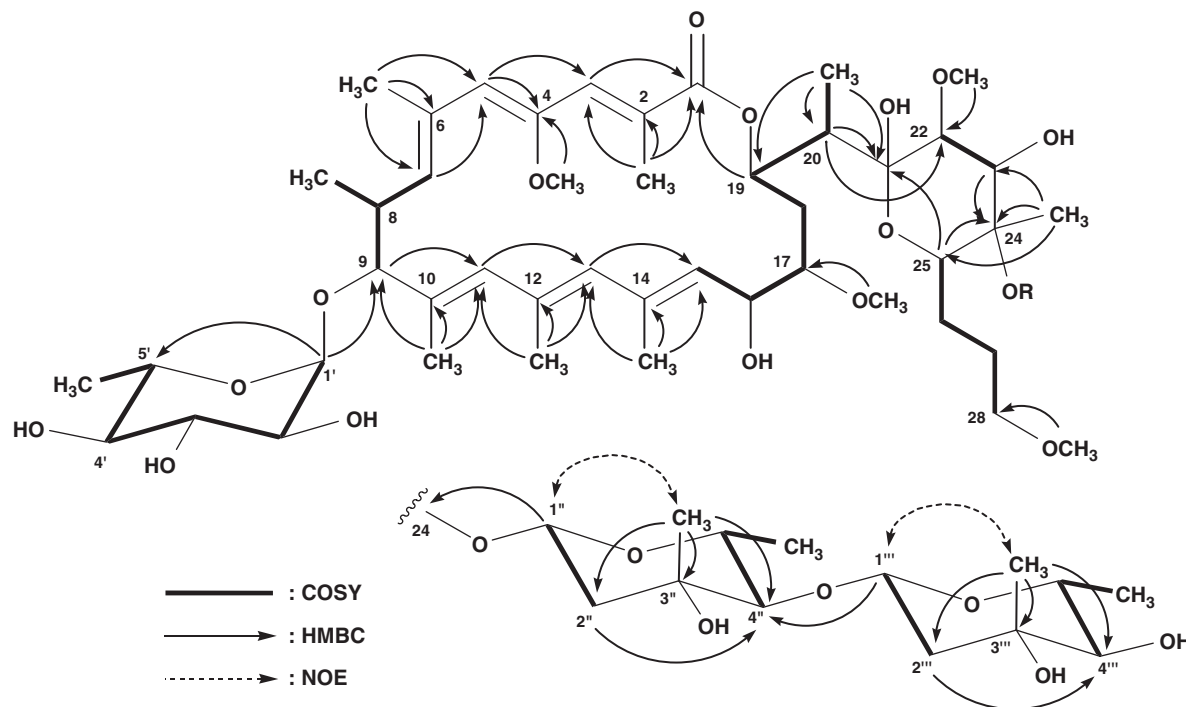
Figure 2 Key correlations in 2-D NMR of ammocidin B.

ammocidin B. A ^{1}H spin network from 15-H to 20-H identified ammocidin C as a 16-deoxyaglycone metabolite. The molecular formula and the upfield shift of C-4″ (δ_C 90.3 in ammocidin B and δ_C 80.1 in ammocidin C) indicated that ammocidin C is the 16-deoxy-4″-O-deolivomycosyl derivative of ammocidin B. Finally, two-dimensional NMR analyses established the planar structure of ammocidin C as shown in Figure 1.

The ^{1}H- and ^{13}C-NMR spectra indicated that ammocidin D consists of the same aglycone as ammocidin B and 6-deoxyglucose as a sole sugar moiety. The molecular formula of ammocidin D and the upfield shift of 24-C (δ_C 82.2 in ammocidin B and δ_C 75.0 in ammocidin D) showed the loss of two olivomycose residues from ammocidin B. The planar structure of ammocidin D was confirmed as shown in Figure 1 by two-dimensional NMR data.

Cytotoxic activities of ammocidins

To determine the cytotoxic activities of the ammocidins, A549 human lung carcinoma cells, MCF-7 human breast carcinoma cells and HCT116 human colon carcinoma cells were tested. The cell

Table 3 Anti-proliferative activities of ammocidins against human cancer cell lines

	IC$_{50}$ (µM)			
	Ammocidin A	Ammocidin B	Ammocidin C	Ammocidin D
A549	0.058	0.073	2.1	6.4
MCF7	0.14	0.10	1.8	5.0
HCT116	0.11	0.38	8.4	23

proliferation assay showed potent cytotoxic activities of ammocidins A and B (Table 3). The IC$_{50}$'s of ammocidins A and B were 0.06–0.4 µM.

DISCUSSION

During our efforts to obtain congeners from the ammocidin-producing strain, we isolated new ammocidin derivatives, ammocidins B, C and D. The main structural differences of these compounds are the

Ammocidins B, C and D from *Saccharothrix* sp. AJ9571
R Murakami *et al*

npg

127

number of olivomycose residues attached to 24-*O*. Whereas ammocidin A contains a digitoxose residue and an olivomycose residue, the sugar chain of ammocidin B consisted of two olivomycose residues. The ammocidins are considered to be good tools to investigate the importance of sugar moieties for the biological activity of 20-membered macrolides.

We evaluated the anti-proliferative effects of ammocidins on human cancer cell lines. Although all ammocidins showed cytotoxic activities, ammocidins A and B were more potent than ammocidins C and D. Thus, deoxysugar moieties attached to 24-*O* play an important role in the anti-proliferative activities of ammocidins. Human cancer cell lines A549 and HCT116 harbor oncogenic *ras* mutation (A549: K-*ras*-G12S, HCT116: K-*ras*-G13D). MCF-7 cells, however, have no *ras* mutation (but harbor PI3KCA mutation). Ammocidins showed potent anti-proliferative activities against all the three cell lines, implying that their anti-proliferative activities might not be due to Ras inhibition. Further biological studies on ammocidins are in progress.

METHODS
Cell culture
The cancer cell lines A549 (lung adenocarcinoma), MCF-7 (breast adenocarcinoma) and HCT-116 (colon carcinoma) were cultured in Dulbecco's modified Eagle's medium supplemented with 10% fetal bovine serum at 37 °C under 5% CO_2 atmosphere.

Assay of anti-proliferative activity
Anti-proliferative activities were measured by using the CellTiter-Glo Luminescent Cell Viability Assay kit (Promega Corporation, Madison, WI, USA), which determines the number of viable cells in a culture based on quantitation of ATP. In brief, cancer cells were seeded at 1×10^3 cells per well in 96-well microplates and cultured overnight. The cells were treated with various concentrations of ammocidins for 48 h. After 50 μl per well of CellTiter-Glo Reagent was added to the cell culture, the luminescence was measured by a ARVO.sx multilabel counter (Wallac Berthold, Turku, Finland). IC_{50} values were determined from the dose–response curves of growth inhibition.

General experimental procedures
NMR spectra were obtained on a Varian NMR System 600 NB CL (Varian NMR Systems, Palo Alto, CA, USA). Methanol-d_4 was used as a solvent and an internal reference. Melting points were determined with a Yanagimoto (Seisakusyo, Japan) micro melting point apparatus. High-resolution electrospray ionization mass spectra were recorded on a Waters LCT-Premier XE mass spectrometer (Waters, Milford, MA, USA). Optical rotations were recorded on a HORIBA SEPA-300 polarimeter (Horiba, Tokyo, Japan). UV spectra were obtained on a HITACHI U-3200 spectrophotometer (Hitachi, Tokyo, Japan). IR spectra were obtained using a HORIBA FT-720 spectrophotometer.

1 Murakami, R, Tomikawa, T, Shin-ya, K, Seto, H & Hayakawa, Y Ammocidin, a new apoptosis inducer in Ras-dependent cells from *Saccharothrix* sp. I. Production, isolation and biological activity. *J Antibiot* **54**, 710–713 (2001).
2 Murakami, R, Tomikawa, T, Shin-ya, K, Seto, H & Hayakawa, Y Ammocidin, a new apoptosis inducer in Ras-dependent cells from *Saccharothrix* sp. II. Physico-chemical properties and structure elucidation. *J Antibiot* **54**, 714–717 (2001).

npg

ORIGINAL ARTICLE

Velleratretraol, an unusual highly functionalized lactarane sesquiterpene from *Lactarius vellereus*

Du-Qiang Luo[1], Li-Yan Zhao[1], Yao-Long Shi[1], Hong-Liang Tang[1], Yu-Ye Li[2], Liu-Meng Yang[2],
Yong-Tang Zheng[2], Hua-Jie Zhu[3] and Ji-Kai Liu[3]

An unusual highly functionalized lactarane sesquiterpene, named velleratretraol (1), was isolated from the ethanol extract of
the fruiting body of the mushroom *Lactarius vellereus*. Its structure was determined through spectroscopic analysis and single-
crystal X-ray diffraction studies. The proposed assignment of the absolute configuration is based on computational results.
It showed weak activity against HIV-1 cells with an effective concentration of $68.0\,\mu g\,ml^{-1}$ and a selectivity index of 2.0.
The Journal of Antibiotics (2009) 62, 129–132; doi:10.1038/ja.2008.25; published online 23 January 2009

INTRODUCTION

The Russulaceae family is one of the largest in the subdivision
Basidiomycotina in Whittaker's Kingdom of Fungi and comprises
hundreds of species.[1] Sesquiterpenes play an important biological role
in a majority of the *Lactarius* species. They are responsible for the
pungent and bitter taste of the milky juice, the color change in the latex
upon air exposure,[2] and they constitute a chemical defense system
against intruders such as bacteria, fungi, animals and insects.[3] The
fungal subdivision Basidiomycotina produces many toxic sesquiterpenes
derived from the protoilludane skeleton. This skeleton is transformed
and rearranged into a multitude of compounds. Fungal sesquiterpenes
formed via the humulane–protoilludane biosynthetic pathway are
characteristic for the subdivision Basidiomycotina. The largest group
of sesquiterpenes, belonging to the classes of lactaranes, secolactaranes,
marasmanes, isolactaranes, norlactaranes and caryophyllanes, are
believed to be biosynthesized from humulane.[4] Fungi of the genus
Lactarius have been shown to be a good source of bioactive secondary
metabolites.[5–7] China is extraordinarily rich in higher fungi, with over
6000 species reported to belong to about 1200 genera. In our on-going
research to explore the biologically active natural products of the higher
fungi of China,[8–12] the chemical constituents of the fruiting bodies of
Lactarius vellereus were investigated. This report describes the isolation
and structure elucidation of an unusual highly functionalized lactarane
sesquiterpene, named velleratretraol (1), and its anti-HIV activity.

RESULTS AND DISCUSSION

Velleratretraol (1) was isolated as colorless crystals. The molecular
formula of 1 was determined to be $C_{15}H_{24}O_6$ on the basis of

high-resolution electrospray ionization mass spectrometry (HR-ESI-
MS) ([M+NH$_4$]$^+$ at *m/z* 318.1911 in combination with ^{1}H- and
^{13}C-NMR data (Table 1)). The IR data suggested the presence of a
hydroxy (3463, 3408 and 3355 cm^{-1}) moiety. The ^{13}C-NMR spectrum
of 1 showed 15 resonances, which could be further classified into three
Me groups (δ, 29.5, 31.6 and 31.8), three CH$_2$ (δ, 40.4, 43.5 and 44.2),
three oxymethines (δ, 71.2, 99.3 and 112.9), two aliphatic methines
(δ, 42.7 and 52.3), three oxygenated quaternary carbon atoms (δ, 82.0,
85.0 and 88.4) and one quaternary carbon atom (δ, 35.9) by analysis
of the DEPT spectra. An analysis of the ^{1}H-NMR spectrum indicated
the presence of three methyl groups at δ=1.03 (s), 1.12 (s) and 1.27
(s). The first two resonances were ascribed to geminal methyl groups,
and the third one was ascribed to the methyl group on the carbon
atom bearing the tetramethylene oxide carbocycle group. In particular,
a doublet occurring at δ=3.73 (d, 11.8) was attributed to the C-4
bearing a secondary OH group, and two resonances at δ=5.55 (s) and
5.35 (s) were assigned at C-14 and C-15, respectively. Its formula
indicated a sesquiterpene skeleton containing 4 degrees of unsatura-
tion. The structure was suggested to be a tetracyclic sesquiterpene.

The key connectivity of the protons and carbon atoms was further
established by the ^{1}H- and ^{13}C-NMR, hetero multiple quantum
correlation spectra, ^{1}H–^{1}H COSY and hetero multiple band correla-
tion (HMBC) spectra. The cross-peaks between H-2 and H-3/H-9,
H-3 and H-2/H-4/H-11, H-9 and H-2, and H-11 and H-3 were
observed in the ^{1}H–^{1}H COSY spectrum. The further connectivity of
the above partial structures was deduced from the HMBC spectrum
(Figure 1). The HMBC correlations from the acetal methine proton
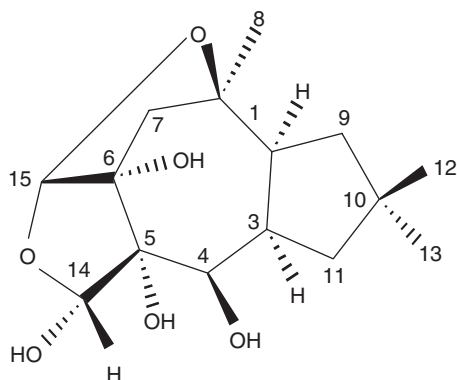(H-15) to the one oxygenated quaternary carbon at δ_c 88.4 (C-1) and

130

Table 1 NMR spectral data for velleratretraol (1) in CD$_3$OD

	^{13}C	^1H	^1H–^1H COSY	HMBC
1	88.4 (s)			
2	52.3 (d)	2.23 (m)	H-3, H-9	C-4, 11
3	42.7 (d)	2.18 (m)	H-2, 4, 11	C-2, 4
4	71.2 (d)	3.73 (d, 11.8)	H-2, 3	C-3, 6, 14
5	85.0 (s)			
6	82.0 (s)			
7	40.4 (t)	2.43 (d, 13.5),		C-1, 2, 5, 6, 8, 15
		1.73 (d, 13.5)		
8	29.5 (q)	1.27 (s)		C-1, 2, 7
9	44.2 (q)	1.37 (d, 13.1)	H-2	C-2, 10, 12, 13
		1.45 (dd, 6.7,		
		12.6)		
10	35.9 (s)			
11	43.5 (t)	1.53 (d, 9.2,	H-3	C-3, 4, 10, 12, 13
		13.9)		
		1.46 (m)		
12	31.6 (q)	1.03 (s)		C-9, 10, 11, 13
13	31.8 (q)	1.12 (s)		C-9, 10, 11, 12
14	99.3 (d)	5.35 (s)		C-4, 5, 15
15	112.9 (d)	5.55 (s)		C-1, 14

Figure 2 The structure of velleratretraol (1).

Figure 3 X-ray crystal structure of 1.

Figure 1 Key 1H–1H COSY (—) and HMBC ($\rightarrow$) correlations of 1.

the oxymethine carbon at δ_c 99.3 (C-14), from the oxymethine proton (δ_H 5.35, H-14) to the acetal carbon at δ_c 112.9 (C-15), 71.2 (C-4) and 85.0 (C-5), as well as from the methylene protons (δ_H 2.43 (d, 13.4), 1.73 (d, 13.5), H-7) to C-1, C-2, C-5, C-6, C-8 and C-15, indicated the connectivity of C-15 via two individual oxygen bridges to both C-14 and C-1. The HMBC correlations from H-12 to C-13, H-2 to C-11 and H-9 to C-3 revealed the presence of dimethylcyclopentane. The HMBC spectrum further gave the correlation from Me-8 (δ_H 1.27 s) to C-1, C-2 and C-7 indicated the methyl group (C-8) was attached at C-1. Further, the above HMBC correlations also implied that four hydroxyl groups were attached to C-4, C-5, C-6 and C-14. By combining all these data, we were able to assign the planar structure 1 to an unusually oxygenated lactarane skeleton (Figure 2), velleratretraol. The structural assignments were further confirmed by an X-ray structure (Figure 3), which established the relative stereochemistry of 1.

For the assignment of absolute configuration, the optical rotation value of compound 1 was computed as −22.7° for (1R, 2S, 3R, 4R, 5S, 6R, 14R and 15R)-1 using the B3LYP/aug-cc-VDZ//B3LYP/6-311+G(d,p) method.[13–15] This value is very close to the observed value of −17.5°, which strongly suggests that the eight stereogenic centers in 1 were 1R, 2S, 3R, 4R, 5S, 6R, 14R and 15R.

Compound 1 has a previously unknown carbon skeleton: we propose the name 'verlleratretraol' for this new skeleton. From a biogenetic point of view, the precursor of 1 may be 8-epi-isolactarorufin or Lactarorufin A, which has been isolated from the Lactarius genus.[16,17] Up to now, none of the known sesquiterpenes has such a skeleton. Therefore, we propose the possible biosynthetic pathway for 1 as shown in Scheme 1, in which hydrolysis, oxidation, reduction and condensation reactions are potentially responsible for the above transformations.

Compound 1 also showed cytotoxicity against C8166 cells (inhibitory concentration of 136.5 μg ml^{-1}) and weak anti-HIV-1 cells activity with an effective concentration of 68.0 μg ml^{-1} and a selectivity index of 2.0.

EXPERIMENTAL SECTION

General experimental procedures

Optical rotations were measured on a Horiba SEPA-300 polarimeter (Horiba, Tokyo, Japan). UV spectra were recorded on a Shimadzu UV-2401PC spectro-photometer (Shimadzu, Kyoto, Japan). IR spectra were obtained with a Tensor
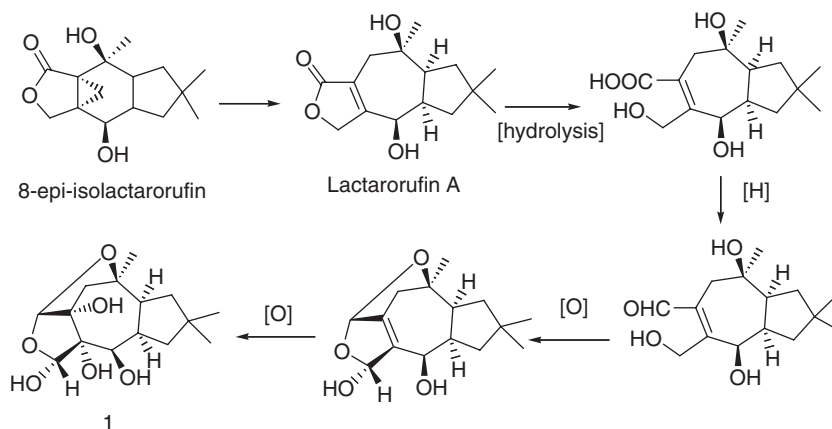
Scheme 1 Biosynthetic pathway proposed for velleratretraol (**1**) synthesis.

27 (Bruker, Karlsruhe, Germany) using KBr pellets. NMR spectra were recorded on Bruker AM-400 and Bruker DRX-500 spectrometers (Bruker) in CD_3OD with TMS as an internal standard. Electrospray ionization and HR-ESI-MS were recorded with an API QSTAR Pulsar I Hybrid LC/MS/MS system (Applied Biosystems, Foster City, CA, USA). Silica gel (200–300 mesh, Qingdao Marine Chemical Inc., Qingdao, PR China) and Sephadex LH-20 (Amersham Biosciences, Uppsala, Sweden) were used for column chromatography. Fractions were monitored by TLC (Qingdao Marine Chemical Inc.). TLC experiments were developed with petroleum ether–EtOAc or $CHCl_3$–MeOH solvent systems, and spots were visualized by heating silica gel plates sprayed with 10% sulfuric acid in EtOH.

Fungal material
The fresh fruiting bodies of *L. vellereus* were collected at the Ailao mountain, Yunnan Province, China in August 2006, and identified by the staff at the Kunming Institute of Botany, Chinese Academy of Science. A voucher specimen was deposited in the Herbarium of the Kunming Institute of Botany, Chinese Academy of Science.

Extraction and isolation
The fresh fruiting bodies of *L. vellereus* (8.0 kg) were extracted with 95% aq. EtOH (30 l). The EtOH soln was evaporated *in vacuo* to give an extract (500 g), which was suspended in water and extracted with EtOAc (5 l). The EtOAc extracts were evaporated under reduced pressure, giving 220 g of a residue, which was subjected to silica gel column chromatography using mixtures of $CHCl_3$ and MeOH (from 100:0 to 50:50; each 500 ml) as the eluents. The fraction eluted by mixtures of $CHCl_3$ and MeOH (90:10; 500 ml) was first evaporated, then redissolved and, finally, further subjected to silica gel column chromatography, eluting with mixtures of EtOAc and MeOH (100:0, 90:10, 80:20, 50:50; each 200 ml) to give 1, 2, 3 and 4 fractions. Fraction 2 eluted with mixtures of EtOAc and MeOH (90:10; 200 ml) was evaporated, redissolved with MeOH and further purified by Sephadex LH-20 chromatography (MeOH) to afford **1** (25 mg) as colorless crystal.

Velleratretraol (1): colorless crystals, m.p. 190–192 °C (MeOH). $[\alpha]_D^{20}$-17.5 (*c* 0.30, MeOH). UV λ_{max} (log ε) (MeOH): 243 (2.54), 204 (2.76) nm. IR (KBr): 3481, 2988, 2959, 2925, 2881, 1638, 1445, 1388, 1297, 1273, 1045, 968 and 900 cm^{-1}. ^{1}H- and ^{13}C-NMR (CD_3OD): see Table 1. HR-ESI-MS (pos.): 318.1911 ($C_{15}H_{24}O_6NH_4$) (0.20 mmu error).

Crystal data for 1. Crystals of **1**, crystallized from MeOH, belong to the orthorhombic space group P2(1)2(1)2(1). Crystal data: $C_{15}H_{24}O_6$, $M=300.34$, $a=5.6443$ (18) Å, $b=8.7693$ (12) Å, $c=28.892$ (4) Å, $V=1430.1$ (3) A3, $Z=4$, $d=1.395$ mg m^{-3}, Mo Kα radiations, linear absorption coefficient 0.107 mm^{-1}. A crystal of dimensions $0.22\times0.03\times0.02$ mm^3 was used for X-ray measurements on a Bruker SMART-1000 diffractometer with a graphite monochromator. The total number of independent reflections measured was 18 085, 2015

of which were considered to be observed (F2>3<F2). The structure was solved by the direct method SHELXS-97 and expanded using difference Fourier techniques, refined by the program and method NOMCSDP[18] and full-matrix least-squares calculations. Hydrogen atoms were fixed at calculated positions. The final indices were $R_f=0.0359$ and $R_w=0.0844$. Crystallographic data for the structure of **1** have been deposited in the Cambridge Crystallographic Data Centre (deposition number: CCDC 683072). Copies of these data can be obtained, free of charge, on application to the CCDC through www.ccdc.cam. ac.uk/conts/retriving.html (or from the Cambridge Crystallographic Data Centre, 12, Union Road, Cambridge CB2 1EZ, UK; fax (internat.): +44-1223/336-033; E-mail: deposit@ccdc.cam.ac.uk).

Reagents and cell culture
AZT (3′-azido-3′-deoxythymidine) and MTT (3-(4,5-dimethylthiazol-2-yl)-2,5-diphenyltetrazolium bromide) were purchased from Sigma-Aldrich (St Louis, MO, USA). Cells were donated by the Medical Research Council (AIDS Reagent Project, UK), and grown in RPMI-1640 medium supplemented with 10% heat-inactivated fetal calf serum (Gibro BRL, Gaithersburg, MD, USA), 2 mM L-glutamine, 10 mM HEPES (4-(2-hydroxyethyl) piperazine-1-ethanesulfonic acid), 50 μM 2-mercaptoethanol, 100 000 IU ml^{-1} penicillin and 100 μg ml^{-1} streptomycin sulfate. All cells and virus were stored and resuscitated by common methods.[19]

Cytotoxicity of compound 1 on C8166 cells
C8166 was one of the host cells for HIV-1. On a microtiter plate, 100 μl of 4×10^5 ml^{-1} cells were seeded. Then 100 μl of various concentrations of **1** was added and the cells were incubated at 37 °C in a humidified atmosphere of 5% CO_2 for 72 h. The cellular toxicity was assessed by an MTT colorimetric assay, the plates were read with a *Bio-Tek Elx* 800 ELISA reader at 595/630 nm and the 50% inhibitory concentration was calculated.

Cytopathic-effect inhibition assay of 1
In the presence of 100 μl of various concentrations of **1**, C8166 cells (4×10^5 ml^{-1}) were infected with HIV-1IIIB at a multiplicity of infection of 0.06. The final volume was 200 μl. The plates were incubated in a humidified incubator at 37 °C and 5% CO_2. AZT (Sigma) was used as drug control. After 3 days of culture, the cytopathic effect was measured by counting the number of syncytia (multinucleated giant cells) in each well under an inverted microscope and the 50% effective concentration was calculated.

organic Chemistry, Nankai University, P R China) for assistance in obtaining the X-ray structure.

1   Whittaker, R. H. New concepts of kingdoms of organisms. *Science* **163,** 150–160 (1969).
2   De Bernardi, M., Garlaschelli, L., Toma, L., Vidari, G. & Vita-Finzi, P. The chemical basis of hot-tasting and yellowing of the mushrooms *Lactarius chrysorrheus* and *L. scrobiculatus*. *Tetrahedron* **49,** 1489–1504 (1993).
3   Sterner, O., Bergmann, R., Kihlberg, J. & Wickberg, B. The sesquiterpenes of *Lactarius vellereus* and their role in a proposed chemical defense system. *J. Nat. Prod.* **48,** 279–288 (1985).
4   Ayer, W. A. & Browne, L. M. Terpenoid metabolites of mushrooms and related basidiomycetes. *Tetrahedron* **37,** 2199–2248 (1981).
5   Garlaschelli, L., Mellerio, G., Vidari, G. & Vita-Finiz, P. New fatty acid esters of drimane sesquiterpenes from *Lactarius uvidus*. *J. Nat. Prod.* **57,** 905–910 (1994).
6   Kopczacki, P. *et al.* Synthesis and antifeedant properties of N-benzoylphenylisoserinates of Lactarius sesquiterpenoid alcohols. *Phytochemistry* **58,** 775–787 (2001).
7   Daniewski, W. M. *et al.* 3, 8-ethers of lactarane sesquiterpenes. *Phytochemistry* **32,** 1499–1502 (1993).
8   Luo, D. Q., Wang, F., Bian, X. Y. & Liu, J. K. Rufuslactone, a new antifungal sesquiterpene from the fruiting bodies of the Basidiomycete *Lactarius rufus*. *J. Antibiot.* **5,** 456–459 (2005).
9   Luo, D. Q., Gao, Y., Yang, X. L., Tang, J. G. & Liu, J. K. Highly oxidized humulane sesquiterpenes from the Basidiomycete *Lactarius mitissimus*. *J. Antibiot.* **60,** 162–165 (2007).
10 Shao, H. J. *et al.* A new cytotoxic lanostane triterpenoid from the Basidiomycete *Hebeloma versipelle*. *J. Antibiot.* **58,** 828–831 (2005).
11 Luo, D. Q. *et al.* Humulane-type sesquiterpenoids from the Mushroom *Lactarius mitissimus*. *J. Nat. Prod.* **69,** 1354–1357 (2006).
12 Wang, F., Luo, D. Q. & Liu, J. K. Aurovertin E, a new polyene pyrone from the Basidiomycete *Albatrellus confluens*. *J. Antibiot.* **56,** 412–415 (2005).
13 Liu, D. Z. *et al.* Vibralactone: a lipase inhibitor with an unusual fused beta-lactone produced by cultures of the basidiomycete *Boreostereum vibrans*. *Org. Lett.* **8,** 5749–5752 (2006).
14 Crawford, T. D., Owens, L. S., Mary, C. T., Schreiner, P. R. & Koch, H. *Ab initio* calculation of optical rotation in (P)-(+)-[4] triangulane. *J. Am. Chem. Soc.* **127,** 1368–1369 (2005).
15 Frisch, M. J. *et al. Gaussian 03 User's Reference*, Gaussian Inc.: Carnegie, PA, (2003).
16 Daniewski, W. M., Gumulka, M. & Przesmycka, D. Sesquiterpenes of Lactarius origin, antifeedant structure–activity relationships. *Phytochemistry* **38,** 1161–1168 (1995).
17 Daniewski, W. M., Kocór, M. & Thorén, S. Isolactarorufin, a novel tetracyclic sesquiterpene lactone from *Lactarius rufus*. *Heterocycles* **5,** 77–84 (1976).
18 Liu, Y. & Wu, B. M. A microcomputer analytic system for crystal structure used in chemical laboratories. *Chin. Chem. Lett.* **3,** 637–640 (1992).
19 Wang, Q., Ding, Z. H., Liu, J. K. & Zheng, Y. T. Xanthohumol, a novel anti-HIV-1 agent purified from Hops *Humulus lupulus*. *Antiviral Res.* **64,** 189–194 (2004).

npg

ORIGINAL ARTICLE

Synthesis and biological properties of 4″-O-acyl derivatives of 8a-Aza-8a-homoerythromycin

Vlado Stimac, Sulejman Alihodzic, Gorjana Lazarevski, Stjepan Mutak, Zorica Marusic Istuk, Andrea Fajdetic, Ivana Palej, Hana Cipcic Paljetak, Jasna Padovan, Branka Tavcar and Vesna Erakovic Haber

A series of 4″-O-acyl derivatives of 8a-aza-8a-homoerythromycins A were synthesized and tested against Gram-positive and Gram-negative bacteria. Derivatives of 8a-aza-8a-homoerythromycin A have potent anti-bacterial activity against not only azithromycin-susceptible strains, but also efflux (M) and inducible macrolide–lincosamide–streptogramin-resistant Gram-positive pathogens. These compounds show moderate to high clearance and low oral bioavailability in preliminary *in vivo* pharmacokinetic studies in rat.
The Journal of Antibiotics (2009) **62**, 133–144; doi:10.1038/ja.2009.1; published online 13 February 2009

INTRODUCTION

Second-generation macrolide anti-biotics, such as clarithromycin[1] (6-O-methylerythromycin A) and azithromycin[2,3] (15-membered aza-lide), have been widely prescribed for upper and lower respiratory tract infections because of their superior anti-bacterial activity, pharmacokinetic properties and fewer gastrointestinal side effects as compared with erythromycin A. However, the therapeutic utility of these macrolides has been severely compromised by the emergence of resistant pathogens.[4]

We recently reported on the synthesis of 3-keto and 3-O-acyl derivatives of 9a- and 8a-aza-8a-homoerythromycins A having anti-bacterial activity against sensitive pathogens as well as against macrolide-resistant Gram-positive pathogens.[5]

In this report we describe a novel series of 4″-O-acyl derivatives of 8a-aza-8a-homoerythromycin A (8a-lactams), having (hetero)ary-lalkyl side chain on 4″-O atom, which showed potent anti-bacterial properties against sensitive pathogens and improved activity against several species of efflux (M) and inducible (iMLS$_B$) macrolide-resistant Gram-positive pathogens.
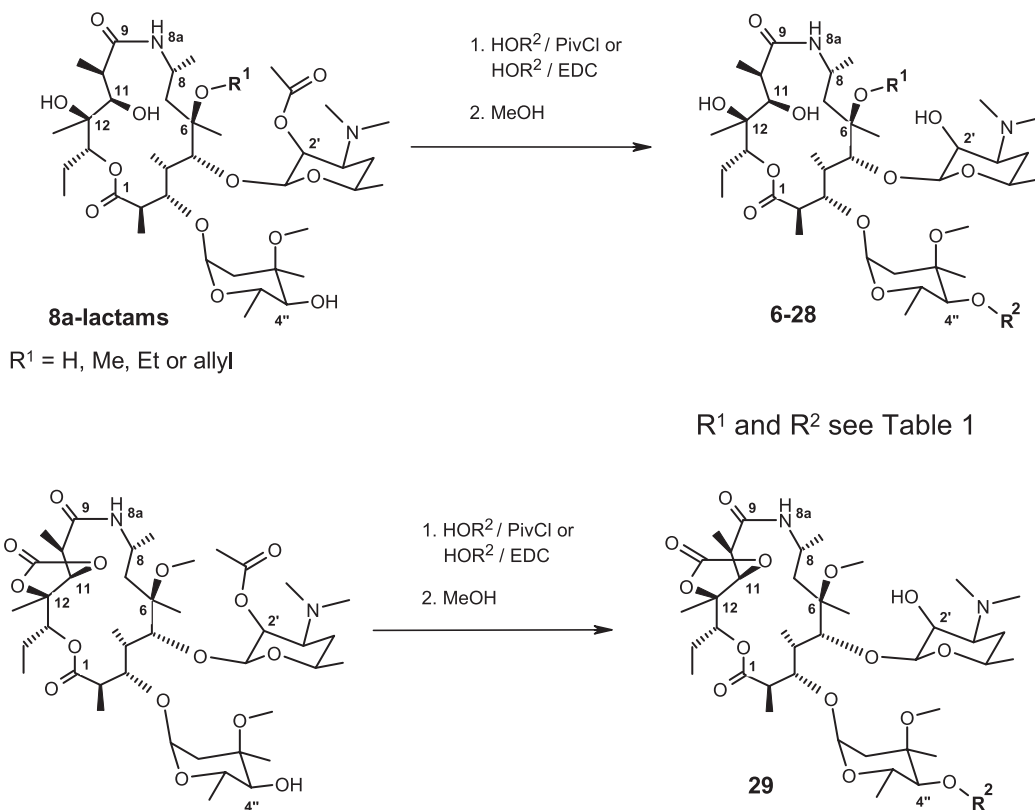
Chemistry

In an attempt to define the structure-activity relationship, 4″-O-acyl derivatives of 8a-lactams have been prepared by modifying several structural units in the molecule. Thus, the length of a linker connecting macrolide and aromatic unit varied from one to five carbon atoms. Unsaturated and saturated analogs were synthesized. Furthermore, 4-nitrophenyl, pyridyl or quinolyl groups were introduced as aromatic substituents, whereas the macrolide moiety had either a free hydroxyl or a free C$_1$-C$_3$-alkoxy group at position C-6.

The synthetic route to the derivatives is presented in Scheme 1. Starting compounds for the synthesis were 6-O-alkyl-8a-aza-8a-homoerythromycins A[5] (**1–5**) having acetyl as 2′-hydroxy-protecting group. Compounds **6**, **13–18**, **22**, **24**, **27** and **29** were prepared by condensation of 2′-protected compounds **1–5** with the corresponding (hetero)arylalkyl-carboxylic acid using 1-[(3-(dimethyl-amino)pro-pyl]-3-ethyl-carbodiimide hydrochloride (EDC) in the presence of 4-(dimethyl-amino)pyridine (DMAP) in dichloromethane. To synthe-size compounds **7–9**, **11**, **23**, **25**, **26** and **28** mixed anhydrides, prepared from the corresponding arylalkyl-carboxylic acid and piva-loyl chloride, were used instead. Subsequent deprotection by stirring overnight in methanol and purification by column chromatography gave the desired 4″-O-acyl derivatives.

Compounds **10**, **12** and **19–21** were obtained by catalytic hydro-genation of the corresponding compounds having a double bond in the linker. Thus, compound **10** was prepared from **9**, compounds **19** and **20** from **16**, compound **12** from **11** and compound **21** from **15**. Although the reaction conditions for compounds **11** and **9** were mild, in addition to reduction of the double bond in the linker, reduction of *p*-nitro to the *p*-amino group occurred. Using more vigorous condi-tions, the quinoline in **15** or **16** can also be reduced to the 1,2,3,4-tetrahydroquinolines **20** and **21**.

Previous reports[6] indicated that conversion of the macrolide 11,12-diol to the corresponding cyclic carbonate may enhance the anti-bacterial activity. The 11,12-carbonate **5** was synthesized by treating the 6-O-methyl-8a-aza-8a-homoerythromycin A with ethylene carbo-nate.[7] Acylation of **5** in the presence of EDC under condition described above provided 4″-O-acyl-11,12-carbonate **29**.

The mass spectra for all new compounds were in agreement with the proposed structure. These results were further confirmed by the

GSK Research Centre Zagreb Ltd, Zagreb, Croatia
Correspondence: Dr V Stimac, GSK Research Centre Zagreb Ltd, Prilaz baruna Filipovica 29, Zagreb, Croatia.
E-mail: vlado.z.stimac@gsk.com

Scheme 1.

NMR spectra of all compounds, which showed two sets of signals, arising from the presence of macrolide and aromatic moieties, respectively, as well as signals reflecting the number of methylene groups in the linker.

In the ^{13}C NMR spectrum, the newly formed ester carbonyl resonates around 170 p.p.m. The significant deshielding of the 4″-H signal in the ^{1}H NMR, together with its long-range coupling to the new ester carbonyl signal (HSQC), provided evidence that the esterification occurred at the 4″-OH group of the macrolide scaffold.

The E-configuration of the double bond was assigned on the basis of the vicinal coupling constant between the olefinic proton pair (for example, $^{3}J=16.05$ Hz in **16**).[8]

Hydrogenation of the double bond in the linker was also confirmed by NMR spectroscopy. For example, in the ^{13}C NMR spectrum of compound **19**, two signals corresponding to the olefinic carbon of the double bond have disappeared and two new methylene signals appeared at δ 35.3 and 28.1 p.p.m. These signals correlated with the proton signals at δ 2.89, 2.66 and 3.18 p.p.m. in the ^{1}H-^{13}C COSY spectra.

RESULTS AND DISCUSSION

In vitro anti-bacterial activity of all compounds was determined against a panel of diverse bacterial strains, covering most important Gram-positive (that is, *Streptococcus pneumoniae*, *S. pyogenes*) and Gram-negative (that is, *Haemophilus influenzae*, *Moraxella catarrhalis*) respiratory tract pathogens and different mechanisms of macrolide resistance. Efflux-mediated resistance gives rise to M phenotype and is characterized by expression of genes encoding efflux pumps, such as mef in *Streptococci* and msr in *Staphylococci* that actively transport macrolide anti-biotics out of bacterial cells. MLSb phenotype occurs due to expression of erm genes that encode ribosomal methyltransferases, a family of enzymes that specifically methylate ribosomal RNA and therefore prevent binding of macrolide, lincosamide and streptogramin B group of anti-biotics. This phenotype is either inducible (giving iMLS phenotype) or constitutive (cMLS).

In all *in vitro* experiments, in addition to starting compounds, azithromycin was used as the reference compound, as it is the 'Gold standard' in macrolide therapy.

Anti-bacterial activities are reported in Tables 1 and 2 as minimum inhibitory concentrations (MIC, in µg ml^{-1}).

In vitro evaluation

Comparing 4-substituted phenyl derivatives (**6–12**) with 4″-O-non-functionalized compounds (**1–4**), an encouraging increase was observed in the level of activity against macrolide-resistant efflux mutants and *E. faecalis*, especially analogs **9** and **11**. However, this was offset by a significant decrease in potency against the Gram-negative organisms *M. catarrhalis* and *H. influenzae*. There appears to be little or no effect on the potency against erythromycin-sensitive strains or constitutively resistant *S. pneumoniae*. The effect of 6-substituent is marginal, although the 6-O-methyl scaffold tends to have a better overall spectrum of activity and potency.

Reduction of the linker double bond and concomitant reduction of the nitro to an amino group (**10**, **12**) diminished potency of compounds compared with their counterparts with unsaturated linker (**9**, **11**), but they are still more active than the starting compounds (**1**, **2**).

Replacement of the nitrophenyl ring by pyridine (**13**) markedly improved the activity against *Streptococcus* efflux mutants (M) but showed no improvement against *Staphylococcus* organisms. Potency

against other strains in the assay is broadly similar in both compounds.

Quinolyl derivatives 14–29 retained similar potency to the nitrophenyl substituent against erythromycin-sensitive strains but showed considerable improvement against the efflux strains (15 vs 9 and 16 vs 11). The improvement was most marked in the 6-hydroxy scaffold (15 vs 9), where there was also an increase in potency against the inducibly resistant Streptococcus strain.

However, activity against the Gram-negative organisms remained weak. Increasing the size of the substituent on 6-hydroxyl was detrimental to potency on the resistant, but not on the sensitive strains (H > Me > Et=Allyl).

Saturation of the linker double bond (19 vs 16) reduces potency against the resistant mutants, as does saturation of hetrocyclic ring (20, 21). There is a minimal difference between 6-hydroxy and 6-methoxy substituents for these changes.

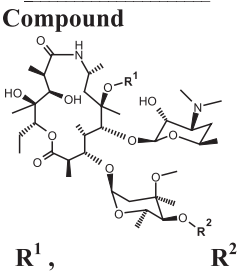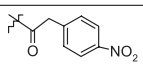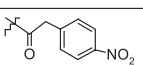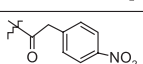**Table 1 Anti-bacterial activity of 4″-O-acyl-6-O-alkyl-8a-aza-8a-homoerythromycins (MIC, $\mu g\,ml^{-1}$)**
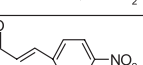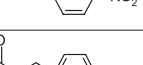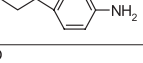
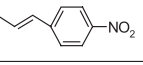| Strain Phenotype / Compound R^1, R^2	Staphylococcus aureus; ATCC13709 eryS	Streptococcus pneumoniae eryS	Streptococcus pyogenes eryS	Staphylococcus aureus M	Streptococcus pneumoniae M	Streptococcus pyogenes M	Staphylococcus aureus iMLS	Streptococcus pyogenes iMLS	Streptococcus pneumoniae cMLS	Moraxella catarrhalis; ATCC23246	Haemophilus influenzae; ATCC49247	Enterococcus faecalis; ATCC29212
Azithromycin	0.5	<0.13	<0.13	>64	8	4	>64	8	>64	<0.13	1	8
1 H, H	1	<0.13	<0.13	>64	32	32	>64	16	>64	0.25	2	8
2 Me, H	0.5	<0.13	<0.13	>64	16	16	>64	8	>64	<0.13	4	4
3 Et, H	0.25	<0.13	<0.13	>64	32	16	>64	16	>64	<0.13	1	8
4 Allyl, H	1	<0.13	<0.13	64	32	16	>64	16	>64	<0.13	4	8
6 H, (p-NO2 phenylacetyl)	8	<0.13	0.25	64	8	32	64	>64	>64	4	16	8
7 Me, (p-NO2 phenylacetyl)	4	<0.13	<0.13	16	2	32	>64	16	64	8	8	4
8 Et, (p-NO2 phenylacetyl)	2	<0.13	<0.13	8	4	16	>64	16	>64	4	4	4
9 H, (p-NO2 cinnamoyl)	0.5	<0.13	<0.13	8	0.25	2	1	4	>64	8	8	<0.13
10 H, (p-NH2 dihydrocinnamoyl)	4	<0.13	0.25	32	4	4	>64	8	>64	4	16	2
11 Me, (p-NO2 cinnamoyl)	1	<0.13	<0.13	1	<0.13	2	16	8	64	8	32	<0.13
12 Me, (p-NH2 dihydrocinnamoyl)	4	0.5	1	16	2	4	64	16	>64	8	8	8
13 Me, (pyridyl acetyl)	8	<0.13	<0.13	>64	0.5	0.5	>64	64	>64	2	16	32
14 Me, (quinolinyl carbonyl)	1	<0.13	<0.13	4	4	32	>64	8	>64	8	8	2

Table 1 Continued

15	H,	0.5	<0.13	<0.13	0.5	<0.13	0.5	1	0.25	>64	4	8	<0.13
16	Me,	1	<0.13	<0.13	2	<0.13	<0.13	8	2	64	8	16	0.5
17	Et,	2	<0.13	0.25	8	4	8	>64	32	>64	2	8	4
18	Allyl,	1	<0.13	<0.13	8	16	16	16	4	32	4	16	4
19	Me,	2	<0.13	0.5	4	4	64	>64	16	>64	8	16	4
20	Me,	1	<0.13	<0.13	4	<0.13	8	64	8	64	8	16	0.5
21	H,	1	<0.13	<0.13	2	0.5	32	64	4	>64	8	8	2
22	Me,	2	<0.13	<0.13	16	0.25	<0.13	64	4	16	8	8	2
23	Me,	1	<0.13	<0.13	4	<0.13	0.25	>64	2	16	2	8	2
24	Me,	2	<0.13	<0.13	4	<0.13	0.5	8	0.5	16	4	4	0.25
25	H,	<0.13	<0.13	<0.13	1	<0.13	2	>64	8	64	2	-	1
26	Me,	1	<0.13	<0.13	8	0.25	<0.13	8	8	16	8	4	1
27	Me,	4	<0.13	0.25	8	2	8	>64	8	>64	8	2	2
28	Me,	2	<0.13	<0.13	8	4	8	>64	16	>64	4	2	2

In vitro susceptibility testing was carried out by standard microdilution broth assay as recommended by NCCLS M7-A5 (2001).

The compound with a quinolyl group attached directly to the 4″-hydroxyl through carbonyl (14) had lower potency than corresponding compounds attached by longer linkers.

Extension of the linker by one carbon (23, 24 vs 16) was detrimental to the level of activity against inducible organisms. However, some of the potency can be regained by saturation of linker double bond (24 vs 23). In both compounds, there is the first indication of activity against the constitutively resistant S. pneumoniae. Extension of the linker by two carbons, in the case of compounds 25 vs 15, decreased activity against inducible strains. Movement of the double bond out of conjugation with the quinoline (27 vs 26) or reduction of the double bond (28 vs 26) was detrimental to potency in these examples.

Attachment of the linker on the 4-position of the quinoline (22), compared with the position 3 (16), retained activity against all sensitive and efflux Streptococcus strains, but was weaker against inducible organisms.

Introduction of a 11,12-cyclic carbonate group (29) reduced overall activity compared with the 11,12-diol derivative (16). A similar slight diminution in overall profile for the 11,12-carbonate was also observed in the case of the 4″-hydroxy analog 5 vs 2.

In vivo evaluation

Pharmacokinetic studies were carried out in rats with several compounds, chosen based on specific substituents on the macrolide moiety in position 6-O and position 4″-O. Compound 2 was screened as a representative of the 4″-hydroxy 8a-aza-8a-homoerythromycin A analogs, and compounds 6, 7, 9, 11 (as diacetate salts), 15 and 16 where selected as analogs with similar substituents in either the 6-O and/or 4″-O positions. Summarized

Table 2 Anti-bacterial activity of 4″-O-acyl-6-O-alkyl-8a-aza-8a-homoerythromycins 11,12-cyclic carbonate derivatives (MIC, µg ml⁻¹)

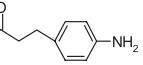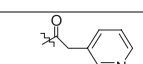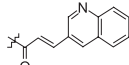| Strain Phenotype / Compound	R^1,	R^2	*Staphylococcus aureus;* ATCC13709 eryS	*Streptococcus pneumoniae* eryS	*Streptococcus pyogenes* eryS	*Staphylococcus aureus* M	*Streptococcus pneumoniae* M	*Streptococcus pyogenes* M	*Staphylococcus aureus* iMLS	*Streptococcus pyogenes* iMLS	*Streptococcus pneumoniae* cMLS	*Moraxella catarrhalis;* ATCC23246	*Haemophilus influenzae;* ATCC49247	*Enterococcus faecalis;* ATCC29212
5	Me,	H	2	<0.13	0.25	64	16	16	>64	4	>64	0.25	8	4
29	Me,	(quinolinyl propenoyl)	8	<0.13	0.25	16	16	16	32	32	>64	8	8	4

Table 3 Summarized pharmacokinetic parameters after [1]intravenous and oral administration to rats, expressed as mean ± s.d.

Compound no.		**2**	**6**	**7**	**9**	**11**	**15**	**16**
Target dose intravenously	mg kg⁻¹	10	5.7	10	10	10	10	10
n^a		4	3	5	3	5	5	5
[1]CL	ml min⁻¹ kg⁻¹	48.0 ± 11.7	87.6 ± 34.2	25.3 ± 7.0	121.0 ± 86.0	143.8 ± 22.0	140 ± 60.0	59.7 ± 37.2
[1]Vss	l kg⁻¹	3.6 ± 1.0	2.8 ± 1.7	4.1 ± 1.5	53.8 ± 36.6	47.3 ± 11.8	41.4 ± 27.2	10.3 ± 8.1
[1]$t_{1/2}$	Hr	1.5 ± 0.1	1.2 ± 0.4	3.8 ± 0.8	13.4 ± 11.9	3.0 ± 0.19	6.7 ± 3.6	3.8 ± 1.7
Oral Fᵇ	%	<1	<1	27.2 ± 11.7	<1	9.4 ± 2.3	3.6 ± 3.3	12.0 ± 7.9

[a]n=number of rats included to express mean ± s.d. values.
[b]Oral F determined based on area under the curve (0–t); compounds administered as salts at target doses of 30 mg kg⁻¹ orally.

pharmacokinetic parameters after intravenous and oral dosing are presented in Table 3.

Compound **2**, lacking the substitution on position 4″-O, has a moderate systemic clearance (Cls) of approximately 56% of liver blood flow (LBF), moderate volume of distribution (Vss) (3.6 l kg⁻¹), short half-life (1.5 h) and oral bioavailability of less than 1%. The lack of systemic availability is most likely due to extrahepatic extraction and/or poor gastrointestinal absorption.

Introduction of a (4-nitrophenyl)acetyl substituent on position 4″-O (compound **6**) resulted in a substantial increase in Cls (≈LBF), a moderate volume of distribution and no improvement in oral bioavailability (<1%). However, methylation of the same analog at position 6-O (compound **7**) gave a lower Cls (≈30% LBF), moderate Vss, longer $t_{1/2}$ (3.3 h) and variable, but substantial increase in oral bioavailability (27%). Lengthening the linker by introducing a double bond between the carbonyl and aromatic moiety (3-(4-nitrophenyl)-2-propenoyl) (compounds **9** and **11**) increased the Cls (>LBF) in both cases, with compound **11** having a variable, but higher oral bioavailability in comparison with compound **9** (≈9 vs <1%). This low bioavailability is most likely due to extensive extrahepatic clearance, in addition to limited absorption. Both compounds had a several fold higher volume of distribution, in comparison with compounds **6** and **7**, and methylation at position 6-O did not improve the oral bioavailability of compound **11** to the extent that was observed in the previous case.

Replacement of the nitrophenyl moiety with a 3-quinolinyl substituent (compounds **15** (6-hydroxy) and **16** (6-methoxy)) resulted in a high Cls, exceeding the LBF in case of compound **15** and ≈70% of LBF with compound **16**. Both compounds had a large Vss, moderate-long $t_{1/2}$ and variable and low bioavailability (3.6 vs 12%, respectively). Yet again, methylation at position 6-O resulted in a slightly higher oral bioavailability. Both compounds showed a delayed absorption, with maximum levels at 8 (compound **15**) and 3 h (compound **16**) upon oral dosing.

In general, the analogs of 4″-O-acyl derivatives of 8a-aza-8a-homoerythromycins tested *in vivo* can be characterized by a moderate (**2**, **7**) to high Cls (**6**, **9**, **11**, **15**, **16**), exceeding the LBF in some cases (**9**, **11**, **15**), suggesting extrahepatic clearance. This is consisted with *in vitro* microsomal CL (in house data), which is low for compounds **7** (0.3 ml min⁻¹ g⁻¹) and **16** (0.8 ml min⁻¹ g⁻¹), and moderate for compound **11** (1.9 ml min⁻¹ g⁻¹) predicting low *in vivo* hepatic metabolism. These derivatives have a moderate (**2**, **6**, **7**) to very high (**9**, **11**, **15**, **16**) volume of distribution, as well as a moderate to long half-life. The oral bioavailability for these compounds is variable and low to moderate, ranging from <1 to 27%, most likely due to extrahepatic clearance, as well as limited absorption. Methylation at position 6-O increased the oral bioavailability in all three cases relative to the non-methylated analog, possibly due to improved absorption or decreased extrahepatic clearance.

138

Conclusions

A series of 4″-*O*-acyl derivatives of 8a-aza-8a-homoerythromycins A have been prepared by varying several structural units on the macrolide scaffold. Thus, 4-nitrophenyl, pyridyl or quinolyl groups were introduced as aromatic substituents linked by an ester bond at the 4″-position of the macrolide scaffold by a spacer of different length. Position 6 of the macrolide moiety was either a free hydroxyl or a C_1-C_3-alkoxy group.

The results indicate improvements in the *in vitro* anti-bacterial activity in comparison with 4″-unsubstituted compounds against efflux or inducibly resistant strains of Gram-positive organisms. Furthermore, activity against the constitutively resistant *S. pneumoniae* was observed.

The compounds evaluated *in vivo* show moderate to high clearances and low oral bioavailabilities in preliminary *in vivo* studies in rat, possibly most likely due to extrahepatic clearance as well as limited absorption.

The overall profile of the reported compounds justifies further structure-based optimization of this series to additionally increase potency against macrolide-resistant strains and to improve pharmacokinetic parameters.

EXPERIMENTAL SECTION
General
All commercial reagents (Merck, Hohenbrunn, Germany; Sigma-Aldrich, Steinheim, Germany) were used as provided unless otherwise indicated.

NMR spectra were recorded on a Bruker Avance DRX500 or Bruker Avance DPX300 spectrometer in $CDCl_3$ or dimethylsulfoxide (DMSO), and chemical shifts are reported in p.p.m. using tetramethylsilane (TMS) as an internal standard. Mass spectra were obtained on a Waters Micromass ZQ mass spectrometer for ES$^+$-MS. Electrospray-positive ion mass spectra were acquired using a Micromass Q-Tof2 hybrid quadrupole time-of-flight mass spectrometer, equipped with a Z-spray interface, over a mass range of 100–1500 Da, with a scan time of 1.5 s and an interscan delay of 0.1 s in a continuum mode. Reserpine was used as the external mass calibrant lock mass ([M+H]$^+$=609.2812 Da). The elemental composition was calculated using a MassLynx v4.1 for the [M+H]$^+$ and the mass error quoted within ± 5 p.p.m. range. In synthetic procedures, column chromatography was carried out over Merck Kieselgel 60 (230–400 mesh) and thin layer chromatography on 0.24 mm silica gel plates Merck TLC 60F$_{254}$. The eluent used was indicated and solvent ratios refer to volume.

In general, organic solutions were dried with anhydrous Na_2SO_4 or K_2CO_3, evaporation and concentration were carried out under reduced pressure below 40 °C, unless otherwise noted.

8a-Aza-8a-homoerythromycin A, 6-*O*-methyl-8a-aza-8a-homoerythromycin A, 6-*O*-ethyl-8a-aza-8a-homoerythromycin A and 6-*O*-allyl-8a-aza-8a-homoerythromycin A were prepared by Beckmann rearrangement of the corresponding oxime derivatives according to the published procedures.[5,9] 2′-*O*-Acetyl-protected derivatives were prepared by the known procedure.[10]

Anti-bacterial activity *in vitro*
Strains were cultured on MH agar (Merck, Germany) except strains belonging to genus *Streptococcus* and *Haemophilus*, which were cultured on blood agar plates (Biomerioux, Craponne, France) and chocolate agar plates (Biomerioux), respectively. MICs were determined by the microtitre liquid dilution method as described by NCCLS[11] except for *Streptococcus* medium, where blood was substituted by 5% horse serum.

In vivo pharmacokinetic studies
Male Wistar Han rats, weighing 300–350 g, were purchased from IFFA CREADO, Lyon, France. The rats were maintained in an air-conditioned animal quarter at a temperature of 22 ± 2 °C and a relative humidity of 50 ± 10%. Water and food (Laboratory Rodent Chow, Nanjing, China) were allowed *ad libitum*. Rats were divided into groups of five and the pharmaco-

kinetic study was performed in a crossover design including a 2-day washout period. Each compound was administered intravenously at 10 mg kg^{-1}, followed by a 2-day washout period and orally at 30 mg kg^{-1} free base equivalent. Compound **6** (as acetate salt) was administered at an intravenous dose of 5.7 mg kg^{-1}. For intravenous dosing, compounds were formulated in 1% dimethyl formamide (DMF)/phosphate buffer, and blood samples (50 µl) were collected at 0.17, 0.33, 0.67, 1, 2, 4, 6, 8, 12 and 24 h. For oral administration, compounds were dissolved in 1% DMF/20% Encapsin (w/v), and saline and blood samples (50 µl) were collected at 0, 0.25, 0.5, 1, 1.5, 2, 4, 6, 8, 12 and 24 h. Blood samples were collected serially from the tail vein, hemolyzed with deionized water in a 1:2 ratio and frozen at −20 °C until analysis.

Sample preparation and bioanalysis
Hemolyzed blood samples (150 µl) in Eppendorf test tubes were treated by protein precipitation with the addition of two volumes of a mixture MeCN/MeOH (1:2), containing an internal standard. A 1 mg ml^{-1} stock solution of each compound was prepared in DMSO, diluted in water and spiked into rat blank blood to prepare duplicate standards ranging from 5 to 25 000 ng ml^{-1}. One set of standards was analyzed at the beginning and one set at the end of each sample batch. Quality control samples (QCs) were prepared from separate stock solutions and analyzed at three concentrations (low, medium, high). The mixtures were centrifuged at 4000 r.p.m. at 4 °C for 10 min and aliquots (0.01 ml) of the resulting supernatant fractions were transferred to a 96-well plate. Samples were analyzed with either a Sciex API 3000 or Sciex API 2000 Triple Quadrupole Mass Spectrometer (Sciex, Division of MDS Inc., Toronto, Canada) coupled to an HP HPLC System (HP1100, Hewlett-Packard, Palo Alto, CA, USA) and an HTS PAL CTC Autosampler (CTC). Samples (5 µl) were injected onto an HPLC column (3 µm Phenomenex Luna C18(2), 2.0×50 mm) and eluted with a gradient at room temperature. The chromatographic conditions consisted of mobile phase A (1000:1 MeCN/formic acid, v/v) and mobile phase B (1000:1 water/formic acid, v/v) that was run over a 6 min gradient at a flow rate of 0.3 ml min^{-1}. A positive ion mode with turbo spray, an ion source temperature of 400–450 °C and a dwell time of 300–400 ms were utilized for mass spectrometric detection. Quantification was performed using multiple reaction monitoring (MRM) at the following transitions for each particular compound: **2** (*m/z* 763.8 to *m/z* 606.3), **15** (*m/z* 930.8 to *m/z* 591.2), **16** (*m/z* 945.3 to *m/z* 606.7), **6** (*m/z* 912.8 to *m/z* 591.7), **7** (*m/z* 926.8 to *m/z* 605.5), **9**, **11** (*m/z* 938.6 to *m/z* 605.4) and internal standard (*m/z* 837.6 to *m/z* 158.4). Linear regression plots of compounds to internal standard peak area ratios versus drug concentrations were derived with $1/x$ or $1/x^2$ weighting. The dynamic range for the blood assay ranged from 0.005 to 10 µg ml^{-1}. Accuracy of the QCs used during the analysis was below 24% (judged by percent deviation from nominal value) for at least two of three concentrations, with a precision of ⩽20% (as judged by relative standard deviation).

Pharmacokinetic analysis
Noncompartmental analysis for all compounds was performed using WinNonlin Professional, version 4.0.1 (Pharsight, Mountain View, CA, USA). Individual blood concentrations and sample times for each animal were used in the analysis. Following intravenous bolus administration, the terminal elimination half-life (t), total area under the curve, concentration-time curve extrapolated to infinity, systemic blood clearance and steady-state volume of distribution were calculated by standard methods. After oral administration, the peak plasma concentration (C_{max}) and the time to C_{max} (T_{max}) were taken directly from individual profiles and the areas under the curve and oral bioavailabilites were determined. Summarized pharmacokinetic parameters were reported as mean values ± s.d. both after intravenous and oral administration.

4″-*O*-[(4-nitrophenyl)acetyl]-8a-aza-8a-homoerythromycin A (6)
To a solution of 2′-*O*-acetyl-8a-aza-8a-homoerythromycin A (0.50 g, 0.63 mmol) in CH_2Cl_2 (25 ml) and DMF (5 ml), 4-(nitrophenyl)acetic acid (0.57 g, 3.15 mmol) was added, and the resulting white suspension was cooled to 0 °C under argon. EDC hydrochloride (0.50 g, 2.62 mmol) was added in one portion, followed by addition of DMAP (0.075 g, 0.62 mmol). The reaction mixture was stirred at room temperature for 5 h. The reaction was quenched by

addition of saturated aqueous NaHCO$_3$ solution (30 ml) and extracted with CH$_2$Cl$_2$ (3×20 ml) at pH 9.5. Combined organic extracts were washed with brine (20 ml), dried over K$_2$CO$_3$ and concentrated *in vacuo*. The brown residue was dissolved in MeOH (30 ml), stirred at room temperature overnight and concentrated to dryness. The residue was purified by flash column chromatography (eluent CH$_2$Cl$_2$/MeOH 9:1) to obtain the title compound **6** (88 mg, 15.3%).

MS (ES) *m/z*: [M+H]$^+$ 912.9.

HRMS (ES positive): calculated for C$_{45}$H$_{74}$N$_3$O$_{16}$ [M+H]$^+$ 912.5069 found 912.5060.

^{1}H NMR (500 MHz, CDCl$_3$) δ 8.20 (Ph-2H), 7.49 (Ph-2H), 5.94 (8a-NH), 5.13 (1″-H), 4.92 (13-H), 4.74 (4″-H), 4.57 (1′-H), 4.38 (5″-H), 4.33 (3-H), 4.20 (8-H), 4.78 (Ph-CH$_2$, 5′-H), 3.57 (5-H), 3.50 (11-H), 3.32 (2′-H), 3.31 (3″-OCH$_3$), 2.83 (3′-H), 2.64 (2-H), 2.52 [3′-N(CH$_3$)$_2$], 2.38 (2″a-H, 10-H), 1.94 (4-H), 1.90 (14a-H), 1.77 (4′a-H), 1.62 (2″b-H), 1.55 (7a-H), 1.45 (14b-H), 1.41 (7b-H), 1.39 (6-CH$_3$), 1.21 (8-CH$_3$, 5′-CH$_3$), 1.19 (10-CH$_3$), 1.18 (2-CH$_3$), 1.14 (5″-CH$_3$), 1.10 (12-CH$_3$), 1.05 (4-CH$_3$), 1.04 (3″-CH$_3$), 0.89 (14-CH$_3$).

^{13}C NMR (125 MHz, DMSO) δ 177.8 (C-1), 176.5 (C-9), 169.9 (4″-OCO), 147.3, 140.9, 130.3, 123.8 (Ph), 102.0 (C-1′), 94.6 (C-1″), 82.9 (C-5), 79.9 (C-4″), 77.2 (C-3), 76.9 (C-13), 74.8 (C-12), 73.9 (C-6), 73.2 (C-3″), 70.6 (C-2′), 70.1 (C-11), 67.7 (C-5′), 65.7 (C-3′), 62.6 (C-5″), 49.5 (3″-OCH$_3$), 45.5 (C-2), 42.9 (C-4), 42.3 (C-7), 41.9 (C-10), 40.7 (CH$_2$), 40.6 (C-8), 40.4 [3′-N(CH$_3$)$_2$], 34.9 (C-2″), 30.3 (C-4′), 21.7 (C-14), 11.3 (14-CH$_3$).

4″-O-[(4-nitrophenyl)acetyl]-6-O-methyl-8a-aza-8a-homoerythromycin A (7)

To a solution of (4-nitrophenyl)acetic acid (0.25 g, 1.4 mmol) in CH$_2$Cl$_2$ (3 ml) triethylamine (TEA) was added (0.13 ml), and the resulting solution was cooled to 0 °C in an ice-bath under argon. Pivaloyl chloride (0.115 ml) was added, the resulting mixture was stirred for 30 min and then pyridine (0.3 ml) and 2′-O-acetyl-6-O-methyl-8a-aza-8a-homoerythromycin A (0.25 g, 0.31 mmol) were added. The reaction was stirred for 6 h and during that time it was allowed to warm to room temperature. The reaction was quenched with saturated aqueous NaHCO$_3$ solution (20 ml). CH$_2$Cl$_2$ (20 ml) was added and aqueous layer was extracted with CH$_2$Cl$_2$ (2×10 ml). Combined organic extracts were washed with brine (20 ml), dried over K$_2$CO$_3$ and concentrated *in vacuo*. The brown foamy residue was dissolved in MeOH (15 ml), stirred at room temperature overnight and concentrated to dryness. Column chromatography (eluent CH$_2$Cl$_2$/MeOH/NH$_4$OH 90:5:0.5) afforded the title compound **7** (0.12 g, 41.8%) as a brown-yellow solid.

MS (ES) *m/z*: [M+H]$^+$ 926.9.

HRMS (ES positive): calculated for C$_{46}$H$_{76}$N$_3$O$_{16}$ [M+H]$^+$ 926.5226 found 926.5222.

^{1}H NMR (500 MHz, CDCl$_3$) δ 8.20 (Ph-H), 7.49 (Ph-H), 5.69 (8a-CONH), 5.07 (1″-H), 4.95 (13-H), 4.71 (4″-H), 4.55 (1′-H), 4.38 (5″-H), 4.17 (8-H), 3.99 (3-H), 3.83 (PhCH$_2$-1H), 3.74 (5′-H), 3.73 (PhCH$_2$-1H), 3.68 (5-H), 3.49 (11-H), 3.31 (3″-OCH$_3$), 3.28 (2′-H), 3.16 (6-OCH$_3$), 2.72 (3′-H), 2.70 (2-H), 2.48 [3′-N(CH$_3$)$_2$], 2.39 (2″a-H), 2.29 (10-H), 1.93 (14a-H), 1.93 (4-H), 1.91 (4′a-H), 1.66 (7a-H), 1.63 (2″b-H), 1.54 (7b-H), 1.46 (14b-H), 1.36 (6-CH$_3$), 1.31 (4′b-H), 1.24 (2-CH$_3$), 1.20 (5′-CH$_3$), 1.18 (10-CH$_3$, 5″-CH$_3$), 1.14 (8-CH$_3$), 1.12 (3″-CH$_3$), 1.06 (4-CH$_3$), 1.04 (12-CH$_3$), 0.90 (14-CH$_3$).

^{13}C NMR (125 MHz, DMSO) δ 177.2 (C-1), 174.4 (C-9), 169.9 (4″-OCO), 147.3, 140.9, 130.3, 123.8 (Ph), 102.3 (C-1′), 95.4 (C-1″), 80.3 (C-5), 79.8 (C-4″), 78.8 (C-6), 77.4 (C-3), 77.2 (C-13), 74.3 (C-12), 73.0 (C-3″), 70.8 (C-2′), 70.4 (C-11), 67.9 (C-5′), 65.5 (C-3′), 62.8 (C-5″), 51.8 (6-OCH$_3$), 49.5 (3″-OCH$_3$), 45.4 (C-2), 42.9 (C-7), 42.4 (C-4), 42.2 (C-10), 41.0 (C-8), 41.0 [3′-N(CH$_3$)$_2$], 40.8 (CH$_2$), 35.1 (C-2″), 21.6 (C-14), 11.2 (14-CH$_3$).

4″-O-[(4-nitrophenyl)acetyl]-6-O-ethyl-8a-aza-8a-homoerythromycin A (8)

A solution of (4-nitrophenyl)acetic acid (0.110 g, 0.61 mmol) and TEA (0.086 ml, 0.63 mmol) in CH$_2$Cl$_2$ (5 ml) was cooled to 0 °C under nitrogen. Pivaloyl chloride (0.075 ml, 0.62 mmol) was added and the reaction mixture was stirred for 0.5 h. To a solution of 2′-O-acetyl-6-O-ethyl-8a-aza-8a-homoerythromycin A (0.100 g, 0.12 mmol) in CH$_2$Cl$_2$ (4 ml), pyridine (0.108 ml,

1.34 mmol) and DMAP (0.015 g, 0.12 mmol) were added. The reaction mixture was allowed to slowly warm to room temperature and was stirred for 20 h, then additional amounts of (4-nitrophenyl)acetic acid (0.110 g, 0.61 mmol), TEA (0.086 ml, 0.63 mmol) and pivaloyl chloride (0.075 ml, 0.62 mmol) were added and the mixture was stirred for additional 20 h. The reaction was quenched by addition of saturated aqueous NaHCO$_3$ solution and extracted with CH$_2$Cl$_2$. Combined organic extracts were washed with brine and dried over K$_2$CO$_3$. The solution was concentrated to form a solid that after deprotection in MeOH at room temperature for 48 h gave the crude product. After chromatography on a silica gel column (eluent CH$_2$Cl$_2$/MeOH/NH$_4$OH 90:5:0.5), the title compound **8** was obtained (0.055 g, 48.7%).

MS (ES) *m/z*: [M+H]$^+$ 940.4.

HRMS (ES positive): calculated for C$_{47}$H$_{78}$N$_3$O$_{16}$ [M+H]$^+$ 940.5382 found 940.5355.

^{1}H NMR (500 MHz, CDCl$_3$) δ 8.20 (Ph-2H), 7.51 (Ph-2H), 6.93 (8a-NH), 5.01 (13-H), 4.91 (1″-H), 4.70 (4″-H), 4.44 (1′-H), 4.38 (5″-H), 3.93 (8-H), 3.90 (3-H), 3.82 (Ph-CH$_2$-), 3.64 (5-H), 3.52 (5′-H), 3.50 (11-H), 3.43 (6-OCH$_2$-), 3.30 (3″-OCH$_3$), 3.25 (2′-H), 2.79 (2-H), 2.68 (3′-H), 2.44 [3′-N(CH$_3$)$_2$], 2.40 (2″a-H), 2.35 (10-H), 2.16 (7a-H), 2.10 (4-H), 1.93 (14a-H), 1.86 (4′a-H), 1.65 (7b-H), 1.62 (2″b-H), 1.49 (14b-H), 1.27 (4′b-H), 0.85 (14-CH$_3$).

^{13}C NMR (125 MHz, DMSO) δ 175.3 (C-9), 174.7 (C-1), 170.0 (4″-OCO), 147.3, 141.0, 130.4, 123.8 (Ph), 103.2 (C-1′), 97.6 (C-1″), 82.6 (C-5), 82.1 (C-3), 79.7 (C-4″), 78.9 (C-6), 77.5 (C-13), 74.1 (C-12), 73.1 (C-3″), 71.1 (C-11), 70.9 (C-2′), 68.7 (C-5′), 65.5 (C-3′), 62.8 (C-5″), 58.9 (6-OCH$_2$CH$_3$), 49.5 (3″-OCH$_3$), 45.4 (C-2), 42.4 (C-7), 41.9 (C-8, C-10), 40.9 (CH$_2$), 40.6 [3′-N(CH$_3$)$_2$], 40.4 (C-4), 35.9 (C-2″), 29.7 (C-4′), 21.4 (C-14), 10.8 (14-CH$_3$).

4″-O-[3-(4-nitrophenyl)-2-propenoyl]-8a-aza-8a-homoerythromycin A (9)

The same method was followed as for the synthesis of compound **8** but starting from 2′-O-acetyl-8a-aza-8a-homoerythromycin A (0.5 g, 0.63 mmol) and 4-nitrocinnamic acid (0.61 g, 3.2 mmol) to obtain the title compound **9** (0.190 g, 32.6%) as a white foam.

MS (ES) *m/z*: [M+H]$^+$ 924.4.

HRMS (ES positive): calculated for C$_{46}$H$_{74}$N$_3$O$_{16}$ [M+H]$^+$ 924.5069 found 924.5034.

^{1}H NMR (500 MHz, CDCl$_3$) δ 8.27 (Ph-2H), 7.79 (Ph-CH=CH), 7.70 (Ph-2H), 6.59 (Ph-CH=CH), 5.83 (8a-NH), 5.17 (1″-H), 4.94 (13-H), 4.84 (4″-H), 4.58 (1′-H), 4.42 (5″-H), 4.35 (3-H), 4.20 (8-H), 3.82 (5′-H), 3.58 (5-H), 3.52 (11-H), 3.36 (3″-OCH$_3$, 2′-H), 3.03 (3′-H), 2.65 (2-H), 2.58 [3′-N(CH$_3$)$_2$], 2.43 (2″a-H), 2.37 (10-H), 1.97 (4′a-H), 1.94 (14a-H), 1.91 (4-H), 1.68 (2″b-H), 1.54 (7-2H), 1.45 (14b-H), 1.40 (6-CH$_3$), 0.90 (14-CH$_3$).

^{13}C NMR (125 MHz, DMSO) δ 177.8 (C-1), 176.4 (C-9), 165.8 (4″-OCO), 148.7, 140.4, 128.6, 124.3 (Ph), 142.7, 121.9 (CH=CH), 102.6 (C-1′), 94.8 (C-1″), 82.6 (C-5), 79.6 (C-4″), 76.9 (C-3, C-13), 74.9 (C-12), 74.1 (C-6), 73.3 (C-3″), 70.8 (C-2′), 70.2 (C-11), 68.0 (C-5′), 65.5 (C-3′), 62.9 (C-5″), 49.6 (3″-OCH$_3$), 45.7 (C-2), 43.1 (C-4), 42.5 (C-7), 42.0 (C-10), 40.8 (C-8), 40.2 [3′-N(CH$_3$)$_2$], 35.1 (C-2″), 29.5 (C-4′), 21.8 (C-14), 11.3 (14-CH$_3$).

4″-O-[3-(4-aminophenyl)propanoyl]-8a-aza-8a-homoerythromycin A (10)

Compound **9** (0.17 g, 018 mmol) was dissolved in MeOH (9 ml), 10% Pd/C catalyst (0.017 g) was added and the reaction mixture was stirred at room temperature under H$_2$ (balloon) for 3 h. The mixture was filtered and MeOH was evaporated under reduced pressure yielding the title compound (0.14 g, 87%) as white foam.

After chromatography on a silica gel column (eluent CH$_2$Cl$_2$/MeOH/NH$_4$OH 90:9:0.5) and precipitation from EtOAc/n-hexane, the title compound **10** was obtained (0.078 g, 55.7%) as a white powder.

MS (ES) *m/z*: [M+H]$^+$ 896.4.

HRMS (ES positive): calculated for C$_{46}$H$_{78}$N$_3$O$_{14}$ [M+H]$^+$ 896.5484 found 896.5487.

^{1}H NMR (500 MHz, CDCl$_3$) δ 6.97 (Ph-2H), 6.61 (Ph-2H), 6.23 (8a-NH), 5.13 (1″-H), 4.92 (13-H), 4.68 (4″-H), 4.56 (1′-H), 4.34 (5″-H), 4.33 (3-H),

4.18 (8-H), 3.74 (5′-H), 3.56 (5-H), 3.50 (11-H), 3.37 (3″-OCH₃), 3.17 (2′-H), 2.85 (Ph-C̲H₂CH₂), 2.66-2.55 (Ph-CH₂C̲H₂, 3′-H), 2.35 (2″a-H, 10-H), 2.30 [3′-N(CH₃)₂], 1.92 (4-H), 1.88 (14a-H), 1.67 (4′a-H), 1.60 (2″b-H), 1.53 (7-2H), 1.42 (14b-H), 1.39 (6-CH₃), 0.89 (14-CH₃).

¹³C NMR (125 MHz, DMSO) δ 177.3 (C-1), 176.0 (C-9), 172.1 (4″-OCO), 144.2, 129.7, 128.5, 114.7 (Ph), 101.8 (C-1′), 94.1 (C-1″), 82.3 (C-5), 78.3 (C-4″), 76.5 (C-3), 76.2 (C-13), 74.2 (C-12), 73.3 (C-6), 72.5 (C-3″), 70.0 (C-2′), 69.4 (C-11), 67.5 (C-5′), 65.1 (C-3′), 62.3 (C-5″), 48.8 (3″-OCH₃), 45.1 (C-2), 42.6 (C-4), 41.9 (C-7), 41.0 (C-10), 40.1 (C-8), 39.7 [3′-N(CH₃)₂], 35.7 (CH₂), 34.4 (C-2″), 29.5 (CH₂), 28.3 (C-4′), 21.2 (C-14), 10.8 (14-CH₃).

4″-*O*-[3-(4-nitrophenyl)-2-propenoyl]-6-*O*-methyl-8a-aza-8a-homoerythromycin A (11)

The same method was followed as for the synthesis of compound **8** but starting from 2′-*O*-acetyl-6-*O*-methyl-8a-aza-8a-homoerythromycin A (0.5 g, 0.62 mmol) and 3-(4-nitrophenyl)-2-propenoic acid (0.60 g, 3.1 mmol) to obtain the title compound **11** (36 mg, 6.2%) as a white powder.

MS (ES) *m/z*: [M+H]⁺ 938.4.

HRMS (ES positive): calculated for C₄₇H₇₆N₃O₁₆ [M+H]⁺ 938.5226 found 938.5199.

¹H NMR (500 MHz, CDCl₃) δ 8.27 (Ph-2H), 7.77 (Ph-CH=C̲H), 7.67 (Ph-2H), 6.59 (Ph-C̲H=CH), 5.71 (8a-NH), 5.11 (1″-H), 4.96 (13-H), 4.83 (4″-H), 4.54 (1′-H), 4.45 (5″-H), 4.19 (8-H), 4.00 (3-H), 3.75 (5′-H), 3.70 (5-H), 3.51 (11-H), 3.36 (3″-OCH₃), 3.21 (2′-H), 3.17 (6-OCH₃), 2.71 (2-H), 2.61 (3′-H), 2.44 (2″a-H), 2.36 [3′-N(CH₃)₂], 2.28 (10-H), 1.94 (14a-H), 1.92 (4-H), 1.72 (4′a-H), 1.69 (7a-H), 1.67 (2″b-H), 1.58 (7b-H), 1.47 (14b-H), 1.37 (6-CH₃), 1.27 (4′b-H), 0.90 (14-CH₃).

¹³C NMR (125 MHz, DMSO) δ 177.1 (C-1), 174.4 (C-9), 165.8 (4″-OCO), 148.7, 140.3, 128.7, 124.3 (Ph), 142.8, 121.7 (CH=CH), 102.7 (C-1′), 95.6 (C-1″), 80.3 (C-5), 79.4 (C-4″), 78.9 (C-6), 77.8 (C-3), 77.2 (C-13), 74.3 (C-12), 73.1 (C-3″), 70.9 (C-2′), 70.4 (C-11), 68.2 (C-5′), 65.5 (C-3′), 63.0 (C-5″), 51.8 (6-OCH₃), 49.6 (3″-OCH₃), 45.6 (C-2), 43.0 (C-7), 42.4 (C-10), 42.3 (C-4), 41.0 (C-8), 40.4 [3′-N(CH₃)₂], 35.2 (C-2″), 29.4 (C-4′), 21.6 (C-14), 11.2 (14-CH₃).

4″-*O*-[3-(4-aminophenyl)propanoyl]-8a-aza-8a-homoerythromycin A (12)

The same method was followed as for the synthesis of compound **10** but starting from compound **11** (0.25 g, 0.27 mmol) to obtain the title compound **12** (0.203 g, 81.5%) as a white powder.

MS (ES) *m/z*: [M+H]⁺ 910.5.

HRMS (ES positive): calculated for C₄₇H₈₀N₃O₁₄ [M+H]⁺ 910.5640 found 910.5636.

¹H NMR (500 MHz, CDCl₃) δ 6.98 (Ph-2H), 6.61 (Ph-2H), 5.59 (8a-NH), 5.05 (1″-H), 4.94 (13-H), 4.68 (4″-H), 4.52 (1′-H), 4.34 (5″-H), 4.17 (8-H), 3.97 (3-H), 3.91 (12-OH), 3.71 (5′-H), 3.67 (5-H), 3.50 (11-H), 3.29 (3″-OCH₃), 3.19 (2′-H), 3.16 (6-OCH₃), 2.85 (Ph-C̲H₂CH₂), 2.69-2.55 (Ph-CH₂C̲H₂, 2-H), 2.37 (2″a-H), 2.34 [3′-N(CH₃)₂], 2.27 (10-H), 1.93 (14a-H), 1.88 (4-H), 1.71 (4′a-H), 1.62 (7a-H), 1.57 (7b-H), 1.44 (14b-H), 1.36 (6-CH₃), 0.89 (14-CH₃).

¹³C NMR (125 MHz, DMSO) δ 177.2 (C-1), 174.4 (C-9), 172.7 (4″-OCO), 144.8, 130.2, 129.1, 115.3 (Ph), 102.6 (C-1′), 95.5 (C-1″), 80.2 (C-5), 78.9 (C-6), 78.8 (C-4″), 77.2 (C-3), 77.2 (C-13), 74.4 (C-12), 73.0 (C-3″), 71.0 (C-2′), 70.5 (C-11), 68.1 (C-5′), 65.5 (C-3′), 63.0 (C-5″), 51.8 (6-OCH₃), 49.4 (3″-OCH₃), 45.6 (C-2), 43.1 (C-7), 42.5 (C-10), 42.3 (C-4), 41.1 (C-8), 40.4 [3′-N(CH₃)₂], 36.3 (CH₂), 35.2 (C-2″), 30.1 (CH₂), 29.4 (C-4′), 21.7 (C-14), 11.2 (14-CH₃).

4″-*O*-(3-pyridinyl)acetyl-6-*O*-methyl-8a-aza-8a-homoerythromycin A (13)

The same method was followed as for the synthesis of compound **6** starting from 2′-*O*-acetyl-6-*O*-methyl-8a-aza-8a-homoerythromycin A (1.0 g, 1.24 mmol) and 3-pyridinylacetic acid hydrochloride (0.646 g, 3.72 mmol). Crude product was purified by column chromatography (eluent CH₂Cl₂/

MeOH/NH₄OH 90:3:0.3) to obtain the title compound **13** (0.085 g, 7.9%) as a white solid.

MS (ES) *m/z*: [M+H]⁺ 883.0.

HRMS (ES positive): calculated for C₄₅H₇₆N₃O₁₄ [M+H]⁺ 882.5327 found 882.5348.

¹H NMR (500 MHz, CDCl₃) δ 8.51, 8.49, 7.65, 7.26 (Py), 5.85 (8a-NH), 5.04 (1″-H), 4.92 (13-H), 4.67 (4″-H), 4.49 (1′-H), 4.37 (5″-H), 4.17 (8-H), 3.96 (3-H), 3.70 (5′-H), 3.65 (5-H), 3.62 (Py-C̲H₂-), 3.49 (11-H), 3.27 (3″-OCH₃), 3.15 (2′-H), 3.13 (6-OCH₃), 2.66 (2-H), 2.52 (3′-H), 2.34 (2″a-H), 2.29 [3′-N(CH₃)₂], 2.25 (10-H) 1.91 (4-H, 14a-H), 1.68 (7a-H, 4′a-H), 1.62 (2″b-H), 1.55 (7b-H), 1.47 (14b-H), 1.34 (6-CH₃), 1.31 (5″-CH₃), 1.18 (5′-CH₃, 2-CH₃, 4′b-H), 1.16 (10-CH₃), 1.14 (12-CH₃), 1.09 (8-CH₃), 1.06 (4-CH₃), 0.98 (3″-CH₃), 0.86 (14-CH₃).

¹³C NMR (125 MHz, DMSO) δ 176.8 (C-1), 174.0 (C-9), 170.0 (4″-OCO), 148.5, 148.4, 136.3, 129.0, 123.4 (Py), 102.3 (C-1′), 95.0 (C-1″), 79.8 (C-5), 79.3 (C-4″), 78.5 (C-6), 77.2 (C-3), 76.7 (C-13), 73.9 (C-12), 72.6 (C-3″), 70.4 (C-2′), 70.0 (C-11), 67.8 (C-5′), 65.1 (C-3′), 62.4 (C-5″), 51.4 (6-OCH₃), 49.1 (3″-OCH₃), 45.2 (C-2), 42.6 (C-7), 42.0 (C-4), 41.9 (C-10), 4.0.5 (C-8), 40.0 [3′-N(CH₃)₂], 38.0 (CH₂), 34.8 (C-2″), 28.5 (C-4′), 21.3 (C-14), 10.28 (14-CH₃).

4″-*O*-(3-quinolinyl)carbonyl-6-*O*-methyl-8a-aza-8a-homoerythromycin A (14)

The same method was followed as for the synthesis of compound **6** starting from 2′-*O*-acetyl-6-*O*-methyl-8a-aza-8a-homoerythromycin A (0.09 g, 0.11 mmol) and 3-quinolinecarboxylic acid (0.095 g, 0.55 mmol). Crude product was purified by column chromatography (eluent CH₂Cl₂/MeOH/NH₄OH 90:5:0.5) to obtain the title compound **14** (0.088 g, 87.1%) as a white powder.

MS (ES) *m/z*: [M+H]⁺ 918.4.

HRMS (ES positive): calculated for C₄₈H₇₆N₃O₁₄ [M+H]⁺ 918.5327 found 918.5319.

¹H NMR (500 MHz, CDCl₃) δ 9.41 (Q2-H), 8.83 (Q8-H), 8.19 (Q4-H), 7.94 (Q5-H), 7.87 (Q7-H), 7.66 (Q6-H), 5.85 (8a-NH), 5.16 (1″-H), 5.01 (4″-H), 4.96 (13-H), 4.65 (1′-H), 4.57 (5″-H), 4.20 (8-H), 4.04 (3-H), 3.83 (5′-H), 3.71 (5-H), 3.53 (11-H), 3.41 (3″-OCH₃) 3.21 (2′-H), 3.18 (6-OCH₃), 2.74 (2-H), 2.67 (3′-H), 2.48 (2″a-H), 2.32 (10-H), 1.96 (14a-H), 1.93 (4-H), 1.78 (4′a-H), 1.73 (2″b-H), 1.62 (7a-H), 1.57 (7b-H), 1.47 (14b-H), 1.37 (6-CH₃), 1.25 (2-CH₃, 5″-CH₃), 1.22 (4′b-H), 1.20 (3″-CH₃), 1.18 (10-CH₃), 1.13 (12-CH₃, 8-CH₃, 4-CH₃), 0.94 (5′-CH₃), 0.91 (14-CH₃).

¹³C NMR (125 MHz, DMSO) δ 177.3 (C-1), 174.1 (C-9), 165.0 (4″-OCO), 149.9, 149.7, 138.7, 131.9, 129.5, 128.8, 127.5, 126.6, 122.6 (Q), 102.6 (C-1′), 95.1 (C-1″), 79.9 (C-5), 79.8 (C-4″), 78.6 (C-6), 77.1 (C-3), 77.0 (C-13), 74.1 (C-12), 72.9 (C-3″), 70.7 (C-2′), 70.2 (C-11), 68.1 (C-5′), 65.5 (C-3′), 63.0 (C-5″), 51.7 (6-OCH₃), 49.4 (3″-OCH₃), 45.4 (C-2), 42.8 (C-7), 42.4 (C-4), 42.1 (C-10), 40.7 (C-8), 40.3 [3′N(CH₃)₂], 34.9 (C-2″), 28.9 (C-4′), 21.5 (C-14), 11.1 (14-CH₃).

4″-*O*-[3-(3-quinolinyl)-2-propenoyl]-8a-aza-8a-homoerythromycin A (15)

The same method was followed as for the synthesis of compound **6** starting from 2′-*O*-acetyl-8a-aza-8a-homoerythromycin A (0.498 g, 0.63 mmol) and 3-(3-quinolinyl)-2-propenoic acid (0.627 g, 3.15 mmol). Crude product was purified by column chromatography (eluent CH₂Cl₂/MeOH/NH₄OH 90:5:0.5) to obtain the title compound **15** (0.250 g, 42.7%) as a yellow solid.

MS (ES) *m/z*: [M+H]⁺ 930.6.

HRMS (ES positive): calculated for C₄₉H₇₆N₃O₁₄ [M+H]⁺ 930.5327 found 930.5315.

¹H NMR (500 MHz, CDCl₃) δ 9.10 (Q2), 8.25 (Q4), 8.11 (Q8), 7.90 (Q5), 7.89 (Q-C̲H=CH), 7.78 (Q7), 7.61 (Q6), 6.68 (Q-CH=C̲H), 6.06 (8a-NH), 5.18 (1″-H), 4.94 (13-H), 4.86 (4″-H), 4.61 (1′-H), 4.45 (5″-H), 4.38 (3-H), 4.20 (8-H), 3.87 (5′-H), 3.62 (5-H), 3.52 (11-H), 3.35 (3″-OCH₃), 3.24 (2′-H), 2.68 (3′-H), 2.66 (2-H), 2.65 (6-OCH₃), 2.43 (2″a-H), 2.41 [3′-N(CH₃)₂], 2.37 (10-H), 1.94 (4-H), 1.91 (14a-H), 1.83 (4′a-H), 1.69 (2″b-H), 1.60 (7a-H), 1.53 (7b-H), 1.44 (14b-H), 1.41 (6-CH₃), 1.29 (4′b-H), 1.22-1.18 (8-CH₃,

5′-CH₃, 5″-CH₃, 2-CH₃, 3″-CH₃ and 10-CH₃), 1.11 (4-CH₃), 1.10 (12-CH₃), 0.91 (14-CH₃).

^{13}C NMR (125 MHz, DMSO) δ 177.4 (C-1), 176.2 (C-9), 165.9 (4″-OCO), 148.3, 148.3, 141.9, 135.7, 130.5, 129.0, 127.3, 127.3, 126.8 (Q), 128.2, 118.9 (-CH=CH-), 102.0 (C-1′), 94.3 (C-1″), 82.4 (C-5), 78.9 (C-4″), 76.9 (C-3), 76.5 (C-13), 74.4 (C-12), 73.6 (C-6), 72.9 (C-3″), 70.2 (C-2′), 69.7 (C-11), 67.7 (C-5′), 65.4 (C-3′), 62.6 (C-5″), 49.2 (3″-OCH₃), 45.3 (C-2), 42.7 (C-4), 42.1 (C-7), 41.4 (C-10), 40.3 [3′N(CH₃)₂], 40.0 (C-8), 35.7 (C-2″), 29.0 (C-4′), 21.4 (C-14), 11.0 (14-CH₃).

4″-*O*-[3-(3-quinolinyl)-2-propenoyl]-6-*O*-methyl-8a-aza-8a-homoerythromycin A (16)

The same method was followed as for the synthesis of compound **6** starting from 2′-*O*-acetyl-6-*O*-methyl-8a-aza-8a-homoerythromycin A (0.500 g, 0.62 mmol) and 3-(3-quinolinyl)-2-propenoic acid (0.740 g, 3.72 mmol). Crude product was purified by column chromatography (eluent CH₂Cl₂/MeOH/NH₄OH 90:5:0.5) to obtain the title compound **16** (0.420 g, 71.8%) as a yellow solid.

MS (ES) *m/z*: [M+H]⁺ 945.1.

HRMS (ES positive): calculated for C₅₀H₇₈N₃O₁₄ [M+H]⁺ 944.5484 found 944.5480.

^{1}H NMR (500 MHz, CDCl₃) δ 9.11 (Q2-H), 8.24 (Q4-H), 8.12 (Q8-H), 7.89 (Q-CH=CH), 7.87 (Q5-H), 7.78 (Q7-H), 7.61 (Q6-H), 6.71 (Q-CH=CH), 5.69 (8a-NH), 5.11 (1″-H), 4.97 (13-H), 4.85 (4″-H), 4.56 (1′-H), 4.47 (5″-H), 4.19 (8-H), 4.01 (3-H), 3.79 (5′-H), 3.71 (5-H), 3.52 (11-H), 3.37 (3″-OCH₃), 3.20 (2′-H), 3.18 (6-OCH₃), 2.71 (2-H), 2.61 (3′-H), 2.45 (2″a-H), 2.35 [3′-N(CH₃)₂], 2.27 (10-H), 1.93 (14a-H), 1.74 (4′a-H), 1.69 (7a-H), 1.69 (2″b-H), 1.59 (7b-H), 1.47 (14b-H), 1.38 (6-CH₃), 1.29 (4′b-H), 1.24 (2-CH₃), 1.23 (5′-CH₃), 1.20 (5″-CH₃), 1.19 (3″-CH₃), 1.18 (10-CH₃), 1.13 (12-CH₃), 1.13 (8-CH₃), 1.11 (4-CH₃), 0.90 (14-CH₃).

^{13}C NMR (125 MHz, DMSO) δ 177.1 (C-1), 174.4 (C-9), 166.2 (4″-OCO), 148.7, 148.7, 136.1, 130.9, 129.5, 128.4, 127.7, 127.6, 127.2 (Q), 142.4, 119.3 (-CH=CH-) 102.8 (C-1′), 95.6 (C-1″), 80.3 (C-5), 79.2 (C-4″), 78.9 (C-6), 77.8 (C-3), 77.2 (C-13), 74.3 (C-12), 73.1 (C-3″), 70.9 (C-2′), 70.4 (C-11), 68.3 (C-5′), 65.6 (C-3′), 63.1 (C-5″), 51.8 (6-OCH₃), 49.6 (3″-OCH₃), 45.6 (C-2), 43.0 (C-7), 42.4 (C-4, C-10), 41.0 (C-8), 40.4 [3′-N(CH₃)₂], 35.2 (C-2″), 29.4 (C-4′), 21.4 (C-14), 11.2 (14-CH₃).

4″-*O*-[3-(3-quinolinyl)-2-propenoyl]-6-*O*-ethyl-8a-aza-8a-homoerythromycin A (17)

The same method was followed as for the synthesis of compound **6** starting from 2′-*O*-acetyl-6-*O*-ethyl-8a-aza-8a-homoerythromycin A (0.100 g, 0.12 mmol) and 3-(3-quinolinyl)-2-propenoic acid (0.146 g, 0.73 mmol). Crude product was purified by column chromatography (eluent CH₂Cl₂/MeOH/ NH₄OH 90:5:0.5) to obtain the title compound **17** (0.044 g, 38.3%).

MS (ES) *m/z*: [M+H]⁺ 958.5.

HRMS (ES positive): calculated for C₅₁H₈₀N₃O₁₄ [M+H]⁺ 958.5640 found 958.5671.

^{1}H NMR (500 MHz, CDCl₃) δ 9.11 (Q2-H), 8.31 (Q4-H), 8.11 (Q8-H), 7.94 (Q-CH=CH), 7.91 (Q5-H), 7.78 (Q7-H), 7.61 (Q6-H), 6.78 (Q-CH=CH), 5.01 (13-H), 4.96 (1″-H), 4.87 (4″-H), 4.49 (5″-H), 4.47 (1′-H), 3.93 (3-H, 8-H), 3.69 (5′-H), 3.51 (11-H), 3.41 (6-OCH₂-), 3.35 (3″-OCH₃), 3.24 (2′-H), 2.82 (2-H), 2.47 (2″a-H), 1.93 (14a-H), 1.70 (2″b-H), 1.48 (14b-H), 0.86 (14-CH₃).

^{13}C NMR (125 MHz, DMSO) δ 175.3 (C-1), 175.2 (C-9), 166.4 (4″-OCO), 149.0, 148.7, 136.0, 130.9, 129.4, 128.6, 127.6, 127.6, 127.1 (Q), 146.7, 119.0 (CH=CH), 103.1 (C-1′), 97.6 (C-1″), 82.5 (C-5), 82.1 (C-3), 79.0 (C-4″), 78.9 (C-6), 77.5 (C-13), 74.1 (C-12), 73.3 (C-3″), 71.0 (C-2′), 70.9 (C-11), 68.7 (C-5′), 65.4 (C-3′), 63.1 (C-5″), 53.4 (6-OCH₂CH₃), 49.6 (3″-OCH₃), 45.4 (C-2), 42.4 (C-7), 42.0 [3′-N(CH₃)₂], 41.9 (C-8), 40.6 (C-4, C-10), 35.9 (C-2″), 29.7 (C-4′), 21.4 (C-14), 15.4 (6-OCH₂CH₃) 10.8 (14-CH₃).

4″-*O*-[3-(3-quinolinyl)-2-propenoyl]-6-*O*-allyl-8a-aza-8a-homoerythromycin A (18)

The same method was followed as for the synthesis of compound **6** starting from 2′-*O*-acetyl-6-*O*-allyl-8a-aza-8a-homoerythromycin A (0.320 g, 0.39 mmol) and 3-(3-quinolinyl)-2-propenoic acid (0.260 g, 1.31 mmol). Crude product

was purified by column chromatography (eluent CH₂Cl₂/MeOH/NH₄OH 90:5:0.5) to obtain the title compound **18** (0.230 g, 61.6%) as a yellowish solid.

MS (ES) *m/z*: [M+H]⁺ 970.7.

HRMS (ES positive): calculated for C₅₂H₇₉N₃O₁₄ [M+H]⁺ 970.7813 found 970.7842.

^{1}H NMR (500 MHz, DMSO) δ 9.28 (s, Q2-H), 8.73 (s, Q4-H), 8.05 (d, Q8-H), 8.00 (d, Q5-H), 7.89 (d, Q-CH=CH), 7.84 (t, Q7-H), 7.68 (t, Q6-H), 6.94 (d, Q-CH=CH), 6.05 (m, 6-OCH₂CHCH₂), 5.77 (s, 8a-NH), 4.98 (d, 1″-H), 4.91 (m, 13-H, 6-OCH₂CHCH₂), 4.78 (d, 4″-H), 4.48 (d, 1′-H), 4.45 (q, 5″-H), 4.02 (m, 8-H), 3.94 (m, 3-H, 6-OCH₂CHCH₂), 3.80 (m, 11-H), 3.62 (d, 5-H), 3.39 (s, 5′-H), 3.35 (s, 3″-OCH₃), 3.08 (t, 2′-H), 2.72 (m, 2-H), 2.61 (m, 3′-H), 2.44 (d, 2″a-H), 2.42 (d, 10-H), 2.29 [s, 3′-N(CH₃)₂], 2.03 (m, 4-H), 1.83 (m, 14a-H), 1.82 (d, 2″b-H), 1.78 (d, 4′a-H), 1.75 (d, 7a-H), 1.40 (m, 14b-H), 1.22 (s, 6-CH₃), 1.13 (5″-CH₃, 3″-CH₃), 1.12 (5′-CH₃), 1.11 (2-CH₃), 1.06 (12-CH₃), 1.02 (4-CH₃), 1.00 (8-CH₃), 0.98 (10-CH₃), 0.83 (14-CH₃).

^{13}C NMR (125 MHz, DMSO) δ 177.2 (C-1), 172.7 (C-9), 165.8 (4″-OCO), 149.6, 147.9, 136.0, 130.8, 128.8, 128.2, 128.7, 127.4, 127.2, 126.9 (Q), 142.2, 119.3 (-CH=CH-), 140.0 (6-OCH₂CH=CH₂), 113.2 (6-OCH₂CH=CH₂), 102.2 (C-1′), 94.5 (C-1″), 79.4 (C-6), 78.5 (C-5), 78.3 (C-4″), 75.9 (C-3), 75.8 (C-13), 74.1 (C-12), 72.4 (C-3″), 71.3 (C-5′), 70.6 (C-2′), 67.0 (C-11), 65.3 (6-OCH₂CH=CH₂), 64.6 (C-3′), 62.5 (C-5″), 49.0 (3″-OCH₃), 44.7 (C-2), 41.7 (C-7), 41.6 (C-4), 40.4 [3′-N(CH₃)₂, C-8, C-10], 34.1 (C-2″), 30.5 (C-4′), 21.2 (C-14), 11.1 (14-CH₃).

4″-*O*-[3-(3-quinolinyl)propanoyl]-6-*O*-methyl-8a-aza-8a-homoerythromycin A (19)
4″-*O*-[3-(1,2,3,4-tetrahydro-3-quinolinyl)propanoyl]-6-*O*-methyl-8a-aza-8a-homoerythromycin A (20)

To a solution of compound **16** (0.061 g, 0.065 mmol) in EtOH (8 ml) HOAc-AcONa buffer (pH 5) was added dropwise to a pH value of 6.5. Then catalyst 10% Pd/C (0.025 g) was added and the reaction mixture was stirred under hydrogen pressure of 1.4 bar for 4 h. The catalyst was filtered off and the filtrate was evaporated under reduced pressure. The residue was partition between water (10 ml) and CH₂Cl₂ (5 ml), the organic layer was separated and the aqueous was extracted with a fresh aliquot of CH₂Cl₂. The combined organic extracts were dried over Na₂SO₄ and evaporated to yield a mixture of the title compounds (0.054 g).

Purification by column chromatography (eluent CH₂Cl₂/MeOH/NH₄OH 90:9:0.5) afforded the title compounds **19** (0.014 g, 23.1%) and **20** (0.031 g, 50.8%).

Compound **19**

TLC *R*f=0.69 (eluent CH₂Cl₂/MeOH/NH₄OH 90:9:1.5).

MS (ES) *m/z*: [M+H]⁺ 946.6.

HRMS (ES positive): calculated for C₅₀H₈₀N₃O₁₄ [M+H]⁺ 946.5640 found 946.5630.

^{1}H NMR (500 MHz, CDCl₃) δ 8.80 (Q2-H), 8.07 (Q8-H), 7.99 (Q4-H), 7.76 (Q5-H), 7.68 (Q7-H), 7.54 (Q6-H), 5.62 (8a-NH), 5.05 (1″-H), 4.94 (13-H), 4.69 (4″-H), 4.49 (1′-H), 4.34 (5″-H), 4.17 (8-H), 3.96 (3-H), 3.93 (12-OH), 3.67 (5′-H), 3.65 (5″-H), 3.50 (11-H), 3.27 (3″-OCH₃), 3.18 (2′-H), 3.15 (Q-CH₂CH₂-, 6-OCH₃), 2.79 (Q-CH₂CH₂-), 2.68 (2-H), 2.61 (3′-H), 2.36 (2″a-H), 2.35 [3′-N(CH₃)₂], 2.26 (10-H), 1.93 (14a-H), 1.90 (4-H), 1.71 (4′a-H), 1.58 (2″b-H), 1.44 (14b-H), 1.27 (4′b-H), 1.18 (2-CH₃, 10-CH₃), 1.13 (5′-CH₃), 1.12 (8-CH₃), 1.05 (5″-CH₃, 4-CH₃), 0.88 (14-CH₃).

^{13}C NMR (125 MHz, DMSO) δ 176.1 (C-1), 173.3 (C-9), 171.0 (4″-OCO), 150.4, 146.0, 133.6, 131.9, 128.2, 128.0, 127.0, 126.4, 125.9 (Q), 101.5 (C-1′), 94.4 (C-1″), 79.1 (C-5), 78.2 (C-4″), 77.8 (C-6), 76.5 (C-3), 76.1 (C-13), 73.3 (C-12), 71.9 (C-3″), 69.8 (C-2′), 69.4 (C-11), 67.0 (C-5′), 64.4 (C-3′), 61.8 (C-5″), 50.8 (6-OCH₃), 48.5 (3″-OCH₃), 44.5 (C-2), 42.0 (C-7), 41.4 (C-10), 41.2 (C-4), 40.0 (C-8), 39.3 [3′N(CH₃)₂], 34.3 (CH₂), 34.1 (C-2″), 28.7 (C-4′), 27.2 (CH₂), 20.6 (C-14), 10.1 (14-CH₃).

Compound **20**

TLC *R*f=0.81 (eluent CH₂Cl₂/MeOH/NH₄OH 90:9:1.5).

MS (ES) *m/z*: [M+H]⁺ 950.7.

142

HRMS (ES positive): calculated for $C_{50}H_{84}N_3O_{14}$ [M+H]$^+$ 950.5954 found 950.5949.

^{1}H NMR (500 MHz, CDCl$_3$) δ 6.96 (THQ6-H), 6.92 (THQ8-H), 6.60 (THQ7-H), 6.49 (THQ5-H), 5.60 (8a-NH), 5.06 (1''-H), 4.94 (13-H), 4.70 (4''-H), 4.55 (1'-H), 4.35 (5''-H), 4.17 (8-H), 3.99 (3-H), 3.73 (5'-H), 3.68 (5-H), 3.50 (11-H), 3.34 (THQ-CH$_2$CH$_2$-), 3.31 (3''-OCH$_3$), 3.26 (2'-H), 3.16 (6-OCH$_3$), 2.97 (THQ-CH$_2$CH$_2$-), 2.84 (THQ3-H), 2.69 (2-H), 2.48 (THQ2-2H), 2.38 (2''a-H), 2.27 (10-H), 1.93 (14a-H), 1.91 (4-H), 1.73 (THQ4-2H, 4'a-H), 1.65 (2''b-H), 1.62 (7a-H), 1.56 (7b-H), 1.45 (14b-H), 1.27 (4'b-H), 0.89 (14-CH$_3$).

^{13}C NMR (125 MHz, DMSO) δ 177.1 (C-1), 174.3 (C-9), 173.1 (4''-OCO), 144.2, 129.5, 126.8, 120.0, 117.0, 113.9 (THQ), 102.2 (C-1'), 95.3 (C-1''), 80.1 (C-5), 78.7 (C-6), 78.6 (C-4''), 76.9 (C-3, C-13), 74.2 (C-12), 72.9 (C-3''), 70.8 (C-2'), 70.3 (C-11), 67.8 (C-5') 65.3 (C-3'), 62.9 (C-5''), 51.8 (6-OCH$_3$), 49.4 (3''-OCH$_3$), 46.6 (CH$_2$), 46.5 (CH$_2$), 45.4 (C-2), 42.9 (C-7), 42.4 (C-10), 42.1 (C-4), 40.9 (C-8), 40.9 [3'N(CH$_3$)$_2$], 35.0 (C-2''), 33.3 (THQ, C-4'), 28.4 (THQ), 21.5 (C-14), 11.1 (14-CH$_3$).

4''-O-[3-(1,2,3,4-tetrahydro-3-quinolinyl)propanoyl]-8a-aza-8a-homoerythromycin A (21)

A similar method was followed as for the synthesis of compound **10** but starting from compound **15** (0.06 g, 0.065 mmol) and at 2 bar pressure to obtain the title product **21** (0.027 g, 44.6%).

MS (ES) m/z: [M+H]$^+$ 936.4.

HRMS (ES positive): calculated for $C_{49}H_{82}N_3O_{14}$ [M+H]$^+$ 936.5797 found 936.5782.

^{1}H NMR (500 MHz, DMSO) δ 7.80 (8a-NH), 6.83 (THQ6-H), 6.80 (THQ8-H), 6.41 (THQ7-H), 6.39 (THQ5-H), 5.66 (THQ1-NH), 4.96 (1''-H), 4.84 (13-H), 4.52 (4''-H), 4.38 (1'-H), 4.34 (5''-H), 4.14 (3-H), 4.10 (2'-OH), 3.97 (12-OH), 3.92 (8-H), 3.66 (5'-H), 3.49 (11-H), 3.38 (5-H), 3.24 (3''-OCH$_3$), 3.20 (THQ4-2H), 3.05 (2'-H), 2.79 (THQ2a-H), 2.72 (THQ2b-H), 2.62 (2-H), 2.42 (THQ-CH$_2$CH$_2$, 10-H), 2.41 (3'-H), 2.35 (THQ3-H), 2.30 (2''a-H), 2.23 [3'-N(CH$_3$)$_2$], 1.97 (4-H), 1.78 (14a-H), 1.68 (2''b-H), 1.62 (4'a-H), 1.57 (THQ-CH$_2$CH$_2$), 1.54 (7a-H), 1.34 (14b-H), 1.27 (7b-H), 1.24 (6-CH$_3$), 0.80 (14-CH$_3$).

^{13}C NMR (125 MHz, DMSO) δ 177.7 (C-1), 175.0 (C-9), 173.2 (4''-OCO), 145.3, 129.4, 126.8, 119.4, 115.6, 113.5 (THQ), 102.7 (C-1'), 94.3 (C-1''), 82.4 (C-5), 78.6 (C-4''), 77.0 (C-3), 76.2 (C-13), 75.1 (C-12), 73.8 (C-6), 72.9 (C-3''), 71.2 (C-11), 70.9 (C-2'), 67.4 (C-5'), 65.2 (C-3'), 62.6 (C-5''), 49.4 (3''-OCH$_3$), 46.1 (THQ), 45.2 (C-2), 42.7 (C-4), 41.2 (C-7), 40.9 [3'-N(CH$_3$)$_2$], 39.6 (C-8), 34.7 (C-2''), 33.3 (THQ), 31.8 (CH$_2$), 31.3 (THQ), 30.7 (C-4'), 28.6 (CH$_2$), 21.9 (C-14), 11.7 (14-CH$_3$).

4''-O-[3-(4-quinolinyl)-2-propenoyl]-6-O-methyl-8a-aza-8a-homoerythromycin A (22)

The same method was followed as for the synthesis of compound **6** starting from 2'-O-acetyl-6-O-methyl-8a-aza-8a-homoerythromycin A (0.050 g, 0.062 mmol) and 3-(4-quinolinyl)-2-propenoic acid (0.062 g, 0.31 mmol). Crude product was purified by column chromatography (eluent CH$_2$Cl$_2$/MeOH/NH$_4$OH 90:5:0.5) to obtain the title compound **22** (0.030 g, 51.3%) as a yellow solid.

MS (ES) m/z: [M+H]$^+$ 944.7.

HRMS (ES positive): calculated for $C_{50}H_{78}N_3O_{14}$ [M+H]$^+$ 944.5484 found 944.5475.

^{1}H NMR (500 MHz, CDCl$_3$) δ 8.97 (Q2-H), 8.50 (Q-CH=CH), 8.17 (Q8-H), 8.16 (Q7-H), 7.79 (Q7-H), 7.65 (Q6-H), 7.54 (Q3-H), 6.67 (Q-CH=CH), 5.66 (8a-NH), 5.12 (1''-H), 4.96 (13-H), 4.87 (4''-H), 4.55 (1'-H), 4.46 (5''-H), 4.17 (8-H), 4.02 (3-H), 3.78 (5'-H), 3.71 (5-H), 3.51 (11-H), 3.37 (3''-OCH$_3$), 3.23 (2'-H), 3.18 (6-OCH$_3$), 2.71 (2-H), 2.68 (3'-H), 2.46 (2''a-H), 2.37 [3'-N(CH$_3$)$_2$], 2.27 (10-H), 1.93 (4-H), 1.93 (14a-H), 1.76 (4'a-H), 1.70 (2''b-H), 1.67 (7a-H), 1.56 (7b-H), 1.47 (14b-H), 1.37 (6-CH$_3$), 1.29 (4'b-H), 1.23 (5'-CH$_3$), 1.20 (2-CH$_3$, 3''-CH$_3$, 5''-CH$_3$), 1.19 (10-CH$_3$), 1.13 (8-CH$_3$, 12-CH$_3$), 1.10 (4-CH$_3$), 0.90 (14-CH$_3$).

^{13}C NMR (125 MHz, DMSO) δ 177.4 (C-1), 174.4 (C-9), 166.3 (4''-OCO), 149.1, 148.7, 135.9, 130.9, 129.3, 128.9, 127.7, 127.6, 127.0 (Q), 142.7, 118.9 (CH=CH), 101.8 (C-1'), 95.3 (C-1''), 80.2 (C-5), 79.0 (C-4''), 78.7 (C-6), 77.3

(C-13), 77.0 (C-3), 74.4 (C-12), 73.2 (C-3''), 70.9 (C-2'), 70.4 (C-11), 67.4 (C-5'), 65.6 (C-3'), 63.2 (C-5''), 51.9 (6-OCH$_3$), 49.6 (3''-OCH$_3$), 45.4 (C-2), 42.8 (C-7), 42.6 (C-10), 42.1 (C-4), 41.1 (C-8), 40.5 [3'-N(CH$_3$)$_2$], 35.0 (C-2''), 29.7 (C-4'), 21.7 (C-14), 11.2 (14-CH$_3$).

4''-O-[4-(3-quinolinyl)-3-butenoyl]-6-O-methyl-8a-aza-8a-homoerythromycin A (23)

The same method was followed as for the synthesis of compound **8** but starting from 2'-O-acetyl-6-O-methyl-8a-aza-8a-homoerythromycin A (0.07 g, 0.09 mmol) and 4-(3-quinolinyl)-3-butenoic acid (0.132 g, 0.62 mmol). Crude product was purified by column chromatography (eluent EtOAc/MeOH 7:3) to obtain the title compound **23** (0.038 g, 44.1%) as a white solid.

MS (ES) m/z: [M+H]$^+$ 958.5.

HRMS (ES positive): calculated for $C_{51}H_{80}N_3O_{14}$ [M+H]$^+$ 958.5640 found 958.5640.

^{1}H NMR (500 MHz, DMSO) δ 8.99 (Q2-H), 8.10 (Q8-H), 8.07 (Q4-H), 7.81 (Q5-H), 7.70 (Q7-H), 7.55 (Q6-H), 6.72 (Q-CH=CH), 6.55 (Q-CH=CH), 5.60 (8a-NH), 5.08 (1''-H), 4.96 (13-H), 4.77 (4''-H), 4.58 (1'-H), 4.40 (5''-H), 4.17 (8-H), 4.01 (3-H), 3.78 (5'-H), 3.71 (5-H), 3.50 (11-H), 3.38 (OCOCH$_2$), 3.36 (3''-OCH$_3$), 3.19 (6-OCH$_3$), 2.71 (2-H), 2.48 [3'-N(CH$_3$)$_2$], 2.43 (2''a-H), 2.29 (10-H), 1.95 (14a-H), 1.93 (4-H), 1.67 (2''b-H), 1.62 (7a-H), 1.54 (7b-H), 1.47 (14b-H), 1.38 (6-CH$_3$), 0.91 (14-CH$_3$).

^{13}C NMR (125 MHz, DMSO) δ 177.1 (C-1), 174.3 (C-9), 170.9 (4''-OCO), 148.9, 147.4, 132.4, 129.5, 129.3, 129.1, 127.9, 127.8, 127.0 (Q), 130.7, 123.8 (-CH=CH-) 102.6 (C-1'), 95.3 (C-1''), 80.1 (C-5), 79.2 (C-4''), 78.7 (C-6), 76.9 (C-3, C-13), 74.2 (C-12), 73.0 (C-3''), 70.8 (C-2'), 70.3 (C-11), 67.8 (C-5'), 65.4 (C-3'), 62.8 (C-5''), 51.8 (6-OCH$_3$), 49.4 (3''-OCH$_3$), 45.3 (C-2), 42.8 (C-7), 42.4 (C-10), 42.0 (C-4), 40.9 (C-8), 40.4 [3'-N(CH$_3$)$_2$], 38.1 (CH$_2$), 35.0 (C-2''), 29.6 (C-4'), 21.5 (C-14), 11.1 (14-CH$_3$).

4''-O-[4-(3-quinolinyl)butanoyl]-6-O-methyl-8a-aza-8a-homoerythromycin A (24)

The same method was followed as for the synthesis of compound **6** starting from 2'-O-acetyl-6-O-methyl-8a-aza-8a-homoerythromycin A (0.10 g, 0.12 mmol) and 4-(3-quinolinyl)butanoic acid (0.13 g, 0.60 mmol). The crude product was purified by column chromatography (eluent EtOAc/MeOH 8:2) to give the title compound **24** (0.028 g, 38.3%) as a yellow solid.

MS (ES) m/z: [M+H]$^+$ 960.5.

HRMS (ES positive): calculated for $C_{51}H_{82}N_3O_{14}$ [M+H]$^+$ 960.5796 found 960.5784.

^{1}H NMR (500 MHz, CDCl$_3$) δ 8.78 (Q2, s, 1H), 8.07 (Q8, d, 1H), 7.97 (Q4, d, 1H), 7.81 (Q5, d, 1H), 7.67 (Q7, m, 1H), 7.54 (Q6, m, 1H), 5.51 (8a-NH, d, 1H), 5.07 (1-H, d, 1H), 4.93 (13-H, dd, 1H), 4.70 (4-H, d, 1H), 4.56 (1'-H, d, 1H), 4.27 (5-H, dq, 1H), 4.13 (8-H, m, 1H), 3.99 (3-H, dd, 1H), 3.70 (5'-H, m, 1H), 3.67 (5-H, d, 1H), 3.46 (11-H, s, 1H), 3.38 (2'-H, m, 1H), 3.30 (3-OCH$_3$, s, 3H), 3.16 (6-OCH$_3$, s, 3H), 2.89 (CH$_2$, m, 2H), 2.68 (2-H, dq, 1H), 2.50, 2.37 (CH$_2$, m, 2H), 2.39 (2a-H, d, 1H), 2.28 (10-H, q, 1H), 2.09 (CH$_2$, m, 2H), 196-1.88 (14a-H, 4-H, m, 2H), 1.64 (2b-H, dd, 1H), 1.57 (7a-H, t, 1H), 1.49-1.43 (7b-H, 14b-H, m, 2H), 0.89 (14-CH$_3$, t, 3H).

4''-O-[5-(3-quinolinyl)-4-pentenoyl]-8a-aza-8a-homoerythromycin A (25)

A solution of 4-pentenoic acid (0.25 ml, 2.4 mmol) and TEA (0.7 ml, 5.1 mmol) in CH$_2$Cl$_2$ (20 ml) was cooled to 0 °C under argon. Pivaloyl chloride (0.6 ml, 4.9 mmol) was added and the reaction mixture was stirred for 0.5 h. To a solution of 2'-O-acetyl-8a-aza-8a-homoerythromycin A (0.5 g, 0.63 mmol) in CH$_2$Cl$_2$ (4 ml), pyridine (0.80 ml, 9.90 mmol) and DMAP (0.08 g, 0.63 mmol) were added. The reaction mixture was allowed to slowly warm to room temperature and then stirred for 2 h. Water (30 ml) was added and pH was adjusted to 4 using 2 M HCl. The residue was partitioned between water and CH$_2$Cl$_2$, and the pH was adjusted to 9 using 2 M NaOH. The organic phase was concentrated to yield an oily residue, which was dissolved in MeOH (110 ml) and stirred at room temperature for 30 h. The MeOH was evaporated and the residue was purified by column chromatography on a silica gel (eluent CH$_2$Cl$_2$/MeOH/NH$_4$OH 90:9:0.5). The 4''-O-(4-pentenoyl)-8a-aza-8a-homoerythromycin A (0125 g, 0.15 mmol) that was obtained was dissolved in DMF

(1.5 ml). Into this solution Pd(II), acetate (2.4 mg) and tri-*o*-tolylphosphine (6.4 mg) were added and the mixture stirred under argon for 20 min. To the solution, 3-bromoquinoline (0.022 ml, 0.15 mmol) and TEA (0.029 ml, 2.1 mmol) were added and the reaction mixture was stirred at 80 °C for 38 h. The mixture was partitioned between water and EtOAc, and evaporation of the organic phase resulted in solid product. Column chromatography (eluent EtOAc/n-hexane/diethylamine 5:5:1) afforded the title compound **25** (0.097 g, 67.4%).

MS (ES) *m/z*: [M+H]$^+$ 958.0.

HRMS (ES positive): calculated for $C_{51}H_{80}N_3O_{14}$ [M+H]$^+$ 958.5640 found 958.5606.

^{1}H NMR (500 MHz, CDCl$_3$) δ 8.94 (Q2-H), 8.06 (Q8-H), 8.00 (Q4-H), 7.78 (Q5-H), 7.67 (Q7-H), 7.54 (Q6-H), 6.60 (-C<u>H</u>=CH), 6.48 (Q-CH=C<u>H</u>), 6.18 (8a-NH), 5.14 (1″-H), 4.92 (13-H), 4.73 (4″-H), 4.57 (1′-H), 4.37 (5″-H), 4.35 (3-H), 4.19 (8-H), 4.17 (8-OH), 3.79 (5′-H), 3.58 (5-H), 3.50 (11-H), 3.30 (3″-OCH$_3$), 2.66-2.55 (2xCH$_2$), 2.39 (2″a-H), 2.37 (10-H), 1.92 (4-H), 1.62 (2″b-H), 1.57 (7a-H), 1.53 (7b-H), 0.90 (14-CH$_3$).

^{13}C NMR (125 MHz, DMSO) δ 177.8 (C-1), 176.6 (C-9), 172.4 (4″-OCO), 149.1, 147.3, 132.0, 130.0, 129.2, 129.1, 127.9, 127.8, 126.8 (Q), 130.8, 128.0 (CH=CH), 102.1 (C-1′), 94.6 (C-1″), 82.8 (C-5), 79.1 (C-4″), 77.2 (C-3), 77.0 (C-13), 74.7 (C-12), 73.9 (C-6), 73.1 (C-3″), 70.5 (C-2′), 70.0 (C-11), 67.9 (C-5′), 65.7 (C-3′), 62.7 (C-5″), 49.4 (3″-OCH$_3$), 45.6 (C-2), 43.0 (C-4), 42.4 (C-7), 41.7 (C-10), 40.6 (C-8), 40.3 [3′-N(CH$_3$)$_2$], 35.0 (C-2″), 33.8, 28.5 (<u>CH$_2$-CH$_2$</u>), 29.7 (C-4′), 21.8 (C-14), 11.3 (14-CH$_3$).

4″-O-[5-(3-quinolinyl)-4-pentenoyl]-6-O-methyl-8a-aza-8a-homoerythromycin A (26)

The same method was followed as for the synthesis of compound **25** but starting from 2′-O-acetyl-6-O-methyl-8a-aza-8a-homoerythromycin A (0.300 g, 0.36 mmol). Column chromatography (eluent EtOAc/MeOH 7:3) afforded the title compound **26** (0.060 g, 17.1%) as a white solid.

MS (ES) *m/z*: [M+H]$^+$ 972.0.

HRMS (ES positive): calculated for $C_{52}H_{82}N_3O_{14}$ [M+H]$^+$ 972.5797 found 972.5793.

^{1}H NMR (500 MHz, CDCl$_3$) δ 8.94 (Q, d, 1H), 8.06 (Q, d, 1H), 8.00 (Q, s, 1H), 7.78 (Q, d, 1H), 7.67 (Q, t, 1H), 7.53 (Q, t, 1H), 6.61 (Q-C<u>H</u>=CH, d, 1H), 6.47 (Q-CH=C<u>H</u>, m, 1H), 5.64 (8a-NH, d, 1H), 5.08 (1-H, d, 1H), 4.94 (13-H, dd, 1H), 4.73 (4″-H, d, 1H), 4.55 (1′-H, d, 1H), 4.36 (5-H, dq, 1H), 4.17 (8-H, m, 1H), 3.99 (3-H, d, 1H), 3.74 (5′-H, m, 1H), 3.69 (5-H, d, 1H), 3.49 (11-H, s, 1H), 3.31 (3-OCH$_3$, s, 3H), 3.24 (2′-H, dd, 1H), 3.16 (6-OCH$_3$, s, 3H), 2.70-2.53 (2-H, 3′-H, 2xCH$_2$,ov, 6H), 2.40 [3′-N(CH$_3$)$_2$, s, 6H] 2.38 (2a-H, d, 1H), 2.28 (10-H, q, 1H), 1.95-1.89 (14a-H, 4-H, 4′a-H, ov, 3H), 1.63 (7a-H, 2b-H, ov, 2H), 1.54 (7b-H, d, 1H), 1.45 (14b-H, m, 1H), 0.89 (14-CH$_3$, t, 3H).

^{13}C NMR (125 MHz, DMSO) δ 177.3 (C-1), 174.3 (C-9), 172.4 (4″-OCO), 149.1, 147.3, 132.1, 130.1, 129.2, 129.1, 128.0, 127.8, 127.0 (Q), 130.7, 128.3 (-CH=CH-), 102.3 (C-1′), 95.4 (C-1″), 80.1 (C-5), 78.9 (C-4″), 78.8 (C-6), 77.3 (C-3), 77.2 (C-13), 74.3 (C-12), 73.0 (C-3″), 70.9 (C-2′), 70.4 (C-11), 67.9 (C-5′), 65.4 (C-3′), 62.9 (C-5″), 51.9 (6-OCH$_3$), 49.5 (3″-OCH$_3$), 45.5 (C-2), 43.0 (C-7), 42.4 (C-10), 42.3 (C-4), 41.0 (C-8), 40.4 [3′-N(CH$_3$)$_2$], 35.1 (C-2″), 33.8, 29.4 (-<u>CH$_2$</u>CH=CH<u>CH$_2$</u>-), 30.0 (C-4′), 21.7 (C-14), 11.2 (14-CH$_3$).

4″-O-[5-(3-quinolinyl)-3-pentenoyl]-6-O-methyl-8a-aza-8a-homoerythromycin A (27)

The same method was followed as for the synthesis of compound **6** starting from 2′-O-acetyl-6-O-methyl-8a-aza-8a-homoerythromycin A (0.050 g, 0.06 mmol) and 5-(3-quinolinyl)-3-pentenoic acid (0.042 g, 0.18 mmol). The crude product was purified by column chromatography (eluent EtOAc/MeOH 7:3) to give the title compound **27** (0.027 g, 46.2%) as a white powder.

MS (ES) *m/z*: [M+H]$^+$ 972.0.

HRMS (ES positive): calculated for $C_{52}H_{82}N_3O_{14}$ [M+H]$^+$ 972.5797 found 972.5792.

^{1}H NMR (500 MHz, CDCl$_3$) δ 8.77 (Q, s, 1H), 8.08 (Q, d, 1H), 7.94 (Q, d, 1H), 7.77 (Q, d, 1H), 7.68 (Q, m, 1H), 7.54 (Q, m, 1H), 5.82, 5.72 (CH=CH, m, 2H) 5.62 (8a-NH, d, 1H), 5.07 (1-H, d, 1H), 4.94 (13-H, dd, 1H), 4.69 (4-H, d, 1H), 4.53 (1′-H, d, 1H), 4.33 (5-H, dq, 1H), 4.15 (8-H, m, 1H), 3.98 (3-H, br d, 1H), 3.73 (5′-H, m, 1H), 3.62 (5-H, d, 1H), 3.59 (CH$_2$, d, 2H) 3.49 (11-H, s, 1H), 3.28 (2′-H, ov, 1H), 3.28 (3-OCH$_3$, s, 3H), 3.22, 3.10 (CH$_2$, m, 2H), 3.16 (6-OCH$_3$, s, 3H), 2.68 (2-H, dq, 1H), 2.40 [3′-N(CH$_3$)$_2$, s, 6H] 2.38 (2a-H, d, 1H), 2.28 (10-H, q, 1H), 1.95-1.90 (14a-H, 4-H, 4′a-H, ov, 3H), 1.65-1.61 (7a-H, 2b-H, ov, 2H), 1.54 (7b-H, d, 1H), 1.47 (14b-H, m, 1H), 0.89 (14-CH$_3$, t, 3H).

^{13}C NMR (125 MHz, DMSO) δ 177.3 (C-1), 174.3 (C-9), 171.4 (4″-OCO), 151.8, 146.9, 134.7, 132.5, 129.1, 128.9, 128.1, 127.4, 126.7 (Q), 132.4, 124.0 (-CH$_2$CH=CHCH$_2$-Q), 102.1 (C-1′), 95.3 (C-1″), 80.0 (C-5), 79.2 (C-4″), 79.0 (C-6), 77.2 (C-3, C-13), 74.3 (C-12), 73.0 (C-3″), 70.8 (C-2′), 70.4 (C-11), 67.7 (C-5′), 65.4 (C-3′), 62.9 (C-5″), 51.9 (6-OCH$_3$), 49.5 (3″-OCH$_3$), 45.4 (C-2), 42.9 (C-7), 42.4 (C-4), 42.2 C-10), 41.0 (C-8), 40.3 [3′-N(CH$_3$)$_2$], 37.6, 36.1 (-<u>CH$_2$</u>CH=CH<u>CH$_2$</u>-Q), 35.0 (C-2″), 31.0 (C-4′), 21.6 (C-14), 11.2 (14-CH$_3$).

4″-O-[5-(3-quinolinyl)pentanoyl]-6-O-methyl-8a-aza-8a-homoerythromycin A (28)

The same method was followed as for the synthesis of compound **8** but starting from 2′-O-acetyl-6-O-methyl-8a-aza-8a-homoerythromycin A (0.100 g, 0.12 mmol) and 5-(3-quinolinyl)pentanoic acid (0.141 g, 0.6 mmol). The crude product was purified by column chromatography (eluent EtOAc/MeOH 7:3) to obtain the title compound **28** (0.022 g, 18.8%) as a white solid.

MS (ES) *m/z*: [M+H]$^+$ 974.0.

HRMS (ES positive): calculated for $C_{52}H_{84}N_3O_{14}$ [M+H]$^+$ 974.5953 found 974.5956.

^{1}H NMR (500 MHz, CDCl$_3$) δ 8.77 (Q, d, 1H), 8.07 (Q, d, 1H), 7.94 (Q, s, 1H), 7.78 (Q, d, 1H), 7.66 (Q, m, 1H), 7.53 (Q, m, 1H), 5.51 (8a-NH, d, 1H), 5.06 (1-H, d, 1H), 4.92 (13-H, dd, 1H), 4.69 (4-H, d, 1H), 4.59 (1′-H, d, 1H), 4.25 (5-H, m, 1H), 4.12 (8-H, m, 1H), 4.00 (3-H, d, 1H), 3.78 (5′-H, m, 1H), 3.69 (5-H, d, 1H), 3.45 (11-H, s, 1H), 3.41 (2′-H, m, 1H), 3.28 (3-OCH$_3$, s, 3H), 3.16 (6-OCH$_3$, s, 3H), 2.84 (CH$_2$, t, 2H), 2.67 (2-H, m, 1H), 2.47, 2.30 (CH$_2$, m, 2H), 2.38 (2a-H, d, 1H), 2.27 (10-H, q, 1H), 1.95-1.88 (14a-H, 4-H, m, 2H), 1.78 (2x CH$_2$, m, 4H), 1.63 (2b-H, dd, 1H), 1.57 (7a-H, t, 1H), 1.49-1.40 (7b-H, 14b-H, m, 2H), 0.88 (14-CH$_3$, t, 3H).

4″O-[3-(3-quinolinyl)-2-propenoyl]-6-O-methyl-8a-aza-8a-homoerythromycin A 11,12-cyclic carbonate (29)

The same method was followed as for the synthesis of compound **6** starting from 2′-O-acetyl-6-O-methyl-8a-aza-8a-homoerythromycin A 11,12-cyclic carbonate (0.950 g, 1.14 mmol) and 3-(3-quinolinyl)-2-propenoic acid (1.36 g, 6.8 mmol). Crude product was purified by column chromatography (eluent CH$_2$Cl$_2$/MeOH/NH$_4$OH 90:3:0.3) to obtain the title compound **29** (0.850 g, 76.8%) as a pale yellow solid.

MS (ES) *m/z*: [M+H]$^+$ 970.9.

HRMS (ES positive): calculated for $C_{51}H_{76}N_3O_{15}$ [M+H]$^+$ 970.5277 found 970.5264.

^{1}H NMR (500 MHz, CDCl$_3$) δ 9.11, 8.26, 8.12, 7.92, 7.78, 7.61 (Q), 7.89 (Q-CH=C<u>H</u>-), 6.75 (Q-C<u>H</u>=CH-), 5.04 (1″-H), 4.96 (13-H), 4.87 (4″-H), 4.59 (1′-H), 4.45 (11-H), 4.42 (5″-H), 4.02 (3-H), 4.07 (8-H), 3.67 (5′-H), 3.63 (5-H), 3.38 (3″-OCH$_3$), 3.18 (6-OCH$_3$), 2.76 (2-H), 2.46 (2″a-H), 2.39 (10-H), 2.39 [3′-N(CH$_3$)$_2$], 1.92 (4-H), 1.87 (14a-H), 1.85 (4′a-H), 1.85 (7a-H), 1.71 (2″b-H), 1.60 (14b-H), 1.55 (7b-H), 1.45 (12-CH$_3$), 1.36 (4′b-H), 1.35 (6-CH$_3$), 1.30 (10-CH$_3$), 1.26 (2-CH$_3$), 1.22 (5″-CH$_3$), 1.21 (5′-CH$_3$), 1.15 (8-CH$_3$, 3″-CH$_3$), 1.01 (4-CH$_3$), 0.92 (14-CH$_3$).

^{13}C NMR (125 MHz, DMSO) δ 176.1 (C-1), 169.8 (C-9), 165.7 (4″-OCO), 152.9 (C=O cyclic carbonate), 148.2, 148.1, 135.5, 130.3, 128.8, 127.8, 127.1, 127.0, 126.6 (Q), 141.9, 118.7 (CH=CH), 102.3 (C-1′), 95.4 (C-1″), 85.1 (C-12), 81.7 (C-11), 79.6 (C-5), 79.0 (C-6), 78.5 (C-4″), 76.7 (C-3), 75.2 (C-13), 76.3 (C-3), 72.5 (C-3″), 70.3 (C-2′), 68.1 (C-5′), 64.8 (C-3′), 62.6 (C-5″), 51.3 (6-OCH$_3$), 49.1 (3″-OCH$_3$), 45.1 (C-2), 41.7 (C-7), 41.6 (C-8), 41.5 (C-4), 41.5 (C-10), 39.7 [3′-N(CH$_3$)$_2$], 34.7 (C-2″), 28.4 (C-4′), 22.0 (C-14), 10.0 (14-CH$_3$).

1 Morimoto, S., Takahashi, Y., Watanabe, Y. & Ōmura, S. Chemical modification of erythromycins. I. Synthesis and antibacterial activity of 6-*O*-methylerythromycin A. *J. Antibiot.* **37,** 187–189 (1984).
2 Djokic, S., Kobrehel, G., Lazarevski, G., Lopotar, N. & Tamburašev, Z. Erythromycin Series. Part 11. Ring Expansion of Erythromycin A Oxime by the Beckmann Rearrangement. *J. Chem. Soc. Perkin Trans. I* **1986,** 1881–1890 (1986).
3 Djokic, S. *et al.* Erythromycin series. Part13. Synthesis, structure elucidation of 10-dihydro-10-deoxo-11-methyl-11-azaerythromycin A. *J. Chem. Research (S)* **1988,** 152–153 (1988).
4 Neue, H. C. The crisis in antibiotic resistance. *Science* **257,** 1064–1073 (1992).
5 Alidhodzic, S. *et al.* Synthesis and antibacterial activity of isomeric 15-membered azalides. *J. Antibiot.* **59,** 753–769 (2006).
6 Fernandes, P. B., Baker, W. R., Freiberg, L. A., Hardy, D. J. & Mcdonald, E. J. New macrolides active against *Streptococcus pyogenes* with inducible or constitutive type of macrolide-lincosamide-streptogramin B resistance. *Antimicrob. Agents Chemother.* **33,** 78–81 (1989).
7 Djokic, S., Kobrehel, G. & Lazarevski, G. Erythromycin series. XII. Antibacterial *in vitro* evaluation of 10-dihydro-10-deoxo-11-azaerythromycin A: synthesis and structure-activity relationship of its acyl derivatives. *J. Antibiot.* **40,** 1006–1015 (1987).
8 Pretsch, E., Clerc, T., Seibl, J. & Simon, W. Tabellen zur Strukturaufklärung organischer Verbindungen mit spektroskopischen Methoden. p H205##(Springer-Verlag, Berlin, Heidelberg, New York, 1976).
9 Wilkening, R. R. *et al.* The synthesis of novel 8a-aza-8a-homoerythromycin derivatives *via* the Beckmann rearrangement of 9(Z)-erythromycin A oxime. *Bioorg. Med. Chem. Lett.* **3,** 1287–1292 (1993).
10 Baker, W. R., Clark, J. D., Stephens, R. L. & Kim, K. H. Modification of macrolide antibiotics. Synthesis of 11-deoxo-11-(carboxyamino)-6-*O*-methyl-erythromycin A 11,12-(cyclic esters) *via* an intramolecular Michael reaction of *O*-carbamates with an alpha, beta-unsaturated ketone. *J. Org. Chem.* **53,** 2340–2345 (1988).
11 Methods for dilution antimicrobial susceptibility tests for bacteria that grow aerobically, Approved standard 5th Ed. NCCLS, M7-A5: 20 (2).

npg

ORIGINAL ARTICLE

Antimycin A-induced cell death depends on AIF translocation through NO production and PARP activation and is not involved in ROS generation, cytochrome *c* release and caspase-3 activation in HL-60 cells

Masaki Ogita[1], Akira Ogita[2], Yoshinosuke Usuki[3], Ken-ichi Fujita[1] and Toshio Tanaka[1]

A respiratory inhibitor, antimycin A (AA), induced an apoptotic-like cell death characterized by nuclear and DNA fragmentation in human leukemia HL-60 cells. This cell death was significantly restricted by a nitric oxide synthase (NOS) inhibitor, N^G-monomethyl-L-arginine (L-NMMA), and a poly(ADP-ribose) polymerase (PARP) inhibitor, 5-aminoisoquinoline (AIQ). Indeed, NO production and PARP overactivation were detected in the cells treated with AA. On the one hand, L-NMMA partly eliminated NO production and on the other, AIQ and L-NMMA also restricted PARP activation. Excessive signals related to PARP overactivation induce the translocation of an apoptosis-inducing factor (AIF) from the mitochondria to the nuclei, resulting in DNA fragmentation. In AA-treated cells, the nuclear translocation of AIF occurred. This translocation was restricted by pretreatment with AIQ and L-NMMA. Although pretreatment with ascorbic acid eliminated the reactive oxygen species (ROS) generation induced by the blockade of complex III by AA, the pretreatment did not protect the cells from AA-induced cell death. Furthermore, cytochrome *c* release or caspase-3 activation was not observed in the cells treated with AA. These results suggest that AA-induced cell death does not depend on respiratory inhibition and the succeeding cascades, but on NO production, PARP overactivation and AIF translocation.
The Journal of Antibiotics (2009) 62, 145–152; doi:10.1038/ja.2009.2; published online 20 February 2009

INTRODUCTION

Antimycin A (AA) inhibits mitochondrial electron transport at complex III,[1] thereby inhibiting respiration. The blockade of electron transport causes a collapse of the proton gradient across the mitochondrial inner membrane. This decreases mitochondrial membrane potential. It also induces the generation of reactive oxygen species (ROS).[2] Both respiratory inhibition and ROS generation are reported to cause cell death in several mammalian cell lines, including mouse leukemia P388, mouse melanoma B16, human oral epidermoid carcinoma KB, human colon adenocarcinoma COLO201 and porcine renal proximal tubule LLC-PK$_1$ cells.[3–6] Most of the cases of cell death induced by AA are classified as being a result of necrosis. However, there are few reports concerning the AA-induced apoptosis of LLC-PK$_1$ and human leukemia HL-60 cells.[4,7] Although it was reported that AA promotes DNA fragmentation and nuclear and cellular disintegrations in HL-60 cells,[4] the detailed mechanism of AA-induced apoptosis has been unclear. The proliferation of respiration-deficient rho0 cells of HL-60 is possible.[8] This mutant generally lacks cytochrome *b* of complex III and various subunits of cytochrome *c* oxidase in addition to F$_1$F$_0$-ATPase.[8] In addition, HL-60 cells are viable, independent of respiration. Therefore, it is unlikely that AA-induced apoptosis depends on respiratory inhibition caused by AA and the succeeding cascades. On the other hand, we recently found that AA-induced cell death accompanied with nuclear and DNA fragmentation and without cellular disintegration did not depend on the release of cytochrome *c* or the activation of caspase-3. In addition to these events, we also found that a nonspecific inhibitor of nitric oxide synthase (NOS), N^G-monomethyl-L-arginine (L-NMMA), and an inhibitor of poly(ADP-ribose) polymerase (PARP) activation, 5-amino-isoquinoline (AIQ), significantly restricted AA-induced cell death.

[1]Department of Biology and Geosciences, Graduate School of Science, Osaka City University, Sumiyoshi-ku, Osaka, Japan; [2]Research Center for Urban Health and Sports, Osaka City University, Sumiyoshi-ku, Osaka, Japan and [3]Department of Molecular Materials Science, Graduate School of Science, Osaka City University, Sumiyoshi-ku, Osaka, Japan
Correspondence: Dr K-i Fujita, Department of Biology and Geosciences, Graduate School of Science, Osaka City University, 3-3-138 Sugimoto, Sumiyoshi-ku, Osaka 558-8585, Japan.
E-mail: kfujita@sci.osaka-cu.ac.jp
Received 2 December 2008; revised 27 December 2008; accepted 13 January 2009; published online 20 February 2009

Nitric oxide (NO) is formed from L-arginine and oxygen by NOS. Cytokines and stimuli, such as bacterial lipopolysaccharides induce NOS in macrophages, including HL-60 cells, which generally differentiate into macrophages in the presence of phorbol 12-myristate 13-acetate. There are many reports related to drug-induced NO production in HL-60 cells.[9,10] In addition, NO-induced apoptosis of HL-60 cells has also been reported.[11,12]

PARP is an abundant nuclear enzyme that is activated by DNA strand breaks or kinks.[13–15] Activated PARP consumes nicotinamide adenine dinucleotide (NAD^+) to transfer poly(ADP-ribose) to specific acceptor proteins.[16,17] PARP activation contributes to DNA repair enzymes and then prevents chromatid exchange.[16,18,19] However, excessive PARP activation can also promote cell death when extensive DNA damage occurs, as in inflammation and ischemia.[17,20] The phenomena in such cell death pathways include mitochondrial depolarization, mitochondrial permeability transition and the release of apoptosis-inducing factor (AIF) from the mitochondria. AIF is released from the mitochondria and moves to the nucleus and then triggers nuclear DNA fragmentation.

In this report, we focus on PARP-mediated cascades to clarify the biochemical process of AA-induced apoptotic-like cell death in HL-60 cells and also discuss the association of free radicals, including reactive oxygen and/or nitrogen species, produced by AA with apoptotic promotion.

MATERIALS AND METHODS

Cell culture
The HL-60 cell line was earlier obtained from the American Type Culture Collection (Manassas, VA, USA).[21] HL-60 cells were cultured in RPMI 1640 medium supplemented with 10% fetal bovine serum along with L-glutamine, penicillin and streptomycin at 37 °C in humidified air containing 5% CO_2. The cells were subcultured twice a week, and only those in the exponential growth phase were used in the following experiments.

Antibodies and chemicals
The antibodies used were obtained from commercial sources as follows: anti-cytochrome *c* (BD Pharmingen, Franklin Lakes, NJ, USA); anti-actin (Sigma, St Louis, MO, USA); anti-AIF (H-300) and anti-PARP-1 (F-2) (Santa Cruz Biotechnology, Santa Cruz, CA, USA); anti-mouse IgG (Promega Corporation, Madison, WI, USA); and anti-rabbit IgG (Bio-Rad, Hercules, CA, USA). AA, puromycin, eukaryotic protease inhibitor cocktail, A23187, thapsigargin, Fluo3-AM, L-NMMA and AIQ were obtained from Sigma. Ac-DEVD-MCA as a caspase-3 substrate, Boc-VLK-MCA as a calpain substrate and Z-LL-H as a calpain inhibitor were obtained from Peptide Institute Inc. (Osaka, Japan). Alamar blue dye was obtained from Diagnostic Systems Inc. (Webster, TX, USA).

Cytotoxicity
Cytotoxicity was determined using Alamar blue assay, as described earlier.[22] Briefly, cells (10^6 cells/ml) were pretreated in quadruplicate in 96-well flat-bottom tissue-culture plates with or without an antioxidant, such as ascorbic acid, for 1 h. After pretreatment, AA was added to the culture and the cells were then incubated for 24 h. After incubation with AA, Alamar blue dye was added to the culture and the cells were further incubated for another 4–8 h. Fluorescence was detected using a Tecan GENios (Männedorf, Switzerland; excitation wavelength at 530 nm, emission wavelength at 590 nm).

Measurement of ROS generation level
Cellular ROS generation was examined by a method dependent on intracellular deacylation and oxidation of 2′,7′-dichlorodihydrofluorescein-diacetate (DCFH-DA) to the fluorescent compound 2′,7′-dichlorofluorescein (DCF).[23] Briefly, exponentially growing cells (10^6 cells/ml) were washed twice with glucose-free modified Gey's buffer (MGB; 145 mM NaCl, 5 mM KCl, 1 mM

Na_2HPO_4, 10 mM HEPES, 1 mM $CaCl_2$, 1 mM $MgSO_4$, pH 7.4) and then stained in MGB with 20 μM DCFH-DA. The stained cells were incubated for 1 h. After incubation, the cells were washed with MGB. The washed cells were treated with AA or H_2O_2 for 1 h. Fluorescence derived from DCF was detected using a Tecan GENios (excitation wavelength at 488 nm, emission wavelength at 525 nm).

Fluorescence staining of the nuclei
Cells (10^6 cells/ml) were cultured with or without drugs for 24 h. The cells were washed with phosphate-buffered saline (PBS). The washed cells were fixed with 1% glutaraldehyde in PBS for 1 h and then washed with PBS twice. The fixed cells were stained with 1 mM Hoechst 33258 in PBS for 5 min. The stained cells were observed under an Olympus fluorescence microscope (Hamburg, Germany) (excitation wavelength at 365 nm, emission wavelength at 420 nm).

Analysis of oligonucleosomal DNA fragmentation
Oligonucleosomal DNA fragmentation was analyzed using a slightly modified agarose gel electrophoresis method, as described earlier.[21] Cells (10^6 cells/ml) were cultured with or without drugs for 24 h. The cells were digested with 50 mM Tris-HCl buffer (pH 7.8) containing 10 mM EDTA, 0.5% SDS and 100 μg ml^{-1} proteinase K at 37 °C for 12 h. DNA was extracted with chloroform/phenol/isoamylalcohol (25:24:1, v/v), precipitated with 0.5 M NaCl/ethanol (1:1, v/v) and then electrophoresed on a 2% agarose gel. DNA fragments were stained with ethidium bromide.

Preparation of cytosolic fraction for detection of cytochrome *c* and AIF release
Cytochrome *c* and AIF release from the mitochondria was detected by western blot analysis using LAS1000 (Fujifilm, Tokyo, Japan). Cells (10^6 cells/ml) were cultured with or without AA in six-well flat-bottom tissue culture plates for 24 h. After cultivation, the cells were washed with a buffer containing 30 mM Tris, 75 mM sucrose, 20 mM glucose, 5 mM KH_2PO_4, 40 mM KCl, 0.5 mM EDTA and 3 mM $MgCl_2$. The cells were lysed by adding 10 μM digitonin for 10 min on ice. The cell lysates were incubated with a eukaryotic protease inhibitor cocktail at 1:1000 volume of the lysates at 37 °C for 7 min. After incubation, the supernatant was harvested by centrifugation at 350 *g* for 3 min at 4 °C. SDS-polyacrylamide gel electrophoresis (PAGE) and western blot analysis were performed using standard protocols.

Caspase-3 and calpain assays
Caspase-3 and calpain activities were measured using fluorometric assays in which the fluorogenic synthetic peptides, Ac-DEVD-MCA and Boc-VLK-MCA, were used as substrates, respectively. Cells (10^6 cells/ml) were cultured with or without drugs in 48-well flat-bottom tissue culture plates for 24 h. After the cultivation, the collected cells were washed with PBS. The pellets were re-suspended in 20 mM HEPES-KOH buffer (pH 6.8) with 250 mM sucrose, 50 mM KCl, 2.5 mM $MgCl_2$ and 1 mM dithiothreitol on ice for 10 min. The cells were lysed by adding 10 μM digitonin for 10 min on ice. The cell lysates were incubated with 14 μM Ac-DEVD-MCA in 100 mM Tris-HCl buffer (pH 7.5) or Boc-VLK-MCA in the same buffer containing 2 mM $CaCl_2$ and 5 mM β-mercaptoethanol at 37 °C for 1 h. Fluorescence intensity was measured using a Tecan GENios (excitation wavelength at 380 nm, emission wavelength at 460 nm). One unit of enzyme activity was defined as the cleavage of 1 pmol of each substrate per minute.

Elevation of intracellular Ca^{2+} level
The rate of Ca^{2+} release was estimated by flow cytometry in which the fluorogenic dye, fluo-3 AM, was used. Cells (10^6 cells/ml) were cultured with 1 mg ml^{-1} fluo-3 AM in 48-well flat-bottom tissue culture plates for 30 min. After incubation, the collected cells were suspended in RPMI 1640 medium containing 6 mM EGTA (ethylene glycol bis(β-aminoethylether)-*N,N,N′,N′*,-tetraacetic acid) and 50 μM β-mercaptoethanol. The fluorescence intensity of each cell was measured using FACS Calibur, LSR (BD, Franklin Lakes, NJ, USA). Measurement of intracellular Ca^{2+} level was started after adding 500 μl of 6 mM EGTA. After a 30-s flow, the sample was added to 20 μl of 5 μM A23187, and the measurement was restarted.

Measurement of NO production level

Intracellular NO production level was determined by fluorometric assay using a NO assay kit (Dojindo Laboratories, Kumamoto, Japan). The principle of this kit is described as follows: NO is oxidized to NO_2^- and NO_3^- in water. The reaction of 2,3-diaminonaphthalene with NO_2^- forms the fluorescent product, 1-(H)-napthotriazole. The fluorescence derived from 1-(H)-napthotriazole is measured (excitation wavelength at 360 nm, emission wavelength at 460 nm). In this kit, NO_3^- is converted into NO_2^- by reductase. Therefore, it is possible to estimate the total NO level using this kit. Cells (10^6 cells/ml) were incubated with or without drugs in 96-well flat-bottom tissue culture plates for 24 h, and 80 µl of the culture was then used for the assay.

Preparation of nuclear fraction for detection of AIF and PARP

Cells (10^6 cells/ml) were washed in cold PBS and suspended in 400 µl of ice-cold hypotonic buffer (10 mM HEPES/KOH, pH 7.9, 2 mM $MgCl_2$, 0.1 mM EDTA, 10 mM KCl, 1 mM dithiothreitol, 0.5 mM PMSF (phenylmethylsulfonyl fluoride) and 1% (v/v) eukaryotic protease inhibitor cocktail) for 10 min on ice. The suspension was vortexed and centrifuged at 15 000 g for 30 s at 4 °C. The supernatant was discarded and the cell pellet was gently re-suspended in 100 µl of ice-cold saline buffer (50 mM HEPES/KOH (pH 7.9), 50 mM KCl, 300 mM NaCl, 0.1 mM EDTA, 10% glycerol, 1 mM DTT, 0.5 mM PMSF, 1% (v/v) eukaryotic protease inhibitor cocktail) on ice for 20 min. The cell suspension was vortexed and centrifuged at 15 000 g for 5 min at 4 °C. The supernatant was stored at −70 °C as a nuclear lysate.

Determination of intracellular NAD^+ level

The NAD^+ concentration was determined as described with a slight modification.[24] Briefly, 10^6 cells were re-suspended in 100 µl of 0.5 M perchloric acid. The obtained cell extracts were neutralized with equal volumes of 1 M KOH and 0.33 M KH_2PO_4/K_2HPO_4 (pH 7.5). After centrifugation, to remove the $KClO_4$ precipitate, 200 µl of NAD^+ reaction mixture (600 mM ethanol, 0.5 mM 3-[4,5 dimethylthiazol-2-yl]-2,5 diphenyltetrazolium bromide, 2 mM phenazine ethosulfate, 5 mM EDTA, 1 mg ml^{-1} bovine serum albumin, 120 mM bicine at pH 7.8) was added to 50 µl of the supernatant or NAD^+ standard, and the mixture was incubated for 5 min at 37 °C. Alcohol dehydrogenase (25 µl) was added to the reaction mixture and the resulting mixture was incubated for 20 min at 37 °C. To stop the reaction, 250 µl of 12 mM iodoacetate was added, and the optical density was then read at 570 nm.

Measurement of intracellular ATP level

Intracellular ATP level was determined by luminescence assay using D-luciferin and luciferase (Toyo Ink, Tokyo, Japan). Cells (10^6 cells/ml) were incubated with or without drugs for 24 h in 96-well flat-bottom tissue culture plates. After incubation, the washed cells were suspended in PBS and 100 µl of luminous dye was then added. After 10 min, the luminescence was detected using a Tecan GENios.

Analysis of membrane potential

The fluorescent stain rhodamine 123 was used as a probe to assess the mitochondrial membrane potential of living HL-60 cells. Membrane potential analysis was described earlier.[25] Cells were treated with 50 µg ml^{-1} AA or 25 µM carbonyl cyanide m-chlorophenylhydrazone (CCCP) for 24 h.

Statistical analysis

Values represent means ± s.d. of at least three independent experiments, unless otherwise indicated.

RESULTS

Cytotoxicity of AA and AA-induced ROS generation in HL-60 cells

After exposure to AA for 24 h, the cells showed a dose-dependent cytotoxicity against AA at concentrations higher than 3 µg ml^{-1} (Figure 1a). In addition, at the concentrations of 0.2–3 µg ml^{-1}, AA also showed a weak cytotoxicity. The IC_{50} of AA was 10 µg ml^{-1}. This IC_{50} was considered to be higher than those of AA in other cell lines, such as P388 B16, and KB.[3] ROS generation was evaluated as DCFH-DA oxidation. This probe was highly reactive with hydrogen peroxide and has been used in evaluating ROS generation in mammalian cells.[23] AA and all the antioxidants tested did not directly react with DCFH-DA (data not shown). In addition, pretreatment of the cells with all the antioxidants tested did not result in ROS generation (Figure 1b). The exposure of HL-60 cells to AA for 1 h induced ROS generation mainly as hydrogen peroxide (Figure 1b). Antioxidants restrict the oxidative damage to cellular components caused by ROS. Indeed, pretreatment with a hydrophilic ascorbic acid prevented nearly all the AA-induced ROS generation (Figure 1b). Other antioxidants, such as α-tocopherol and N-acetyl cysteine, showed no effect. On the other hand, pretreatment with ascorbic acid hardly altered the cytotoxicity of AA (Figure 1c).

AA-induced apoptotic-like cell death of HL-60 cells

In AA-treated cells, nuclear fragmentation, chromatin condensation and formation of apoptotic bodies were observed, as well as in those treated with a typical apoptotic inducer, puromycin, which inhibits cytoplasmic protein synthesis (Figure 1e). Although the puromycin-treated cells showed cellular disintegration, most of the AA-treated cells did not show such effects. Oligonucleosomal DNA fragments were also detected in the DNA fraction extracted from AA-treated cells (Figure 1d).

Cytochrome c release from the mitochondria and caspase-3 activity

AA did not activate caspase-3 (Figure 2a). Interestingly, the activity of caspase-3 was significantly lower than that in the case of the drug-free control. On the other hand, puromycin activated caspase-3.

CCCP, which induces the depolarization of mitochondrial inner membrane, apparently caused the release of cytochrome c. In the case of AA treatment, the level of cytochrome c release from the mitochondria was similar to that in the control (Figure 2b).

Intracellular Ca^{2+} level and calpain activity

In a positive control, a calcium ionophore, A23187, induced a massive increase in intracellular Ca^{2+} level immediately after its addition (data not shown). On the other hand, AA slightly increased intracellular Ca^{2+} level after 24-h incubation (Figure 2c). This observation indicates that AA is not merely a calcium ionophore rather it promotes a slight Ca^{2+} release by a mechanism different from that of A23187.

The activation of calpains is also stimulated by endoplasmic reticulum (ER) stress by Ca^{2+} release into the cytosol.[7] Thapsigargin, which is an ER Ca^{2+}-ATPase inhibitor, increased calpain activity (Figure 2d). In addition, AA significantly increased calpain activity. Furthermore, pretreatment with the calpain inhibitor, Z-LL-H, significantly suppressed the AA-induced increase in calpain activity (Figure 2d). However, pretreatment with the inhibitor did not decrease the cytotoxicity of AA (Figure 2e).

NO production

In the pretreatment with L-NMMA, which is a nonspecific inhibitor of NOS, a four-fold increase in the IC_{50} of AA was observed, indicating that the cytotoxicity of AA was significantly restricted by pretreatment with L-NMMA (Figure 3a). Moreover, we detected NO production in AA-treated cells (Figure 3b). AA did not directly react with 2,3-diaminonapthalene as a probe for NO detection (data not shown). In addition, pretreatment with L-NMMA decreased the NO production level of AA-treated cells by 55%. On the other hand, a slight decrease in NO production level was observed in AA-treated cells pretreated with N-acetyl cysteine.
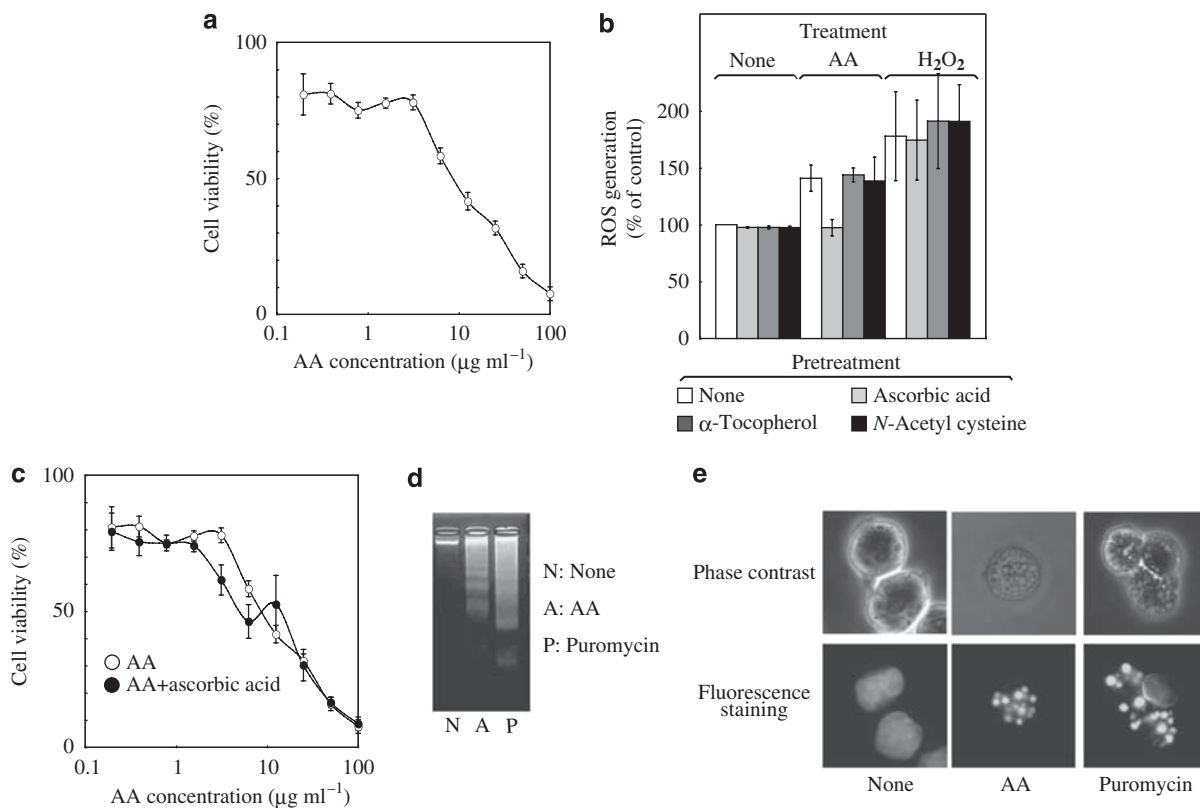
Figure 1 Effects of AA on HL-60 cells. (a) Cytotoxicity of AA. After the treatment of HL-60 cells with AA for 24 h, cytotoxicity was evaluated using Alamar blue assay. (b) ROS generation induced by AA. HL-60 cells were pretreated with or without 25 μM of each antioxidant for 1 h. Addition of no drug (None), 50 μg ml^{-1} AA (AA) or 10 μg ml^{-1} hydrogen peroxide (H$_2$O$_2$) into the culture was carried out, and the cells were further incubated for 1 h before the measurement of ROS generation level. ROS generation was defined as 100% in the control experiment, in which incubation was carried out without antioxidant and AA. (c) Cytotoxicity of AA under a suppressed condition of ROS. HL-60 cells were pretreated with 0 or 25 μM ascorbic acid for 1 h. After pretreatment, AA was added to the culture and the cells were then incubated for 24 h. Cytotoxicity was evaluated using Alamar blue assay. (d) Oligonucleosomal DNA fragmentation induced by AA. HL-60 cells were treated with 50 μg ml^{-1} AA or 10 μg ml^{-1} puromycin for 24 h. (e) Nuclear fragmentation induced by AA. HL-60 cells were treated for 24 h with 50 μg ml^{-1} AA or 10 μg ml^{-1} puromycin. The fluorescence staining of nuclei was performed using 200 μM Hoechst 33258 for 5 min.

Detection of AIF release and cleaved PARP-1

Pretreatment with AIQ, which restricts the activation of PARP,[26] significantly restricted the cytotoxicity of AA (Figure 3c), indicating that the progression of AA-induced cell death depends on PARP activation. AIF directly translocates from the mitochondrial inner membrane to the nucleus and then participates in the execution of DNA fragmentation. This is stimulated by activated calpains or PARP cycle.[27,28]

The release of AIF into the cytosol and its translocation into the nuclei were not detected in a control experiment (Figure 3d). On the other hand, AA induced the migration of AIF to the nuclei (Figure 3d). In addition, in the case of pretreatment with AIQ, 45 and 30% decreases in cytosolic and nuclear AIF levels, respectively, were observed after AA treatment. Moreover, in the case of pretreatment with L-NMMA, 70 and 63% decreases in cytosolic and nuclear AIF levels, respectively, were observed after AA treatment. These indicate that the AA-induced AIF migration was partly suppressed in the cells pretreated with AIQ and L-NMMA. The cleaved PARP-1, which is an activated form, was detected in cells treated with AA. In addition, this activation was clearly inhibited by pretreatment with AIQ and L-NMMA (Figure 3d).

Intracellular NAD$^+$ and ATP levels

Decreases in the NAD$^+$ and ATP levels were observed in AA-treated cells (Figures 4a and b). PARP activation results in a rapid decline in the levels of cellular NAD$^+$ and ATP as substrates.[27] These results suggest that AA-induced apoptosis is involved in PARP activation. Furthermore, the NAD$^+$ level in AA-treated cells pretreated with AIQ and L-NMMA was partly but significantly restored as compared with that in cells treated with only AA (Figure 4a). On the other hand, the ATP level in AA-treated cells pretreated with AIQ and L-NMMA was slightly restored to the control level (Figure 4b).

Mitochondrial membrane potential of AA-treated cells

The release of AIF from the mitochondria is caused by the decrease in mitochondrial membrane potential.[29] We detected the decrease in the mitochondrial membrane potential in AA-treated cells. The decrease in the membrane potential of AA-treated cells was similar to that of CCCP-treated cells (Figure 4c). In addition, L-NMMA and AIQ significantly restricted the AA-induced decrease in the membrane potential.

DISCUSSION

AA specifically binds to the bc1 complex in the mitochondrial electron transport chain, thereby inhibiting respiration and then inducing ROS generation. Cell death induced by AA was classified as mostly being a result of necrosis and partially being a result of apoptosis. In many cell lines, the toxic effect of AA is extremely strong; the range of IC$_{50}$ was 0.01–0.2 μg ml^{-1}.[30] This is probably directly caused by the inhibition
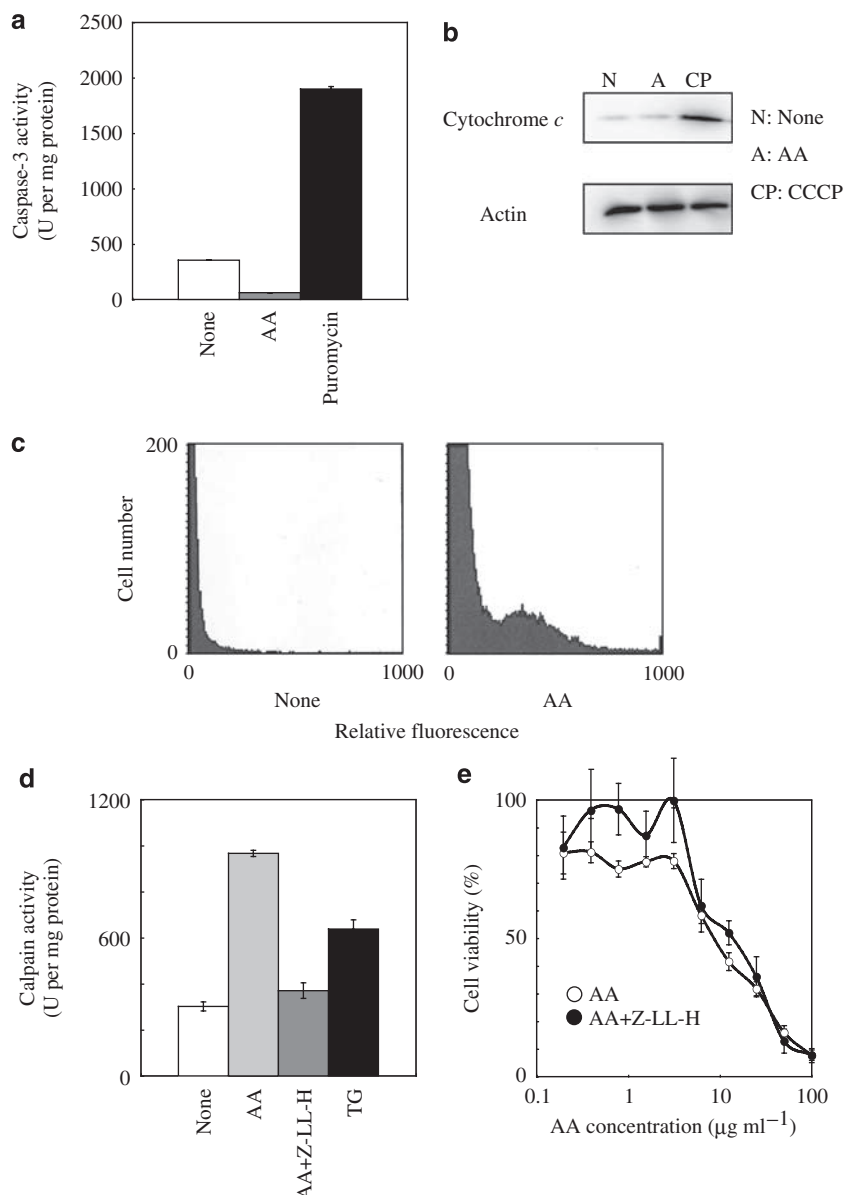
Figure 2 Effects of AA on mitochondrial- and ER-related apoptotic responses of HL-60 cells. (**a**) No activation of caspase-3 in HL-60 cells was treated with AA. HL-60 cells treated with $50\,\mu g\,ml^{-1}$ AA or $10\,\mu g\,ml^{-1}$ puromycin for 24 h. None indicates no treatment with drugs. (**b**) No release of cytochrome *c* from the mitochondria in HL-60 cells treated with AA. HL-60 cells were treated with no drug, $50\,\mu g\,ml^{-1}$ AA or $25\,\mu M$ carbonyl cyanide *m*-chlorophenylhydrazone (CCCP) for 24 h followed by western blot analysis as described in the Materials and Methods section. β-Actin was used as an internal control to show that the amounts of proteins subjected to SDS-PAGE were the same. Data are representative of one of three independent experiments. (**c**) Slight increase in intracellular Ca^{2+} level induced by AA. HL-60 cells were incubated with AA at 0 (None) or 50 (AA) $\mu g\,ml^{-1}$ for 24 h. The washed cells were stained with $5\,\mu g\,ml^{-1}$ Fluo3-AM and then analyzed by flow cytometry to estimate the intracellular Ca^{2+} level. (**d**) Calpain activation induced by AA. HL-60 cells were pretreated with 0 (None, AA and TG) or 25 (AA+Z-LL-H) μM, calpain inhibitor, Z-LL-H, for 1 h. After pretreatment, no drug (None), $50\,\mu g\,ml^{-1}$ AA (AA and AA+Z-LL-H) or $2\,\mu g\,ml^{-1}$ thapsigargin (TG) was added to the culture and the cells were then incubated for 24 h. (**e**) No restoration of AA-induced cytotoxicity by the calpain inhibitor. HL-60 cells were pretreated with 0 (AA) or 25 (AA+Z-LL-H) μM Z-LL-H for 1 h. After pretreatment, AA was added to the culture and the cells were then incubated for 24 h before Alamar blue assay.

of respiration and ROS generation at complex III. On the other hand, AA dose dependently induced the death of HL-60 cells at concentrations higher than $3\,\mu g\,ml^{-1}$. The IC$_{50}$ was $10\,\mu g\,ml^{-1}$ (Figure 1a). It is possible to obtain respiration-deficient rho0 cells of HL-60,[8] indicating proliferation without oxygen respiration. Although AA-induced ROS generation was eliminated in HL-60 cells by pretreatment with ascorbic acid (Figure 1b), the pretreatment hardly altered the toxicity of AA (Figure 1c). Therefore, for AA-induced cell death, factors other

than respiratory inhibition or its indirect or secondary effects, such as ROS generation, are considered in the case of HL-60 cells. Nuclear and DNA fragmentations were detected, but cellular disintegration was not observed in the AA-treated cells, indicating that AA induced a type of apoptotic-like cell death.

Many stimuli are transmitted as a cascade of apoptotic execution signals starting from the mitochondria, namely the signals generated by various environmental changes are consolidated into the
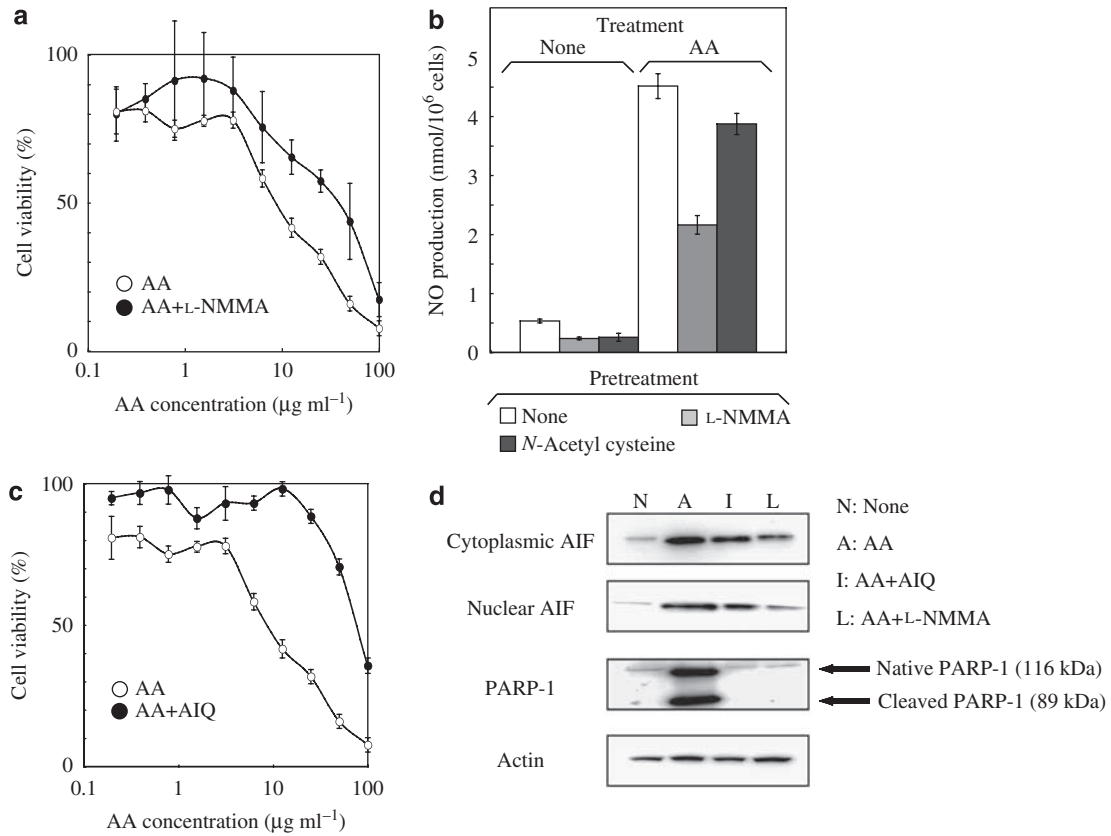
Figure 3 Effects of AA on NO production and PARP-related apoptotic responses of HL-60 cells. (**a**) Restoration of AA-induced cytotoxicity by a NOS inhibitor L-NMMA. HL-60 cells were pretreated with 0 (AA) or 1 (AA+L-NMMA) mM L-NMMA for 1 h. After pretreatment, AA was added to the culture and the cells were then incubated for 24 h before Alamar blue assay. (**b**) NO production in AA-treated cells. HL-60 cells were pretreated with or without 1 mM L-NMMA and 5 mM N-acetyl cysteine for 1 h. After pretreatment, AA at 0 (None) or 50 (AA) μg ml⁻¹ was added to the culture and the cells were further incubated for 24 h. (**c**) Restoration of AA-induced cytotoxicity by the PARP inhibitor AIQ. HL-60 cells were pretreated with 0 (AA) or 10 (AA+AIQ) nM AIQ for 1 h. After pretreatment, AA was added to the culture and the cells were further incubated for 24 h before Alamar blue assay. (**d**) Detection of AIF in the cytoplasm and the nuclei, and activation of PARP-1 induced by AA. HL-60 cells were pretreated with no inhibitor (N and A), 10 nM AIQ (I) and 1 mM L-NMMA (L) for 1 h. After pretreatment, 0 (N) or 50 (A, I and L) μg ml⁻¹ AA was added to the culture and the cells were then incubated for 24 h followed by western blot analysis as described in the Materials and methods section. β-Actin was used as an internal control to show that the amounts of proteins subjected to SDS-PAGE were the same. Data are representative of one of three independent experiments.
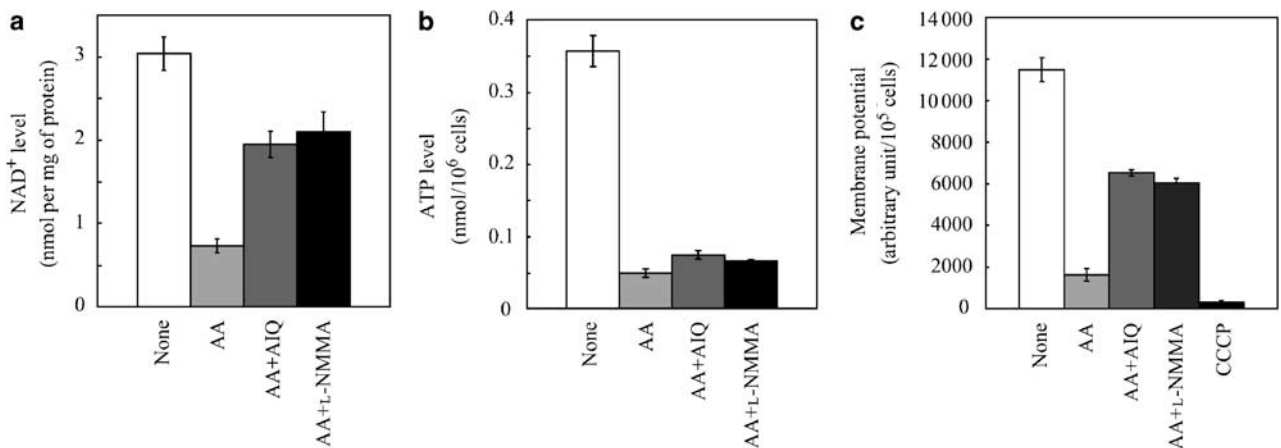

Figure 4 Effects of AA on NAD⁺ and ATP levels, and membrane potential on HL-60 cells. (**a**) Reduction of intracellular NAD⁺ level induced by AA. HL-60 cells were pretreated with no inhibitor (None and AA), 10 nM AIQ (AA+AIQ) and 1 mM L-NMMA (AA+L-NMMA) for 1 h. After pretreatment, AA at 0 (None) or 50 (AA, AA+AIQ and AA+L-NMMA) μg ml⁻¹ was added to the culture and the cells were then incubated for 24 h. (**b**) Decrease in intracellular ATP level induced by AA. HL-60 cells were pretreated with 0 (None and AA), 10 nM AIQ (AA+AIQ) and 1 mM L-NMMA (AA+L-NMMA) for 1 h. After pretreatment, AA at 0 (None) or 50 (AA, AA+AIQ and AA+L-NMMA) μg ml⁻¹ was added to the culture and the cells were then incubated for 24 h. (**c**) Loss of the mitochondrial membrane potential induced by AA. HL-60 cells were pretreated with 0 (None, AA and CCCP), 10 nM AIQ (AA+AIQ) and 1 mM L-NMMA (AA+ L-NMMA) for 1 h. After pretreatment, AA at 0 (None) or 50 (AA, AA+AIQ and AA+L-NMMA) μg ml⁻¹, or 10 μM CCCP (CCCP) was added to the culture and the cells were then incubated for 24 h.

mitochondria first, then cytochrome c and AIF are released from the mitochondria.[31] Interestingly, AA did not cause the release of cytochrome c but that of AIF in HL-60 cells (Figures 2b and 3c). This is supported by a report that AA prevents NO-induced apoptosis by blocking cytochrome c release independent of Bcl-2 expression in the rat gastric mucosa cell line RGM-1.[32] This apoptosis was triggered by a pure NO donor, 1-hydroxy-2-oxo-3,3-bis(2-aminoethyl)-1-triazene. On the other hand, we found that treatment with a high concentration of AA, such as $50 \, \mu g \, ml^{-1}$, induced cellular NO production in HL-60 cells (Figure 3b).

AIF translocation from the mitochondria to the nuclei occurs through PARP activation when Ca^{2+} influx was observed. Ca^{2+} influx activates calcium-dependent cytoplasmic proteins, such as neuronal NOS, in the brain. NO produced in the presence of increased levels of ROS leads to peroxynitrite formation, resulting in oxidative DNA damage. Excessive DNA damage overactivates PARP. PARP activation and/or its related signals stimulate the translocation of AIF from the mitochondria to the nuclei through the loss of mitochondrial membrane potential, resulting in nuclear apoptosis. The loss of mitochondrial membrane potential is reported to trigger the release of AIF.[33] We showed the loss of mitochondrial membrane potential in AA-treated cells (Figure 4c).

L-NMMA is an inhibitor of three isotypes of NOS (endothelial NOS, neuronal NOS and inducible NOS). This inhibitor partly eliminated NO production but significantly restricted the cytotoxicity of AA (Figure 3a). The protective effect of this inhibitor suggests that NO induced the death of AA-treated HL-60 cells. In HL-60 cells, the activation of inducible NOS was reported.[12] Therefore, it may be considered that AA-induced cell death is involved in NO production by inducible NOS.

Caspase-3 is activated in apoptotic inductions dependent on cytochrome c release. The AA-induced cell death did not depend on a cascade by the release of cytochrome c from the mitochondria or the activation of caspase-3 (Figures 2a and b), indicating the possibility that this apoptotic execution occurs only through AIF release.

In nuclear extracts of AA-treated cells, we detected cleaved PARP-1, or its active form, and AIF (Figure 3c). In addition, AIQ, which is an inhibitor of PARP activation, restricted the cytotoxicity of AA, PARP activation and AIF translocation. In addition, in AA-treated cells, both NAD^+ and ATP levels were lower than those in control cells. The NAD^+ level was partly restored by AIQ and L-NMMA (Figure 4a). These results support the observed AA-induced PARP-1 activation. On the other hand, the ATP level was slightly restored by AIQ and L-NMMA (Figure 4b). This result indicates that the cause of the decreased ATP level in AA-treated cells might be factors such as the inhibition of the electron transport chain and/or unknown mechanisms.

ER stress-induced apoptosis could be induced by only AIF release without cytochrome c release from the mitochondria.[34] When ER experiences potent stress, Ca^{2+} is released into the cytosol from ER, and calpains are then activated. Although the intracellular Ca^{2+} level was slightly elevated (Figure 2c) and calpains were strongly activated in the cells treated with AA (Figure 2d), the calpain inhibitor used hardly decreased the cytotoxicity of AA (Figure 2e). These results suggest that the AA-induced cell death is not due to ER stress.

Recently, another target of AA has been reported. AA interacts with the BH3 domain (Bcl-2 homology domain 3)-binding hydrophobic groove of anti-apoptotic proteins Bcl-2 and Bcl-x_L.[35] The BH3 domain is present in the Bcl proteins that promote and restrict apoptotic cell death. AA induces the loss of mitochondrial membrane potential in addition to the mitochondria overexpressing Bcl-2 and Bcl-x_L, thereby

probably inducing the apoptosis of the murine hepatocyte cell line TAMH. Bcl-2 and Bcl-x_L restrict cytochrome c release.[36] This result is in conflict with our results, wherein AA did not cause the release of cytochrome c. On the other hand, there is a report that AA prevents cytochrome c release independent of Bcl-2 expression when NO-induced apoptosis is suppressed by AA.[32] This is consistent with our results.

In conclusion, our results taken together showed that AA induced cellular NO production, PARP overactivation and translocation of AIF from the mitochondria to the nuclei, resulting in the apoptotic-like cell death of HL-60. Further investigations are required to clarify the mechanism by which cytochrome c release from the mitochondria is restricted by AA.

1 Pham, N. A., Robinson, B. H. & Hedley, D. W. Simultaneous detection of mitochondrial respiratory chain activity and reactive oxygen in digitonin-permeabilized cells using flow cytometry. Cytometry 41, 245–251 (2004).
2 Bernardi, P. Modulation of the mitochondrial cyclosporin A-sensitive permeability transition pore by the proton electrochemical gradient. Evidence that the pore can be opened by membrane depolarization. J. Biol. Chem. 267, 8834–8839 (1992).
3 Kaushal, G. P., Ueda, N. & Shah, S. V. Role of caspases (ICE/CED 3 proteases) in DNA damage and cell death in response to a mitochondrial inhibitor, antimycin A. Kidney Int. 52, 438–445 (1997).
4 Malcolm, A. K. & Monica, A. Antimycin A-induced apoptosis of HL-60 cells. Cytometry 49, 106–112 (2002).
5 Takimoto, H., Machida, K., Ueki, M., Tanaka, T. & Taniguchi, M. UK-2A, B, C and D, novel antifungal antibiotics from Streptomyces sp. 517-02. IV. Comparative studies of UK-2A with antimycin A_3 on cytotoxic activity and reactive oxygen species generation in LLC-PK_1 cells. J. Antibiot. 52, 480–484 (1999).
6 Fujita, K., Kiso, T., Usuki, Y., Tanaka, T. & Taniguchi, M. UK-2A, B, C and D, novel antifungal antibiotics from Streptomyces sp. 517-02 VI (3). Role of substituents on dilactone ring of UK-2A and antimycin A_3 against generation of reactive oxygen species in porcine renal proximal tubule LLC-PK_1 cells. J. Antibiot. 57, 687–690 (2004).
7 Broker, L. E., Kruyt, F. A. & Giaccone, G. Cell death independent of caspases: a review. Clin. Cancer Res. 11, 3155–3162 (2005).
8 Hail, N. Jr. & Lotan, R. Apoptosis induction by the natural product cancer chemopreventive agent deguelin is mediated through the inhibition of mitochondrial bioenergetics. Apoptosis 9, 437–447 (2004).
9 Everett, S. A. et al. Nitric oxide involvement in the toxicity of hydroxyguanidine in leukaemia HL60 cells. Br. J. Cancer Suppl. 27, S172–S176 (1996).
10 Oguro, A., Kawase, T. & Orikasa, M. NaF induces early differentiation of murine bone marrow cells along the granulocytic pathway but not the monocytic or preosteoclastic pathway in vitro. In Vitro Cell Dev. Biol. Anim. 39, 243–248 (2003).
11 Laouar, A., Glesne, D. & Huberman, E. Protein kinase C-beta, fibronectin, alpha(5)-beta(1)-integrin, and tumor necrosis factor-alpha are required for phorbol diester-induced apoptosis in human myeloid leukemia cells. Mol. Carcinog. 32, 195–205 (2001).
12 Bhushan, S. et al. A triterpenediol from Boswellia serrata induces apoptosis through both the intrinsic and extrinsic apoptotic pathways in human leukemia HL-60 cells. Apoptosis 12, 1911–1926 (2007).
13 de Murcia, G. et al. Structure and function of poly(ADP-ribose) polymerase. Mol. Cell. Biochem. 138, 15–24 (1994).
14 de Murcia, G. & Ménissier-de Murcia, J. Poly(ADP-ribose) polymerase: a molecular nick-sensor. Trends Biochem. Sci. 19, 172–176 (1994).
15 Lautier, D., Lagueux, J., Thibodeau, J., Ménard, L. & Poirier, G. G. Molecular and biochemical features of poly(ADP-ribose) metabolism. Mol. Cell. Biochem. 122, 171–193 (1993).
16 D'Amours, D., Desnoyers, S., D'Silva, I. & Poirier, G. G Poly(ADP-ribosyl)ation reactions in the regulation of nuclear functions. Biochem. J. 342, 249–268 (1999).
17 Virág, L. & Szabó, C. The therapeutic potential of poly(ADP-ribose) polymerase inhibitors. Pharmacol. Rev. 54, 375–429 (2002).
18 Bryant, H. E. et al. Specific killing of BRCA2-deficient tumours with inhibitors of poly(ADP-ribose) polymerase. Nature 434, 913–917 (2005).
19 Oei, S. L., Keil, C. & Ziegler, M. Poly(ADP-ribosylation) and genomic stability. Biochem. Cell Biol. 83, 263–269 (2005).
20 Eliasson, M. J. et al. Poly(ADP-ribose) polymerase gene disruption renders mice resistant to cerebral ischemia. Nat. Med. 3, 1089–1095 (1997).
21 Wang, X. The expanding role of mitochondria in apoptosis. Genes Dev. 15, 2922–2933 (2001).
22 Kiso, T., Usuki, Y., Ping, X., Fujita, K. & Taniguchi, M. L-2,5-dihydrophenylalanine, an inducer of cathepsin-dependent apoptosis in human promyelocytic leukemia cells (HL-60). J. Antibiot. 54, 810–817 (2001).
23 Carter, W. O., Narayanan, P. K. & Robinson, J. P. Intracellular hydrogen peroxide and superoxide anion detection in endothelial cells. J. Leukoc. Biol. 55, 253–258 (1994).

24 Zong, W. X., Ditsworth, D., Bauer, D. E., Wang, Z. Q. & Thompson, C. B. Alkylating DNA damage stimulates a regulated form of necrotic cell death. *Genes Dev.* **18,** 1272–1282 (2004).

25 Burger, A. M. *et al.* Tyrphostin AG17, [(3,5-Di-tert-butyl-4-hydroxybenzylidene)-malononitrile], inhibits cell growth by disrupting mitochondria. *Cancer Res.* **55,** 2794–2799 (1995).

26 Szabó, G. *et al.* Poly(ADP-ribose) polymerase inhibition reduces reperfusion injury after heart transplantation. *Circ. Res.* **90,** 100–106 (2002).

27 Yu, S. W., Wang, H., Dawson, T. M. & Dawson, V. L. Poly(ADP-ribose) polymerase-1 and apoptosis inducing factor in neurotoxicity. *Neurobiol. Dis.* **14,** 303–317 (2003).

28 Polster, B. M., Basanez, G., Etxebarria, A., Hardwick, J. M. & Nicholls, D. G. Calpain I induces cleavage and release of apoptosis-inducing factor from isolated mitochondria. *J. Biol. Chem.* **280,** 6447–6454 (2005).

29 Hong, S. J., Dawson, T. M. & Dawson, V. L. Nuclear and mitochondrial conversations in cell death: PARP-1 and AIF signaling. *Trends Pharmacol. Sci.* **25,** 259–264 (2004).

30 Ueki, M. *et al.* UK-3A, a novel antifungal antibiotic from *Streptomyces* sp. 517-02: fermentation, isolation, structural elucidation and biological properties. *J. Antibiot.* **50,** 551–555 (1997).

31 Ferri, K. F. & Kroemer, G. Organelle-specific initiation of cell death pathways. *Nat. Cell Biol.* **3,** E255–E263 (2001).

32 Dairaku, N. *et al.* Oligomycin and antimycin A prevent nitric oxide-induced apoptosis by blocking cytochrome *c* leakage. *J. Lab. Clin. Med.* **143,** 143–151 (2004).

33 Susin, S. A. *et al.* Two distinct pathways leading to nuclear apoptosis. *J. Exp. Med.* **192,** 571–580 (2000).

34 Newcomb, E. W., Lukyanov, Y., Smirnova, I., Schnee, T. & Zagzag, D. Noscapine induces apoptosis in human glioma cells by an apoptosis-inducing factor-dependent pathway. *Anticancer Drugs* **19,** 553–563 (2008).

35 Tzung, S. P. *et al.* Antimycin A mimics a cell-death-inducing Bcl-2 homology domain 3. *Nat. Cell Biol.* **3,** E43–E46 (2001).

36 Yang, J. *et al.* Prevention of apoptosis by Bcl-2: release of cytochrome *c* from mitochondria blocked. *Science* **275,** 1129–1132 (1997).

npg

ORIGINAL ARTICLE

A novel assay of bacterial peptidoglycan synthesis for natural product screening

Ryo Murakami[1], Yasunori Muramatsu[2], Emiko Minami[2], Kayoko Masuda[2], Yoshiharu Sakaida[3], Shuichi Endo[3], Takashi Suzuki[3], Osamu Ishida[3], Toshio Takatsu[2], Shunichi Miyakoshi[1,4], Masatoshi Inukai[1,5] and Fujio Isono[1]

Although a large number of microbial metabolites have been discovered as inhibitors of bacterial peptidoglycan biosynthesis, only a few inhibitors were reported for the pathway of UDP-MurNAc-pentapeptide formation, partly because of the lack of assays appropriate for natural product screening. Among the pathway enzymes, D-Ala racemase (Alr), D-Ala:D-Ala ligase (Ddl) and UDP-MurNAc-tripeptide:D-Ala-D-Ala transferase (MurF) are particularly attractive as antibacterial targets, because these enzymes are essential for growth and utilize low-molecular-weight substrates. Using dansylated UDP-MurNAc-tripeptide and L-Ala as the substrates, we established a cell-free assay to measure the sequential reactions of Alr, Ddl and MurF coupled with translocase I. This assay is sensitive and robust enough to screen mixtures of microbial metabolites, and enables us to distinguish the inhibitors for D-Ala–D-Ala formation, MurF and translocase I. D-cycloserine, the D-Ala-D-Ala pathway inhibitor, was successfully detected by this assay ($IC_{50}=1.7\,\mu g\,ml^{-1}$). In a large-scale screening of natural products, we have identified inhibitors for D-Ala–D-Ala synthesis pathway, MurF and translocase I.

INTRODUCTION

The emergence of drug-resistant bacteria is an unavoidable problem in anti-infectious therapy. One of the strategies to overcome this problem is to find new anti-bacterial agents towards novel targets. Bacterial peptidoglycan synthesis is a rich source of such targets, because most enzymes in this pathway are unique in bacteria and essential for growth.[1–4] In fact many antibiotics, including the clinically important beta-lactam and glycopeptides antibiotics, are peptidoglycan synthesis inhibitors. Although most of these antibiotics target the later stage of peptidoglycan synthesis, such as transpeptidation and/or transglyco-sylation steps, only a few inhibitors are known for enzymes involved in the earlier stage of UDP-MurNAc-pentapeptide formation. In the cytoplasm, the D-Ala–D-Ala dipeptide is synthesized from L-Ala by pyridoxal phosphate-dependent D-alanine racemase (Alr) and ATP-dependent D-Ala:D-Ala ligase (Ddl). The dipeptide is transferred to UDP-MurNAc-tripeptide (UDP-MurNAc-L-Ala-γ-D-Glu-m-DAP) by ATP-dependent D-Ala–D-Ala adding enzyme UDP-MurNAc-tripeptide:D-Ala–D-Ala transferase (MurF) to form UDP-MurNAc-pentapeptide. Then, phospho-N-acetylmuramyl-pentapeptide trans-locase (translocase I, MraY) catalyzes the transfer of the MurNAc-pentapeptide moiety to the lipid carrier undecaprenyl phosphate to form lipid I. To date, a variety of nucleoside antibiotics have been reported as translocase I inhibitors,[5] such as mureidomycins,[6]

pacidamycins,[7] napsamycins,[8] liposidomycins,[9] tunicamycin,[10] capur-amycins,[11–17] muraymycins[18] and caprazamycins.[19,20] In contrast, only a few inhibitors have been reported for the steps of UDP-MurNAc-pentapeptide formation. D-cycloserine and O-carba-myl-D-serine are known inhibitors for D-Ala–D-Ala pathways Alr and Ddl,[21–23] and recently a few synthetic compounds were reported as MurF inhibitors.[24] To date, there are some reports on the assay method for D-Ala–D-Ala pathway[25,26] and MurF,[27,28] but none of them are high-throughput functional assays appropriate for large-scale natural product screenings. In this paper, we describe the development of a cell-free assay to measure the sequential reactions of D-Ala–D-Ala formation and MurF coupled with translocase I. To prepare sufficient amount of the substrate dansylated UDP-MurNAc-tripeptide, we also established a large-scale fermentation protocol of UDP-MurNAc-tripeptide. With this method, we carried out a high-thoughput screening of natural products, whose result is also presented.

MATERIALS AND METHODS

Chemicals

Undecaprenyl phosphate was purchased from Larodan Fine Chemicals (Malmo, Sweden). D-cycloserine was purchased from Sigma (St Louis, MO, USA).

[1]Exploratory Research Laboratories II, Daiichi-Sankyo Co., Ltd, Kitakasai, Edogawa-ku, Tokyo, Japan; [2]Exploratory Research Laboratories I, Daiichi-Sankyo Co., Ltd, Kitakasai, Edogawa-ku, Tokyo, Japan and [3]Process Technology Research Laboratories I, Daiichi-Sankyo Co., Ltd, Aza-ohtsurugi, Shimokawa, Izumi-machi, Iwaki-shi, Fukushima, Japan
[4]Current address: Gunma National College of Technology, 580, Toriba-machi, Maebashi, Gunma prefecture 371-8530, Japan.
[5]Current address: Department of Pharmaceutical Sciences, International University of Health and Welfare, 2600-1, Kitakanemaru, Ohtawara, Tochigi prefecture 324-8501, Japan.
Correspondence: Dr R Murakami, Exploratory Research Laboratories II, Daiichi-Sankyo Co., Ltd, 1-16-13, Kitakasai, Edogawa-ku, Tokyo 134-8630, Japan.
E-mail: murakami.ryo.bw@daiichisankyo.co.jp
Received 29 September 2008; accepted 14 January 2009; published online 20 February 2009

Plasmid construction

The alr, ddlA, murF and mraY genes were amplified by PCR using *Escherichia coli* K-12 DNA as a template. These products were digested with BamHI, HindIII and cloned between the corresponding sites of the pET28a plasmid vector (Novagen, Madison, WI, USA). In this construct, each gene is expressed under the control of an IPTG-inducible promoter with an N-terminal His$_6$ extension.

Enzyme preparation

E. coli BL21(DE3) harboring a recombinant plasmid with alr, ddl or murF was grown at 37 °C in 2×YT medium containing 25 μg ml^{-1} of kanamycin. At an A_{600} of 0.6, IPTG was added at a final concentration of 1 mM, and incubation was continued for 6 h at 37 °C with shaking. The cells harvested by centrifugation were washed with 50 mM Tris-HCl buffer (pH 8.0) containing 0.1 mM MgCl$_2$, and re-suspended in the same buffer at 4 °C. After disruption of the cells by sonication, the remaining cells were removed by centrifugation (5000 g, 10 min) and the supernatant was adsorbed onto the Ni-NTA-agarose column (QIAGEN, Germantown, MD, USA). Elution was carried out at 4 °C first with 50 mM Tris-HCl buffer (pH 8.0), and thereafter eluted with 50 mM Tris-HCl buffer (pH 8.0) and 200 mM imidazole. The purified enzyme solutions were stored at −80 °C.

Translocase I was prepared as follows: *E. coli* strain C43 (DE43) harboring recombinant plasmid pET-mraY was grown at 37 °C in 2×YT medium containing 25 μg ml^{-1} of kanamycin. At an A_{600} of 0.7, IPTG was added at a final concentration of 1 mM, and incubation was continued for 16 h at 25 °C with shaking. The cells harvested by centrifugation were washed with 50 mM Tris-HCl buffer (pH 8.0) containing 0.1 mM MgCl$_2$, and re-suspended in the same buffer at 4 °C. After disruption of the cells by sonication, the remaining cells were removed by centrifugation (5000 g, 10 min), and membrane fragments were collected by ultracentrifugation (105 000 g, 60 min) at 4 °C. The pellet was washed with the same buffer and re-suspended in solubilization buffer consisting of 50 mM Tris-HCl buffer (pH 8.0), 0.1 mM MgCl$_2$, 1% Triton X-100 and 30% (v/v) glycerol. The suspension was stirred for 30 min at 4 °C to solubilize the enzyme. After removal of insoluble materials by ultracentrifugation using the same conditions as described above, the resulting crude enzyme solution was stored at −80 °C.

Preparation of UDP-MurNAc-tripeptide

Based on the method reported earlier,[29] we established a large-scale fermentation of UDP-MurNAc-tripeptide. *Bacillus cereus* SANK70880 was inoculated into each of twelve 2-l Erlenmeyer flasks containing 500 ml of the medium consisting of bactopeptone 0.5%, yeast extract 0.5%, meat extract 0.5%, glucose 0.2%, KH$_2$PO$_4$ 0.2% and CB-442 0.01% (NOF Co., Ltd, Tokyo, Japan), and was incubated on a rotary shaker (210 rpm) at 37 °C for 24 h. Then 6 l of the culture was transferred into a 600-l tank containing 300 l of the same medium as mentioned above. The fermentation condition is as follows: temperature 37 °C, initial aeration rate 1 vvm, stirrer speed 83 rpm, dissolved oxygen 5 p.p.m., and pressure 100 kPa. After 2 h of fermentation (A_{600}=0.85), D-cycloserine (final concentration 100 μg ml^{-1}) was added. Cells were harvested by centrifugation for 30 min after addition of D-cycloserine. The pellet (515 g) was washed, suspended in 1-l phosphate buffer, and boiled at 100 °C for 15 min. After centrifugation at 9000 rpm for 30 min, the supernatant was adsorbed onto Sephadex A-25 (2.5 l). The column was washed with 100 mM KCl (12 l) and eluted with 300 mM KCl (20 l). The eluate was adjusted to pH 2.0 with 1 M HCl and adsorbed onto a SEPABEADS SP207 column (2.5 l). The column was washed with 0.01 M HCl (10 l) and water (2 l), and eluted with 20% MeOH (10 l). The eluate was lyophilized to give a powder of UDP-MurNAc-tripeptide (3.8 g) with >95% purity as confirmed by HPLC.

Dansylation of UDP-MurNAc-tripeptide

UDP-MurNAc-tripeptide (5 μmol) was dissolved in a 1:1 (v/v) mixture (150 ml) of 0.25 M NaHCO$_3$ and ME$_2$CO, and dansyl chloride (210 μmol) was added. The solution was stirred for 4 h at room temperature in the dark. The Me$_2$CO was evaporated off and the aqueous solution was chromatographed on a Bio-Gel P2 column (Bio-Rad, Hercules, CA, USA) with water. Fractions containing UDP-MurNAc-dansyltripeptide were identified using HPLC and lyophilized. UDP-MurNAc-dansyltripeptide was stored at −20 °C.

Translocase I-coupled fluorescence-based assay

MurF and translocase I coupling reaction was carried out in a 96-well microtiter polystyrene plate (Corning Coaster, Corning, NY, USA, #3694). The assay mixture contains 100 mM Tris-HCl (pH 8.6), 50 mM KCl, 25 mM MgCl$_2$, 0.2% Triton X-100, 37.5 μM undecaprenyl phosphate, 100 μM UDP-MurNAc-dansyltripeptide, 250 μM D-Ala–D-Ala, 250 μM ATP and 8% glycerol. The reaction was initiated by the addition of 10 μl (5 μg) of MurF and translocase I (1–4 μg) mixture, and monitored by measuring the increase of fluorescence at 538 nm (excitation at 355 nm). The Alr, Ddl, MurF and translocase I coupling reaction was carried out as described above, except that 150 μM L-Ala was used instead of D-Ala–D-Ala, and a four-enzyme mixture (10 μl) including Alr (0.5 μg) and Ddl (0.5 μg). The assay condition in 384-well plate format was the same as that in the 96-well plate format described above, except that the assay volume was half of that in the 96-well plate format and reaction time in the screening mode was 60 min.

HPLC assay

HPLC detection of the MurF activity was carried out as described by Duncan et al.[30] with slight modifications. The reaction mixture containing 100 mM Tris-HCl (pH 8.6), 40 mM KCl, 10 mM MgCl$_2$, 200 μM UDP-MurNAc-tripeptide, 200 μM D-Ala–D-Ala, 200 μM ATP and 8% glycerol was added to 10 μl of MurF and incubated. The reaction was stopped by boiling at 100 °C for 3 min, and after being centrifuged at 11 000 rpm for 10 min, the supernatant was analyzed by HPLC with Symmetry C18 column (eluent 3% acetonitrile–0.3% TEAP aq. (pH 3.0); flow rate 1.0 ml min^{-1}; detection 260 nm).

RESULTS AND DISCUSSION

Fluorescence-based determination of MurF activity

Brandish et al.[31] reported the assay to measure translocase I activity by determining the difference in fluorescent intensities of the substrate UDP-MurNAc-dansylpentapeptide and the product dansylated lipid I. We applied this method to high-throughput screening of natural products and discovered novel translocase I inhibitors.[13–17,32–35] As the assay is sensitive and robust enough, we tried to measure MurF activity by coupling with this reaction (Figure 1). For that purpose, we first established a large-scale fermentation protocol for UDP-MurNAc-tripeptide to prepare the labeled substrate UDP-MurNAc-dansyltripeptide. From a 300-l culture of D-cycloserine-treated *Bacillus cereus*, we obtained 3.8 g of UDP-MurNAc-tripeptide with >95% purity. Then we used UDP-MurNAc-tripeptide or UDP-MurNAc-dansyltripeptide as the substrate for the detection of MurF activity. In cell-free MurF assay, each substrate was converted to the corresponding product, UDP-MurNAc-pentapeptide or UDP-MurNAc-dansylpentapeptide, which was confirmed by HPLC analysis.[30] This indicated that UDP-MurNAc-dansyltripeptide was used as the substrate of MurF, and suggested that MurF activity could be measured in a high-throughput mode by coupling translocase I.

To exemplify this, we used D-Ala–D-Ala and UDP-MurNAc-dansyltripeptide as the substrates instead of UDP-MurNAc-dansylpentapeptide for the translocase I reaction. We observed a small increase of the fluorescence intensity without MurF, but in the presence of MurF the fluorescence intensity was dramatically increased (Figure 2), which suggested that MurF and translocase I reactions were efficiently coupled in this assay condition. The reaction was also dependent on D-Ala–d-Ala as expected. The minor increase of the fluorescence without MurF was reduced in the absence of translocase I (Figure 2), suggesting that dansylated tripeptide could be incorporated into lipid I by translocase I.

Determination of Alr and Ddl activity

Next, we incorporated the D-Ala–D-Ala biosynthesis pathway in this coupling reaction by adding L-Ala instead of D-Ala–D-Ala in
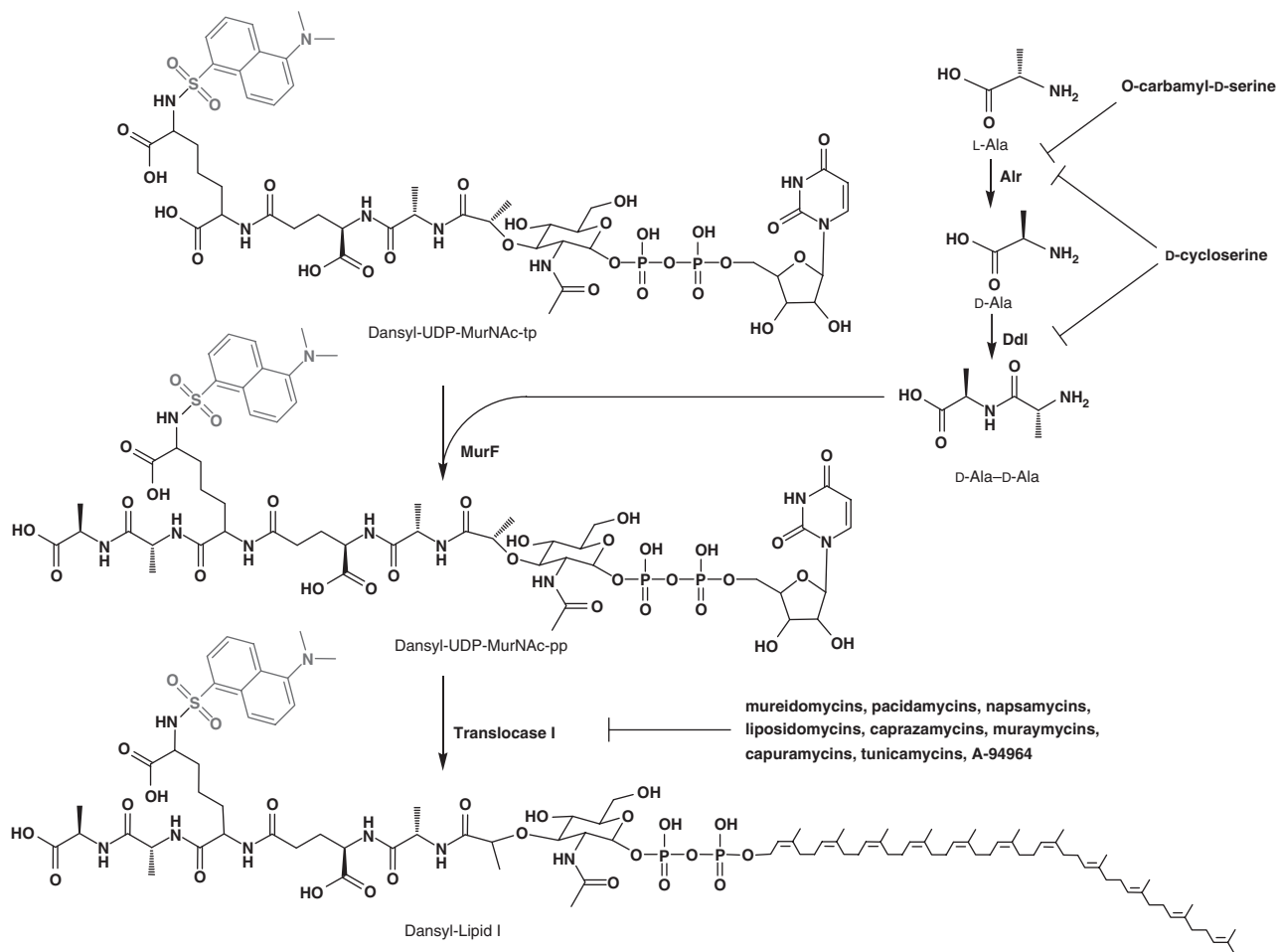
Figure 1 Fluorescence-based assay of D-Ala–D-Ala pathway, MurF and translocase I. In bacterial peptidoglycan biosynthesis, the UDP-MurNAc-pentapeptide is synthesized from L-Ala and UDP-MurNAc-tripeptide by Alr, Ddl and MurF. Then, translocase I converts UDP-MurNAc-pentapeptide to lipid I. A novel assay method to measure the sequential reactions of Alr, Ddl and MurF coupled with translocase I was designed by using dansylated UDP-MurNAc-tripeptide as the substrate. In this assay, the fluorescence intensity was expected to increase by enzymatic reactions.
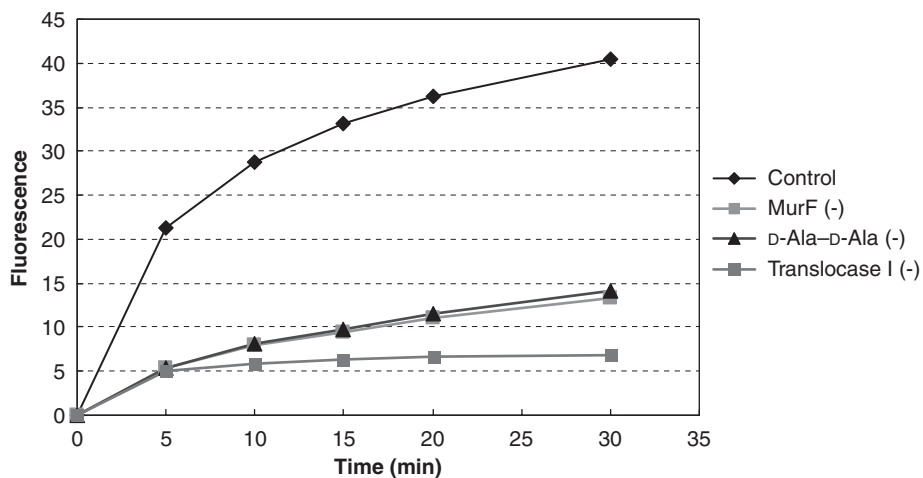

Figure 2 Time course of MurF and translocase I coupling reaction. MurF and translocase I coupling reaction was initiated by the addition of MurF and translocase I enzyme into the assay mixture described in 'Materials and methods', and monitored by measuring the increase of fluorescence at 538 nm (excitation at 355 nm).
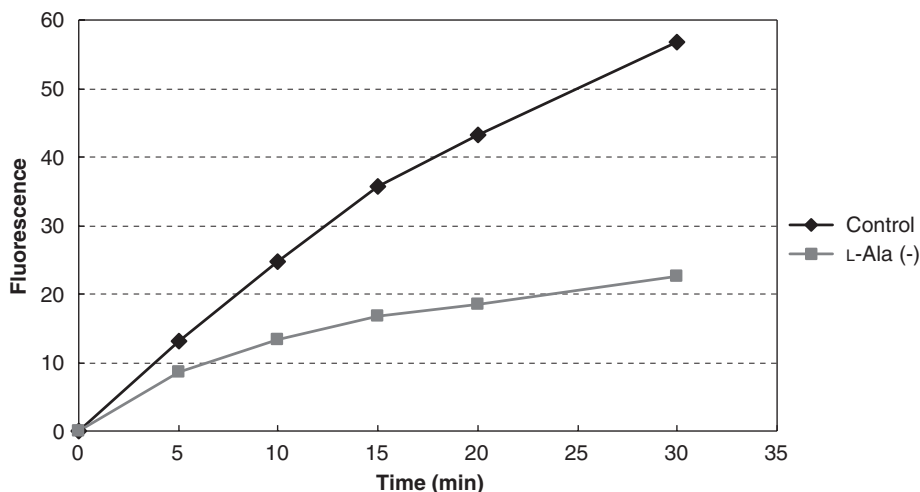
Figure 3 Time course of Alr, Ddl, MurF and translocase I coupling reaction. Alr, Ddl, MurF and translocase I coupling reaction was carried out as shown in Figure 2, except that 150 μM L-Ala was used instead of D-Ala–D-Ala, and a four-enzyme mixture instead of the two.
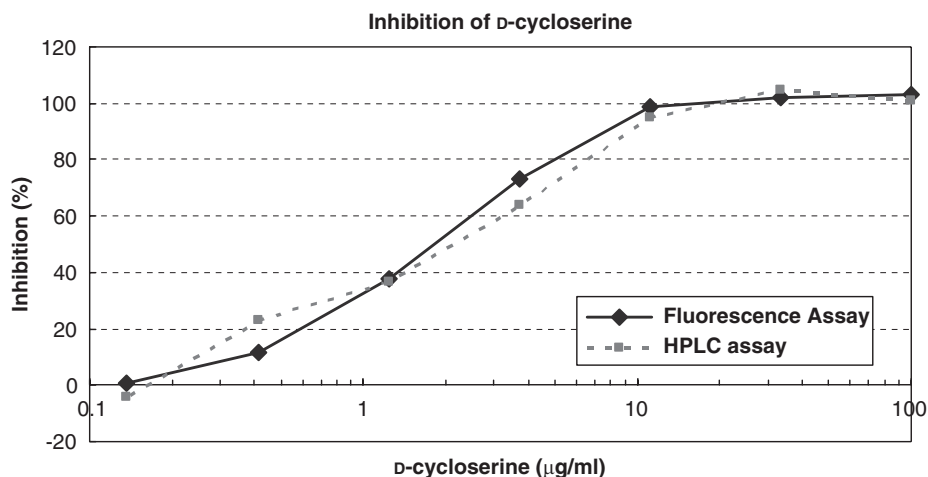

Figure 4 Assay validation by D-cycloserine. The inhibitory activity of D-cycloserine for Alr, Ddl, MurF and translocase I coupling reaction was checked by both HPLC and fluorescence-based assay.

the assay mixture and also by supplying Alr and Ddl enzymes. The fluorescence intensity was increased largely depending on L-Ala (Figure 3). We confirmed the contribution of D-Ala–D-Ala pathway in this reaction by checking the inhibitory activity of D-cycloserine (Figure 4). The IC_{50} value of D-cycloserine was estimated as 1.7 μg ml^{-1} (=17 μM), which is compatible with that obtained in the HPLC assay.[25]

Screening of microbial metabolites for inhibitors of UDP-MurNAc-pentapeptide formation

Our goal is to obtain inhibitors for Alr, Ddl and MurF from microbial metabolites using this assay. We optimized the assay condition in 384-well plate format with Z' values in the range from 0.6 to 0.8 (Figure 5), and carried out a large-scale screening of microbial metabolites (actinomycetes, fungi and bacteria metabolites). On screening some samples showed positive activities (hit rate approximately 0.5%). After retesting these samples with initial fluorescence-based screening, we

checked their inhibitory activities by HPLC assay with all four enzymes. Next, these hit samples were tested in the translocase I reaction as well as in the MurF plus translocase I reaction, and categorized according to the inhibitory activities in these three assay conditions. We identified the translocase I inhibitors reported earlier, such as capuramycins, mureidomycins, liposidomycins and tunicamycins (data not shown). In addition, we found F-11334A1 as an inhibitor of the D-Ala–D-Ala pathway (IC_{50}=20 μM), and (−)-epigallocatechin gallate and pleurotin as MurF inhibitors (IC_{50}=9 μM and 41 μM, respectively) (Figure 6). F-11334A1 was earlier reported as an inhibitor of neutral sphingomyelinase.[36] Pleurotin was discovered as an anti-bacterial substance by Robbin *et al.*[37] and (−)-epigallocatechin gallate was reported to have an anti-bacterial activity.[38] The relationship between the reported activities for these compounds and our current observation remains to be further studied. Nevertheless, the method described here is robust enough to screen a large number of mixture samples in
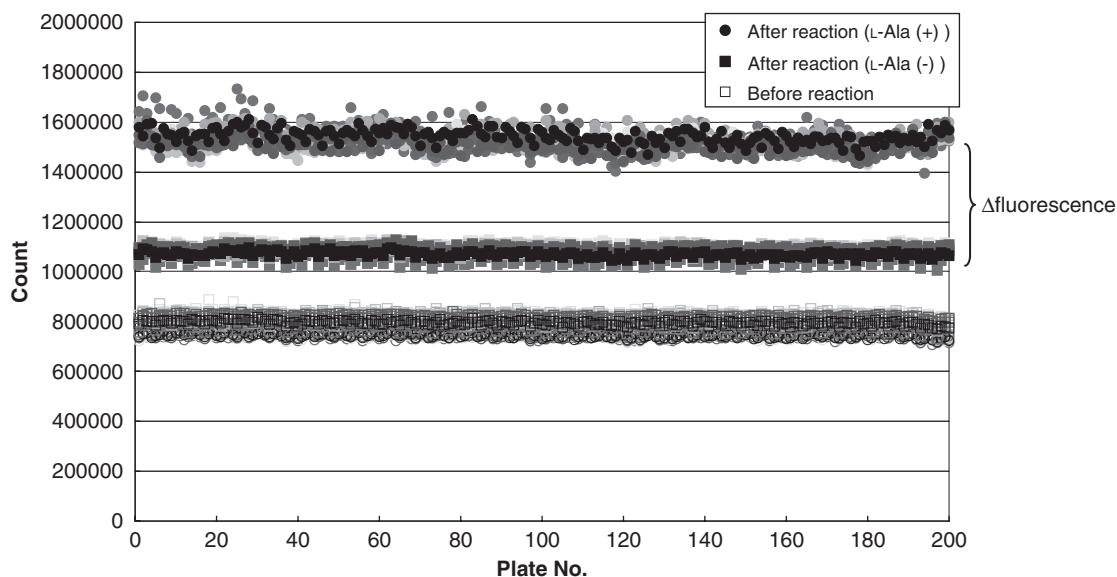
Figure 5 High-throughput screening of D-Ala–D-Ala pathway, MurF and translocase I. Variation among wells in the 384-well plate format was checked. Fluorescence enhancement depending on Alr, Ddl, MurF and translocase I reaction was determined by deducting the count after reaction (L-Ala (−)) from the count after reaction (L-Ala (+)). Therefore, Z' value was derived from data points such that the 'maximum' signal was obtained by deducting the count before reaction from that after reaction (L-Ala (+)) and the 'minimum' signal was obtained by deducting the count before reaction from that after reaction (L-Ala (−)).
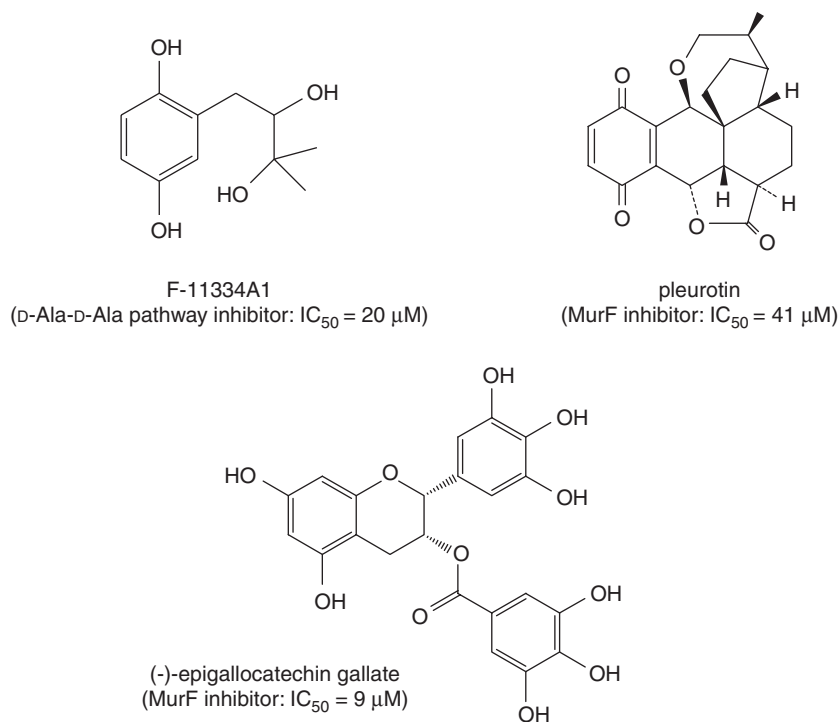

F-11334A1
(D-Ala-D-Ala pathway inhibitor: IC$_{50}$ = 20 μM)

pleurotin
(MurF inhibitor: IC$_{50}$ = 41 μM)

(-)-epigallocatechin gallate
(MurF inhibitor: IC$_{50}$ = 9 μM)

Figure 6 Identification of inhibitors from our screening. Chemical structures and inhibitory activities of inhibitors from our novel fluorescence-based assay of D-Ala–D-Ala pathway, MurF and translocase I are shown.

a high-throughput mode, and will greatly facilitate a discovery of novel antibiotics.

1 Lugtenberg, E. J., De Haas-Menger, L. & Ruyters, W. H. Murein synthesis and identification of cell wall precursors of temperature-sensitive lysis mutants of *Escherichia coli. J. Bacteriol.* **109**, 326–335 (1972).

2 Lugtenberg, E. J. & v Schijndel-van Dam, A. Temperature-sensitive mutants of *Escherichia coli* K-12 with low activities of the L-alanine adding enzyme and the D-alanyl-D-alanine adding enzyme. *J. Bacteriol.* **110**, 35–40 (1972).

3 Lugtenberg, E. J. & v Schijndel-van Dam, A. Temperature-sensitive mutant of *Escherichia coli* K-12 with an impaired D-alanine:D-alanine ligase. *J. Bacteriol.* **113**, 96–104 (1973).

4 Boyle, D. S. & Donachie, W. D. MraY is an essential gene for cell growth in *Escherichia coli. J. Bacteriol.* **180**, 6429–6432 (1998).

5 Brandish, P. E. *et al.* Modes of action of tunicamycin, liposidomycin B and mureidomycin A: inhibition of phospho-*N*-acetylmuramyl-pentapeptide translocase from *Escherichia coli. Antimicrob. Agents Chemother.* **40**, 1640–1644 (1996).

6 Inukai, M. *et al.* Mureidomycin A-D, novel peptidylnucleoside antibiotics with spheroplast forming activity. I. Taxonomy, fermentation, isolation and physico-chemical properties. *J. Antibiot.* **42,** 662–666 (1989).

7 Karwowski, J. P. *et al.* Pacidamycins, a novel series of antibiotics with anti-*Pseudomonas aeruginosa* activity. I. Taxonomy of the producing organism and fermentation. *J. Antibiot.* **42,** 506–511 (1989).

8 Chatterjee, S. *et al.* Napsamycins, new *Pseudomonas* activity antibiotics of mureidomycin family from *Streptomyces* sp. HIL Y-82, 11372. *J. Antibiot.* **47,** 595–598 (1994).

9 Ubukata, M. & Isono, K. The structure of liposidomycin B, an inhibitor of bacterial peptidoglycan synthesis. *J. Am. Chem. Soc.* **110,** 4416–4417 (1988).

10 Takatsuki, A., Arima, K. & Tamura, G. Tunicamycin, a new antibiotic. I. Isolation and characterization of tunicamycin. *J. Antibiot.* **24,** 215–223 (1971).

11 Yamaguchi, H. *et al.* Capuramycin, a new nucleoside antibiotic. Taxonomy, fermentation, isolation and characterization. *J. Antibiot.* **39,** 1047–1053 (1986).

12 Seto, H. & Otake, N. The structure of a new nucleoside antibiotic, capuramycin. *Tetrahedron Lett.* **29,** 2343–2346 (1988).

13 Muramatsu, Y. *et al.* Studies on novel bacterial translocase I inhibitors. I. Taxonomy, fermentation, isolation, physico-chemical properties and structure elucidation of A-500359A, C, D and G. *J. Antibiot.* **57,** 243–252 (2003).

14 Muramatsu, Y., Ishii, M. M. & Inukai, M. Studies on novel bacterial translocase I inhibitors, A-500359s. II. Biological activities of A-500359 A, C, D and G. *J. Antibiot.* **56,** 253–258 (2003).

15 Muramatsu, Y. *et al.* Studies on novel bacterial translocase I inhibitors, A-500359s. III. Deaminocaprolactam derivatives of capuramycin: A-500359 E, F, H, M-1 and M-2. *J. Antibiot.* **56,** 259–267 (2003).

16 Ohnuki, T., Muramatsu, Y., Miyakoshi, S., Takatsu, T. & Inukai, M. Studies on novel bacterial translocase I inhibitors, A-500359s. IV. Biosynthesis of A-500359s. *J. Antibiot.* **56,** 268–279 (2003).

17 Muramatsu, Y. *et al.* Studies on novel bacterial translocase I inhibitors, A-500359s. V. Enhanced production of capuramycin and A-500359A in *Streptomyces griseus* SANK 60196. *J. Antibiot.* **59,** 601–606 (2006).

18 McDonald, L. A. *et al.* Structures of the muraymycins, novel peptidoglycan biosynthesis inhibitors. *J. Am. Chem. Soc.* **124,** 10260–10261 (2002).

19 Igarashi, M. *et al.* Caprazamycin B, a novel anti-tuberculosis antibiotic, from *Streptomyces* sp. *J. Antibiot.* **56,** 580–583 (2003).

20 Igarashi, M. *et al.* Caprazamycins, novel lipo-nucleoside antibiotics, from *Streptomyces* sp. II. Structure elucidation of caprazamycins. *J. Antibiot.* **58,** 327–337 (2005).

21 Strominger, J. L., Threnn, R. H. & Scott, S. S. Oxamycin, competitive antagonist of the incorporation of D-alanine into uridine nucleotide in *Staphylococcus aureus*. *J. Am. Chem. Soc.* **81,** 3803 (1959).

22 Strominger, J. L., Ito, E. & Threnn, R. H. Competitive inhivition of enzymatic reactions by oxamycin. *J. Am. Chem. Soc.* **82,** 998–999 (1960).

23 Lynch, J. L. & Neuhaus, F. C. On the mechanism of action of the antibiotic O-carbamyld-serine in *Streptococcus faecalis*. *J. Bacteriol.* **91,** 449–460 (1966).

24 Gu, Y. G. *et al.* Structure-activity relationships of novel potent MurF inhibitors. *Bioorg. Med. Chem. Lett.* **14,** 267–270 (2004).

25 Vicario, P. P., Green, B. G. & Katzen, H. M. A single assay for simultaneously testing effectors of alanine racemase and/or D-alanine: D-alanine ligase. *J. Antibiot.* **40,** 209–216 (1987).

26 Chen, D. *et al.* Development of a homogeneous pathway for screening inhibitors of bacterial D-Ala-D-Ala biosynthesis. In *43rd Interscience Conference on Antimicrobial Agents and Chemotherapy (ICAAC)* (abstracts F-1456), (2003).

27 Comess, K. M. *et al.* An ultraefficient affinity-based high-throughput screening process: application to bacterial cell wall biosynthesis enzyme MurF. *J. Biomol. Screen.* **11,** 743–754 (2006).

28 Baum, E. Z. *et al.* Utility of muropeptide ligase for identification of inhibitors of the cell wall biosynthesis enzyme MurF. *Antimicrob. Agents Chemother.* **50,** 230–236 (2006).

29 Kohlrausch, U. & Holtje, J. V. One-step purification procedure for UDP-N-acetylmuramyl-peptide murein precursors from *Bacillus cereus*. *FEMS Microbiol. Lett.* **62,** 253–257 (1991).

30 Duncan, K., van Heijenoort, J. & Walsh, C. T. Purification and characterization of the D-Alanyl-D-Alanine-adding enzyme from *Escherichia coli*. *Biochemistry* **29,** 2379–2386 (1990).

31 Brandish, P. E. *et al.* Slow binding inhibition of phospho-*N*-acetylmuramyl-pentapeptide-translocase (*Escherichia coli*) by mureidomycin A. *J. Biol. Chem.* **271,** 7609–7614 (1996).

32 Muramatsu, Y. *et al.* A-503083 A, B, E and F, novel inhibitors of bacterial translocase I, produced by *Streptomyces* sp. SANK 62799. *J. Antibiot.* **57,** 639–646 (2004).

33 Murakami, R. *et al.* A-102395, a new inhibitor of bacterial translocase I, produced by *Amycolatopsis* sp. SANK 60206. *J. Antibiot.* **60,** 690–695 (2007).

34 Murakami, R. *et al.* A-94964, a novel inhibitor of bacterial translocase I, produced by *Streptomyces* sp. SANK 60404 I. Taxonomy, fermentation, isolation and biological activity. *J. Antibiot.* **61,** 537–544 (2008).

35 Fujita, Y., Murakami, R., Muramatsu, Y., Miyakoshi, S. & Takatsu, T. A-94964, a novel inhibitor of bacterial translocase I, produced by *Streptomyces* sp. SANK 60404 II. Physico-chemical properties and structure elucidation. *J. Antibiot.* **61,** 545–549 (2008).

36 Tanaka, M., Nara, F., Yamasato, Y., Ono, Y. & Ogita, T. F-11334s, new inhibitors of membrane-bound neutral sphingomyelinase. *J. Antibiot.* **52,** 827–830 (1999).

37 Robbins, W. J., Kavanagh, F. & Hervey, A. Antibiotic substances from basidiomycetes I. *Pleurotus griseus.*. *Proc. Natl Acad. Sci. USA* **33,** 171–176 (1947).

38 Ikigai, H., Nakae, T. & Shimamura, T. Bactericidal catechins damage the lipid bilayer. *Biochim. Biophys. Acta* **1147,** 132–136 (1993).

npg

ORIGINAL ARTICLE

Novel 24-membered macrolides, JBIR-19 and -20 isolated from *Metarhizium* sp. fE61

Ikuko Kozone[1], Jun-ya Ueda[1], Machika Watanabe[2], Satoru Nogami[2], Aya Nagai[1], Shigeki Inaba[3], Yoshikazu Ohya[2], Motoki Takagi[1] and Kazuo Shin-ya[4]

In the course of our screening program for active compounds that induce cell morphological changes of *Saccharomyces cerevisiae*, the culture broth of an entomopathogenic fungus *Metarhizium* sp. fE61 exhibited a unique morphological phenotype. We conducted an activity-guided isolation from the fermentation broth of *Metarhizium* sp. fE61 to yield two new macrolide compounds named JBIR-19 (1) and -20 (2) as active substances. Their structures were determined to be 24-membered macrolide analogs containing a 2-aminoethyl phosphate ester on the basis of NMR and other spectroscopic data. Compounds 1 and 2 induced striking elongated morphology of *S. cerevisiae* at concentrations of 3.1 and 13 μM, but showed weak antiyeast activity at MICs of 200 and >200 μM, respectively.

INTRODUCTION

Cell morphology is tightly linked to cellular processes and functions in virtually all eukaryotic organisms. In the budding yeast *Saccharomyces cerevisiae*, cell morphology reflects various cellular events, including progression through the cell cycle, establishment of cell polarity and regulation of cell-size control.[1] Change of the cell morphology often occurs as a consequence of cellular differentiation, cellular toxicity, other critical cellular events or signaling. Therefore, we can estimate the target of compounds from the information of yeast morphological changes induced by the compounds. In addition, the observation of morphological changes that provides a different viewpoint from antifungal activity-based screening could be one of the screening methods to discover bioactive compounds with novel skeletons, although these compounds do not show direct cytocidal activity in yeast. Accordingly, we carried out the chemical screening focusing on a specific morphology of *S. cerevisiae*.

We observed visually the cell morphology of diploid wild-type *S. cerevisiae* treated with microbial metabolites by phase contrast microscopy, and screened for inducers of abnormal morphological phenotypes. In the results, we found active ingredients in the fermentation broth of an entomopathogenic fungus identified as *Metarhizium* sp. We carried out activity-guided separation from the culture broth to isolate two new 24-membered macrolide compounds

designated as JBIR-19 (1) and -20 (2). This study describes the fermentation, isolation, structure elucidation and biological activity of 1 and 2, in addition to the taxonomy of the producing micro-organism.

MATERIALS AND METHODS

General experimental procedures

The melting point was determined with a Yanagimoto micro melting point apparatus (Kyoto, Japan). Optical rotations were operated on a Horiba SEPA-300 polarimeter (Kyoto, Japan). HR-ESI (electrospray ionization)-MS data were recorded on a Waters LCT-Premier XE mass spectrometer (Milford, MA, USA). UV and IR spectra were measured on an Hitachi U-3200 spectrophotometer (Tokyo, Japan) and an Horiba FT-720 spectrophotometer (Kyoto, Japan), respectively. The ^{1}H and ^{13}C NMR spectra were taken on a Varian NMR System 500 NB CL (Palo Alto, CA, USA) in DMSO-d_6, with the residual solvent peak as internal standard (δ_C 39.7, δ_H 2.49 p.p.m.). The ^{31}P NMR spectra were taken on a Varian NMR System 400 MR in DMSO-d_6 with phosphoric acid as internal standard (δ_P 0 p.p.m.). Analytical TLC was carried out on precoated silica gel 60 F$_{254}$ plates (0.25 mm thickness; Merck, Darmstadt, Germany), and a phosphomolybdic acid solution was used for the detection. Normal- and reversed-phase medium pressure liquid chromatography was performed on a Purif-Pack SI-60 and a Purif-Pack ODS-100 (Moritex, Tokyo, Japan), respectively. Preparative reversed phase HPLC was carried out on a Senshu Pak PEGASIL ODS (20 i.d.×150 mm; Senshu Scientific, Tokyo,

[1]Biomedicinal Information Research Center (BIRC), Japan Biological Informatics Consortium (JBIC), Koto-ku, Tokyo, Japan; [2]Department of Integrated Biosciences, Graduate School of Frontier Sciences, University of Tokyo, Kashiwa, Chiba, Japan; [3]NITE Biotechnology Development Center (NBDC), Department of Biotechnology, National Institute of Technology and Evaluation (NITE), Kisarazu, Chiba, Japan and [4]Biomedicinal Information Research Center (BIRC), National Institute of Advanced Industrial Science and Technology (AIST), Koto-ku, Tokyo, Japan
Correspondence: Dr K Shin-ya, Biomedicinal Information Research Center (BIRC), National Institute of Advanced Industrial Science and Technology (AIST), 2-42 Aomi, Koto-ku, Tokyo 135-0064, Japan. E-mail: k-shinya@aist.go.jp or Dr M Takagi, Biomedicinal Information Research Center (BIRC), Japan Biological Informatics Consortium (JBIC), 2-42 Aomi, Koto-ku, Tokyo 135-0064, Japan.
E-mail: motoki-takagi@aist.go.jp
Received 8 December 2008; revised 13 January 2009; accepted 19 January 2009; published online 6 February 2009

Japan) with detection by a Waters 2996 photodiode array detector and a Waters 3100 mass detector. Reagents and solvents were of the highest grade available.

Microorganism

The producing organism, designated as fE61, was isolated by the SDS-YE method[2] from a soil sample collected in Kyoto Prefecture, Japan. The soil was treated with a solution containing 6% Bacto-Yeast Extract (BD Biosciences, San Jose, CA, USA) and 0.05% sodium dodecyl sulfate at 40 °C for 20 min. The solution was diluted with water and plated onto potato dextrose agar plates at 27 °C for a few weeks. The fungal colonies that appeared on the plate were transferred to potato dextrose agar slant and the strains were maintained.

The fE61 strain was identified through sequence analysis of the ribosomal DNA ITS region and the microscopic feature was observed by using a Zeiss Axio Plan 2 imaging system (Carl Zeiss, Oberkochen, Germany).

Wild-type diploid *Saccharomyces cerevisiae* strain (BY4743: *MATa/MATα*; *his3Δ1/his3Δ1*; *leu2Δ0/leu2Δ0*; *met15Δ0/MET15*; *LYS2/lys2Δ0*; *ura3Δ0/ura3Δ0*) was obtained from the European *Saccharomyces cerevisiae* Archive for Functional Analysis (EUROSCARF).[3]

Medium

The seed medium, potato dextrose, was composed of $2.4 \, g \, l^{-1}$ Potato dextrose broth (BD Biosciences). The production medium consisted of 15 g oatmeal (Quaker, Chicago, IL, USA) and 50 ml V8 Mix Juice (Campbell Soup Company, Camden, NJ, USA) in 500-ml Erlenmeyer flasks.

Yeast cells were grown in a Yeast-Peptone-Dextrose (YPD) medium containing 1% Bacto-Yeast Extract (BD Biosciences), 2% Bacto-Peptone (BD Biosciences) and 2% dextrose.

Cell morphology assay

For morphological screening, diploid wild-type *S. cerevisiae* was grown in 96-well microtiter plates with YPD liquid media. The culture of logarithmically growing wild-type cells was diluted to 2×10^4 cells per ml, dispensed 100 μl to each well in 96-well microtiter plates and incubated in the presence of 5% screening sample at 25 °C with constant shaking. After a day's incubation, the cells were observed by phase contrast microscopy (AXIO Imager M1, Carl Zeiss).

Antibiotic assay

The MIC determinations of **1** and **2** were conducted in 96-well microtiter plates with YPD liquid media. The culture of logarithmically growing wild-type *S. cerevisiae* cells was diluted to 2×10^4 cells per ml and incubated in the presence of different concentrations of compounds at 25 °C with constant shaking. MIC was determined as the lowest concentration of drugs at which no significant visible growth occurred after a day. The cell number was observed by phase contrast microscopy (AXIO Imager M1, Carl Zeiss).

RESULTS AND DISCUSSION

Taxonomy and fermentation

The producing microorganism showed 99.2% similarity to *Metarhizium anisopliae* var. *anisopliae* (EU307926) using sequence analysis of ribosomal DNA and morphological features such as profusely branched conidiophores forming a sporulating layer and dry subhyaline phialoconidia compacted into regular chains and columns.[4,5] Hence, the strain was identified as *Metarhizium* sp.

Metarhizium sp. fE61 was cultivated in a 50-ml test tubes containing 15 ml of a seed medium. The test tubes were shaken on a reciprocal shaker (355 r.p.m.) at 27 °C for 3 days. Aliquots (5 ml) of the culture were transferred to 500-ml Erlenmeyer flasks containing the production medium and incubated in static culture at 27 °C for 14 days.

Isolation

The solid culture (eight flasks) was extracted with 80% aq. Me₂CO. After concentration *in vacuo*, the aqueous concentrate was partitioned with EtOAc (1000 ml) and *n*-BuOH (1500 ml), successively. The

Table 1 Physicochemical properties of 1 and 2

	1	*2*
Appearance	Colorless amorphous powder	colorless amorphous powder
Melting point	160–162 °C	126–128 °C
$[\alpha]_D^{25}$ (MeOH)	+31.9 (*c* 0.7)	+25.9 (*c* 0.3)
HR-ESI-MS (*m/z*) found	550.3142 (M+H)⁺	534.3166 (M+H)⁺
calculated	550.3145	534.3196
	(for $C_{26}H_{49}NO_9P$)	(for $C_{26}H_{49}NO_8P$)
UV λ_{max} (MeOH) nm (ε)	204 (1093)	204 (1007)
IR v_{max} (KBr) cm⁻¹	3400, 1730, 1630	3400, 1726, 1631

BuOH layer was evaporated to dryness *in vacuo*, and the dried residue (1.9 g) was applied to reversed phase medium-pressure liquid chromatography and developed with an MeOH-water stepwise system (0, 10, 20, 30, 40, 50, 60, 70, 80, 90 and 100%) to yield an active fraction (97.0 mg) in 80% MeOH eluate. The active fraction was chromatographed on normal phase medium-pressure liquid chromatography with CHCl₃-MeOH (3:2). The active eluates were purified by the preparative reversed phase HPLC, developed with 75% MeOH-H₂O, including 0.1% formic acid (flow rate: $10 \, ml \, min^{-1}$) to yield **1** (13.1 mg, Rt 16 min), and **2** (6.1 mg, Rt 22 min).

Structure elucidation

The physicochemical properties of **1** and **2** were summarized in Table 1. Compound **1** was obtained as a colorless amorphous powder, and its molecular formula was established as $C_{26}H_{48}NO_9P$ by HR-ESI-MS data [*m/z* 550.3142 (M+H)⁺], and was also supported by ¹³C, ¹H and ³¹P NMR data. IR spectrum showed absorbance for hydroxyl (v_{max} 3400 cm⁻¹) and ester carbonyl (v_{max} 1730 cm⁻¹) groups. The direct connectivity between each proton and carbon was established by the HSQC (heteronuclear single quantum coherence) spectrum, and the ¹³C and ¹H NMR spectral data for **1** are shown in Table 2. Three partial structures were established by double-quantum filtered (DQF)-COSY and heteronuclear multiple bond correlation (HMBC) spectra as follows:

A spin coupling between oxymethylene protons of 25-H (δ_H 3.86) and aminomethylene protons of 26-H (δ_H 2.94) indicated the presence of ethanolamine moiety (Figure 1). The sequence from a terminal methyl proton 24-H (δ_H 1.13) to methylene protons 16-H (δ_H 1.308) through an oxymethine proton 23-H (δ_H 4.80), methylene protons 22-H (δ_H 1.50, 1.43), 21-H (δ_H 1.310), 20-H (δ_H 2.01 ∼ 1.88), two olefinic protons 19-H (δ_H 5.36), 18-H (δ_H 5.30) and methylene protons 17-H (δ_H 2.01 ∼ 1.88) was observed in DQF-COSY spectrum. The ¹H-¹³C long-range couplings from methylene protons 16-H, 18-H and 19-H to an allylic carbon C-17 (δ_C 31.6), and from 18-H, 19-H, 22-H and 23-H to an allylic carbon C-20 (δ_C 31.7) also supported the connectivity of allylic carbons. Thus, a 2-oxy-6-nonene moiety was established as a partial structure of **1** as shown in Figure 1. The stereochemistry at C-18 was deduced to possess an *E* configuration from its coupling constant ($J_{18,19}$=15.0 Hz). Another sequence from methylene protons 2-H (δ_H 2.28, 2.22) to methylene protons 10-H (δ_H 1.40, 1.23) through methylene protons 3-H (δ_H 1.64), 4-H (δ_H 1.56), an oxymethine proton 5-H (δ_H 3.75), two epoxy protons 6-H (δ_H 2.89, δ_C 58.4), 7-H (δ_H 2.85, δ_C 57.7), two oxymethine protons 8-H (δ_H 2.91, δ_C 75.3) and 9-H (δ_H 3.36, δ_C 72.1) established a 2,3,6-trioxy-4,5-epoxynonane moiety. The existence of an epoxy group at the position of C-6 and C-7 was determined by their characteristic ¹³C shifts, and its stereochemistry was determined as *trans* by its coupling

Table 2 ^{13}C (125 MHz) and ^{1}H (500 MHz) NMR spectra of **1** and **2**

	1		**2**	
Position	δ_C	δ_H (multiplicity, J in Hz)	δ_C	δ_H (multiplicity, J in Hz)
1	172.6		172.6	
2	33.9	2.28 (dt, 16.1, 7.1); 2.22 (dt, 16.1, 7.1)	34.0	2.26 (t, 7.0)
3	20.0	1.64 (pentet, 7.1)	20.1	1.60 (m)
4	32.2	1.56 (m)	32.2	1.55 (m)
5	74.4	3.75 (dq, 8.6, 5.6)	74.7	3.72 (dq, 8.1, 5.9)
6	58.4	2.89 (d, 1.5)	60.5	2.74 (br d, 5.8)
7	57.7	2.85 (dd, 7.1, 1.5)	53.6	2.88 (br t, 5.8)
8	75.3	2.91 (m)	39.6	1.74 (dt, 13.4, 5.4); 1.30 (m)
9	72.1	3.36 (m)	67.7	3.59 (p, 5.1)
10	25.6	1.40 (m); 1.23 (m)	28.22	1.310 (m)
11 ~ 15	31.8	1.44 (m); 1.233 (m)	36.4	1.36 (m); 1.305 (m)
	28.8	1.23 (m)	28.5	1.235 (m)
	28.7	1.23 (m)	28.5	1.235 (m)
	28.5	1.23 (m)	27.4	1.23 (m)
	27.4	1.22 (m)	24.8	1.240 (m)
16	28.3	1.308 (m)	28.21	1.310 (m)
17	31.6	2.01–1.88 (m)	31.5	2.01–1.87 (m)
18	130.6	5.30 (dd, 15.0, 5.5)	130.6	5.29 (dd, 15.0, 5.5)
19	130.4	5.36 (dd, 15.0, 5.5)	130.3	5.34 (dd, 15.0, 5.5)
20	31.7	2.01–1.88 (m)	31.7	2.01–1.87 (m)
21	24.9	1.310 (m)	24.9	1.315 (m)
22	34.7	1.50 (m); 1.43 (m)	34.7	1.51 (m); 1.43 (m)
23	70.2	4.80 (sex, 6.3)	70.2	4.80 (sex, 6.1)
24	20.1	1.13 (d, 6.1)	20.1	1.13 (d, 6.4)
25	61.4	3.86 (br s)	61.5	3.84 (m)
26	41.1	2.94 (br s)	41.2	2.92 (br s)

constant ($J_{6,7}$=1.5 Hz). The ^{1}H-^{13}C long-rang couplings from 23-H, 2-H, 3-H to an ester carbonyl carbon C-1 (δ_C 172.6), together with ^{1}H-^{1}H correlations from both of 10-H and 16-H to the remaining methylene chain (C_5H_{10} unit for 11-H to 15-H, δ_H 1.44–1.21), established a 24-membered macrolide skeleton (Figure 1). A peak of δ_P at −0.448 ppm in ^{31}P NMR spectra indicated the presence of a phosphoric acid or a phosphoryl group. The oxymethylene carbon C-5 (δ_C 74.4) and the oxymethine carbon C-25 (δ_c 61.4) were observed as doublet signals ($^2J_{C-5,P}$=6.5 Hz, $^2J_{C-25,P}$=4.8 Hz, respectively), whereas their neighboring carbons were observed as doublet or broad singlet signals (C-4: δ_C 32.2, br d, $^3J_{C-4,P}$=3.5 Hz; C-6: d, $^3J_{C-6,P}$=4.8 Hz; C-26: δ_C 41.1, br s), suggesting C-5 and C-25 to be connected through a phosphodiester bond. Thus, the structure of **1** was determined as shown in Figure 2.

Compound **2** was obtained as a colorless amorphous powder and has a molecular formula, $C_{26}H_{48}NO_8P$, based on HR-ESI-MS data [m/z 534.3166 (M+H)$^+$]. IR spectrum indicated the presence of hydroxyl (v_{max} 3400 cm^{-1}) and an ester carbonyl (v_{max} 1726 cm^{-1}) groups. The NMR spectral data (Table 2) were similar to those of **1**, and HR-ESI-MS data showed the difference of 16 mass units as an oxygen atom compared with that of **1**. A peak of a phosphoric acid or a phosphoryl group at δ_P −0.436 p.p.m. in the ^{31}P NMR spectra showed as the same as that of **1**. A spin coupling between oxymethylene protons of 25-H (δ_H 3.84) and aminomethylene protons of 26-H (δ_H 2.92), the sequences from methylene protons 2-H (δ_H 2.26) to methylene protons 10-H (δ_H 1.310), and from a methyl proton 24-H (δ_H 1.13) to methylene protons 16-H (δ_H 1.310) were observed in an ^{1}H-^{1}H DQF-COSY experiment in the same manner as those of **1**

(Figure 1), whereas remarkable difference was observed at a methylene carbon C-8 (δ_C 39.6; δ_H 1.74, 1.30), which was high-field shifted compared with the hydroxyl methine carbon C-8 of **1** (δ_C 75.3; δ_H 2.91). The geochemistry of the olefin at C-18 (δ_C 130.6) was determined as *trans* from its coupling constant ($J_{18,19}$=15.0 Hz), similar to that of **1**. On the other hand, the stereochemistry of the oxacyclopropane ring between C-6 (δ_C 60.5) and C-7 (δ_C 53.6) was determined as *cis* from its coupling constant ($J_{6,7}$=5.8 Hz). Therefore, **2** was established to be an 8-deoxy derivative of **1** (Figure 2).

We, herein, isolated two 24-membered macrolide compounds with phosphate ester **1** and **2** from the culture broth of *Metarhizium* sp. fE61. *Metarhizium* sp. is known to be entomopathogenic fungus and produces several secondary metabolites, such as nonribosomal peptides (destruxins,[6] serinocyclins[7]), nor-triterpenoids (helvolic acids,[8] viridoxins[9]) and polyene compounds (aurovertins,[10] NG-391, NG-393[11]). **1** and **2** are the first report that *Metarhizium* sp. produces macrolide compounds. The similar carbon framework to **1** and **2** is only reported as eushearilide, isolated from *Eupenicillium shearii*[12] as a fungal metabolite. The structures of **1** and **2**, however, differ from that of eushearilide in the presence of highly oxygenated functional groups (epoxy and hydroxyl), the substituted position of the phosphate ester and the olefinic groups.

Biological activity
We evaluated the cell morphological change of diploid wild-type *S. cerevisiae* by **1** and **2** using visual observation with phase contrast microscopy. The cells treated with **1** and **2** showed striking elongated morphology at the concentrations of 3.1 and 13 μM, respectively
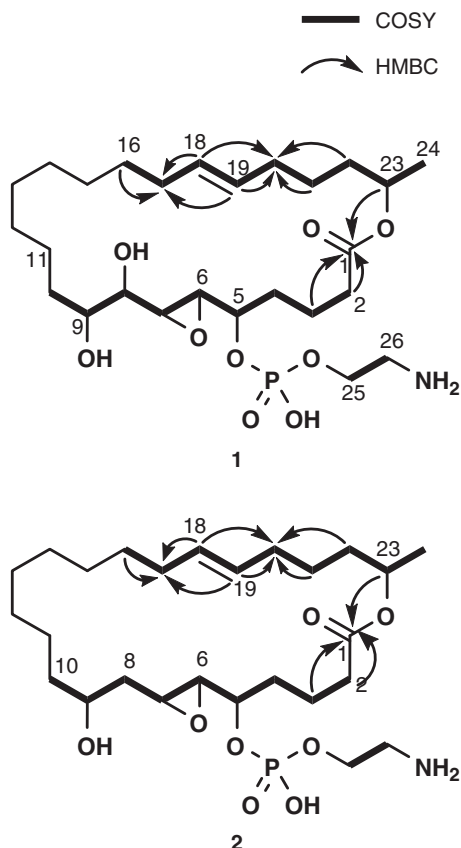
Figure 1 Key correlations in 2D NMR for **1** and **2** (^{1}H-^{1}H DQF-COSY and HMBC).

JBIR-19 (**1**) : R = OH
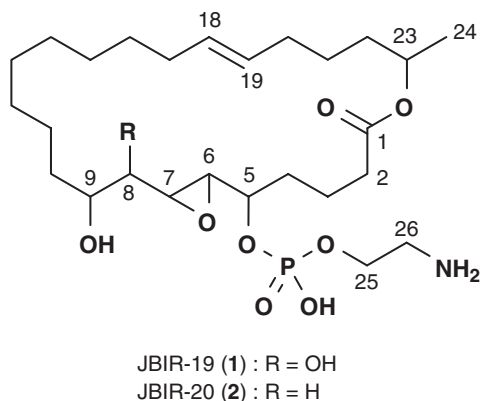JBIR-20 (**2**) : R = H
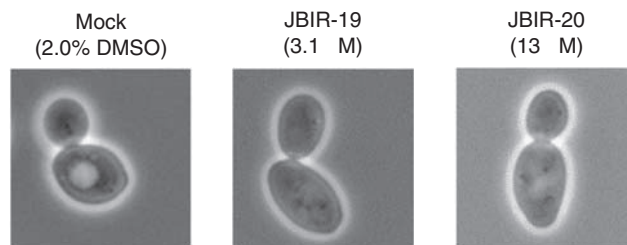
Figure 2 Structures of **1** and **2**.

Figure 3 Phase contrast images of diploid wild-type *S. cerevisiae* grown in the presence or absence of **1** and **2**.

(Figure 3). To the contrary, **1** exhibited weak antimicrobial activity at MICs of 200 μM, whereas **2** did not show antimicrobial activity at the concentration of 200 μM. As the cyclin-dependent kinases and/or mitotic cyclins mutants of *S. cerevisiae* indicate striking elongated morphology, the cell morphology is closely related to M phase progression in the cell cycle.[13] Thus, these results suggest that **1** and **2** inhibit M phase progression and induce striking elongated morphology. Studies on detailed biological activity of **1** are now underway.

1 Ohya, Y. *et al*. High-dimensional and large-scale phenotyping of yeast mutants. *Proc. Natl. Acad. Sci. USA* **102,** 19015–19020 (2005).
2 Hayakawa, M. & Nonomura, H. A new method for the intensive isolation of actinomycetes from soil. *Actinomycetol* **3,** 95–104 (1989).
3 Brachmann, C. B. *et al*. Designer deletion strains derived from *Saccharomyces cerevisiae* S288C: a useful set of strains and plasmids for PCR-mediated gene disruption and other applications. *Yeast* **14,** 115–132 (1998).
4 Mavridou, A., Cannone, J. & Typas, M. A. Identification of group-I introns at three different positions within the 28S rDNA gene of the entomopathogenic fungus *Metarhizium anisopliae* var *anisopliae*. *Fungal. Genet. Biol.* **31,** 79–90 (2000).
5 Domsch, K. H., Gams, W. & Anderson, T. *Compendium of soil fungi*, 2nd edn. (IHW-Verlag & Verlagsbuchhandlung, Eching, 2007).
6 Liu, B. L., Chen, J. W. & Tzeng, Y. M. Production of cyclodepsipeptides destruxin A and B from *Metarhizium anisopliae*. *Biotechnol. Prog.* **16,** 993–999 (2000).
7 Krasnoff, S. B. *et al*. Serinocyclins A and B, cyclic heptapeptides from *Metarhizium anisopliae*. *J. Nat. Prod.* **70,** 1919–1924 (2007).
8 Lee, S. Y., Kinoshita, H., Ihara, F., Igarashi, Y. & Nihira, T. Identification of novel derivative of helvolic acid from *Metarhizium anisopliae* grown in medium with insect component. *J. Biosci. Bioeng.* **105,** 476–480 (2008).
9 Gupta, S. *et al*. Viridoxins A and B: Novel toxins from the fungus *Metarhizium flavoviride*. *J. Org. Chem.* **58,** 1062–1067 (1993).
10 Azumi, M. *et al*. Aureovertins F-H from the entomopathogenic fungus *Metarhizium anisopliae*. *J. Nat. Prod.* **71,** 278–280 (2008).
11 Krasnoff, S. B. *et al*. Production of mutagenic metabolites by *Metarhizium anisopliae*. *J. Agric. Food Chem.* **54,** 7083–7088 (2006).
12 Hosoe, T. *et al*. A new antifungal macrolide, eushearilide, isolated from *Eupenicillium shearii*. *J. Antibiot.* **59,** 597–600 (2006).
13 Ahn, S. H. *et al*. Enhanced cell polarity in mutants of the budding yeast cyclin-dependent kinase Cdc28p. *Mol. Biol. Cell* **12,** 3589–3600 (2001).

npg

NOTE

Xylarinols A and B, two new 2-benzoxepin derivatives from the fruiting bodies of *Xylaria polymorpha*

In-Kyoung Lee[1], Yun-Woo Jang[1], Young-Sook Kim[1], Seung Hun Yu[2], Kui Jae Lee[1], Seung-Moon Park[1], Byung-Taek Oh[1], Jong-Chan Chae[1] and Bong-Sik Yun[1]

Basidiomycetes, as decomposers of forest litter, represent an ecologically important group of organisms in the environment, and are known to produce a large variety of secondary metabolites with unique chemical structures and interesting biological activities.[1] The genus *Xylaria* has been known to produce a diverse class of bioactive compounds, including cytochalasin analogs with chemokine receptor antagonistic activity and cytotoxicity,[2] multiplolides A, B and xylariamide A with antifungal activity,[3,4] xylarenals A and B with neuropeptide Y receptor antagonistic activity[5] and xyloketals A–E, acetylcholinesterase inhibitors.[6] Earlier, we reported two antifungal substances, xylarinic acids A and B, from the methanolic extract of *Xylaria polymorpha*.[7] Our ongoing investigation for novel chemical constituents from *X. polymorpha* has resulted in the isolation of two new 2-benzoxepin derivatives with ABTS (2,2′-azinobis(3-ethylbenzothiazoline-6-sulfonate)) radical scavenging activity. Benzoxepin is very rare in naturally occurring compounds. In this paper, we describe the isolation and structure determination of xylarinols A (1) and B (2), and their biological activity.

Xylarinols were isolated from the fruiting bodies of *X. polymorpha*, as shown in Figure 1. The collected fruiting bodies were ground and then extracted twice with methanol (MeOH) at room temperature for 2 days. After removal of MeOH under reduced pressure, the concentrate was partitioned between chloroform and water and then ethyl acetate and water. The ethyl acetate-soluble portion was chromatographed on a column of silica gel and eluted with increasing amounts (2.0, 5.0, 10, 20 and 50%, stepwise) of MeOH in $CHCl_3$ to give two fractions, which exhibited moderate ABTS radical scavenging activity. One was purified by Sephadex LH-20 column chromatography with $CHCl_3$–MeOH (1 : 1, v/v), followed by preparative reversed-phase HPLC with 40% aqueous MeOH at a flow rate of $6.0\,ml\,min^{-1}$ to yield xylarinol A (1, 1.0 mg). The other fraction was purified by preparative reversed-phase HPLC with 30% aqueous MeOH at a flow rate of $6.0\,ml\,min^{-1}$ to provide xylarinol B (2, 1.7 mg).

Xylarinol A was isolated as a white powder and showed a molecular ion peak at m/z 176 in the electron impact mass measurement. Its high-resolution electron impact mass measurement provided an accurate mass at m/z 176.0472 [M^+, $\Delta-0.1$ mmu], establishing its molecular formula as $C_{10}H_8O_3$. The UV spectrum in MeOH exhibited absorption maxima at 205 (log ε 4.75), 217 (log ε 4.63), 277 (log ε 4.43) and 316 (log ε 4.07) nm. The IR spectrum suggested the presence of a hydroxyl group ($3444\,cm^{-1}$) and an α,β-unsaturated ester group ($1651\,cm^{-1}$). The ^1H-NMR spectrum showed signals due to 1,2,3-trisubstituted benzene ring at δ 7.28, 6.95 and 6.94, two olefinic methine peaks assigned to a *cis*-1,2-disubstituted double bond unit at δ 7.31 (J=12.0 Hz) and 6.29 (J=12.0 Hz), and a methylene peak at δ 5.24. In the ^{13}C-NMR spectrum, an ester carbonyl carbon at δ 169.6, an oxygen-bearing sp^2 carbon at δ 154.9, five sp^2 methines, two sp^2 quaternary carbons and an oxymethylene at δ 61.4 were evident (Table 1). The ^1H–^1H COSY spectrum revealed two partial structures, and the heteronuclear multiple quantum correlation spectrum established the proton-bearing carbons, as shown in Figure 2. The structure of 1 was unambiguously determined by the heteronuclear multiple bond correlation spectrum. The long-range correlations from H-6 to C-8 and C-9a, and from H-8 to C-6 and C-9a revealed the presence of 2,3-disubstituted-phenol moiety in 1. The oxepinone ring system was determined by the heteronuclear multiple bond correlations of H-1 to C-3 (δ 169.6), C-5a (δ 137.3) and C-9a (δ 121.7), of H-4 to C-3 (δ 169.6) and C-5a (δ 137.3), and of H-5 to C-9a (δ 121.7). Finally, the heteronuclear multiple bond correlations from H-1 to C-9 (δ 154.9) and from H-5 to C-6 (δ 120.7) completed the structure of 1 as shown in Figure 2. Therefore, the structure of 1 was determined to be 9-hydroxy-1*H*-benzo[*c*]oxepin-3-one, a new benzoxepin derivative.

Xylarinol B was obtained as a yellow powder with a specific rotation value of −3.32 (*c* 0.1, MeOH). The molecular formula of 2 was established to be $C_{12}H_{16}O_4$ by the high-resolution EI-MS providing a molecular ion peak at m/z 224.1050 [M^+, $\Delta+0.1$ mmu]. The UV

[1]Division of Biotechnology, College of Environmental & Bioresource Sciences, Chonbuk National University, Jeonju, Jeonbuk, Korea and [2]Department of Applied Biology, Chungnam National University, Daejeon, Korea
Correspondence: Dr B-S Yun, Division of Biotechnology, College of Environmental & Bioresource Sciences, Chonbuk National University, Jeonju, Jeonbuk 561-756, Korea.
E-mail: bsyun@chonbuk.ac.kr

Fruiting bodies of *Xylaria polymorpha*
(dry weight, 285 g)

│ extracted with MeOH

MeOH extract

│ partitioned between chloroform and H$_2$O

Water layer

│ partitioned with ethyl acetate

Ethyl acetate-soluble portion

│ concentrated *in vacuo*

Silica gel column chromatography

│ eluted with CHCl$_3$:MeOH=50:1~2:1

Sephadex LH-20 column chromatography │ │ Preparative HPLC

│ eluted with CHCl$_3$:MeOH=1:1 │ │ ODS column : 20 x 150 mm
│ │ │ solvent : 30%MeOH
Preparative HPLC │ │ flowrate : 6.0 ml/min

│ ODS column : 20 x 150 mm │ │ Xylarinol B (1.7 mg)
│ solvent : 40%MeOH
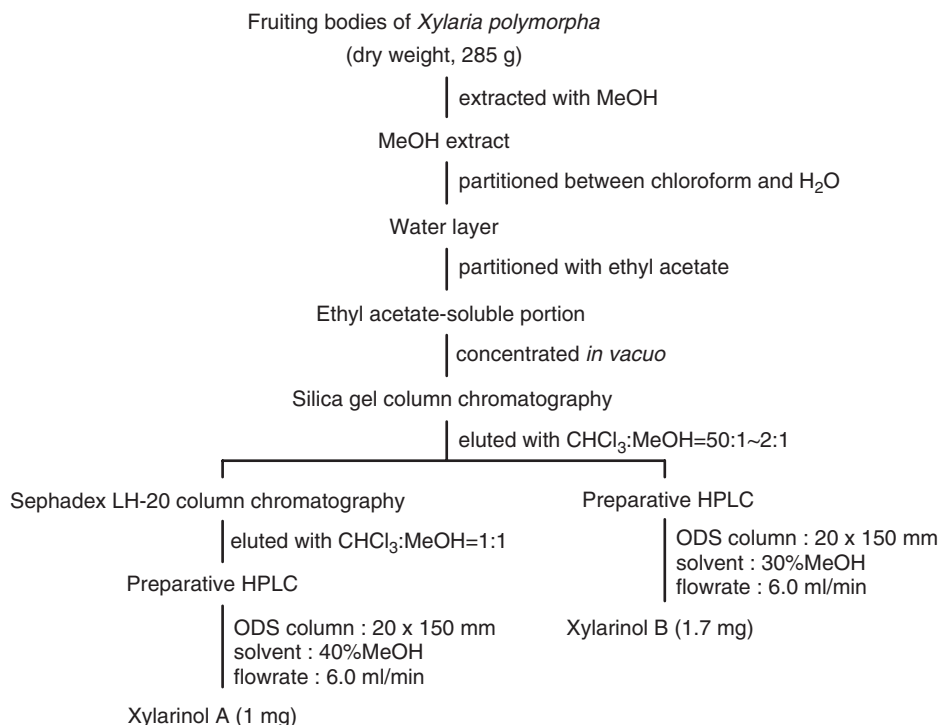│ flowrate : 6.0 ml/min

Xylarinol A (1 mg)

Figure 1 Purification procedures of xylarinol A (**1**) and B (**2**).

Table 1 ^{1}H- and ^{13}C-NMR spectral data of xylarinols A (**1**) and B (**2**)

Positions	Xylarinol A		Xylarinol B	
	δ_H	δ_C	δ_H	δ_C
1a	5.24 (2H, s)[a]	61.4	5.05 (1H, dd, *J*=12.0, 2.8)	71.3
1b			4.95 (1H, d, *J*=12.0)	
3		169.6	3.70 (1H, m)	73.5
4	6.29 (1H, d, *J*=12.0)	121.6	1.82 (2H, m)	40.5
5	7.31 (1H, d, *J*=12.0)	141.7	5.41 (1H, m)	82.6
5a		137.3		145.7
6	6.95 (1H, d, *J*=7.8)	120.7	6.67 (1H, d, *J*=7.8)	113.0
7	7.28 (1H, t, *J*=7.8)	130.1	7.10 (1H, t, *J*=7.8)	130.2
8	6.94 (1H, d, *J*=7.8)	117.1	6.64 (1H, d, *J*=7.8)	114.8
9		154.9		152.9
9a		121.7		126.1
1′			3.61 (1H, m)	72.0
2′			1.16 (3H, d, *J*=6.4)	18.6

NMR spectra were measured in CD$_3$OD (25 °C) at 400 MHz for ^{1}H and 100 MHz for ^{13}C.
[a]Integral, multiplicity and coupling constants in Hz are given in parentheses.

spectrum in MeOH exhibited absorption maxima at 211 (log *ε* 3.93), 222 (log *ε* 3.87), 269 (log *ε* 3.29) and 276 (log *ε* 3.28) nm, and its IR spectrum suggested the presence of a hydroxyl group at 3433 cm^{-1}. The ^{1}H-NMR spectrum exhibited signals assignable to 1,2,3-trisubstituted benzene at *δ* 7.10, 6.67 and 6.64, three oxygenated methines at *δ* 5.41, 3.70 and 3.61, one nonequivalent oxygenated methylene at *δ* 5.05 and 4.95, one methylene at *δ* 1.82, and one methyl at *δ* 1.16. The ^{13}C-NMR spectrum showed 12 carbons, which were identified as an oxygen-bearing sp^2 carbon at *δ* 152.0, three sp^2 methines, two sp^2 quaternary carbons, three oxymethines, one oxymethylene, one methylene and one methyl by the DEPT spectrum. Two partial structures were established on the basis of the proton multiplicity

and *J* values, as well as ^{1}H–^{1}H COSY spectral data, as shown in Figure 2. The proton at *δ* 5.05 (H-1a) of the nonequivalent oxygenated methylene protons was split as a doublet of doublet by the geminal coupling of 12.0 Hz and homoallylic coupling of 2.8 Hz to H-5, which was confirmed by the COSY data. These partial structures were unambiguously connected by the heteronuclear multiple bond correlation spectrum, which showed the long-range correlations of H-1 to C-5a and C-9a, of H-4 to C-3 and C-5a, of H-6 to C-5, C-8, and C-9a, and of H-8 to C-9a, establishing the presence of benzoxepin moiety. Therefore, the structure of **2** was determined as 1,3,4,5-tetrahydro-3-(1-hydroxyethyl)benzo[*c*]oxepin-5,9-diol, a new benzoxepin derivative. The relative configuration of oxepin ring was proposed by the NOE experiments. NOE enhancements of H-1a, H-3 and H-4 by irradiation of H-5 were observed, and H-1a showed NOE with H-5, suggesting that methine protons of H-1a, H-3 and H-5 were coplanar (Figure 2).

Benzoxepin is known to be very rare in naturally occurring compounds. To date, several 1-benzoxepin and 1-benzoxepinone derivatives have been isolated from *Marsamiellus ramealis*,[8] *Mycena galopus*[9] and *Pterula* species[10,11] as antibiotics or inhibitors of NADH. We evaluated the antimicrobial activity of compounds **1** and **2** by the conventional paper disk (Advantec, Tokyo, Japan; 8 mm in diameter) method[7] at a concentration of 50 μg per disk. Fifteen test microorganisms, including 12 phytopathogenic fungi (*Pythium ultinum, Fusarium oxysporium*, *Magnaporthe grisea*, *Aspergillus niger*, *Alternaria panax*, *Phytophthora capsici*, *Alternaria mali*, *Alternaria porri*, *Botrytis cinerea*, *Rhizoctonia solani, Fulvia fulva, Cylindrocarpon destructans*) and three bacteria (*Salmonella sendai*, *Staphylococcus aureus*, *Bacillus subtilis*), were used. However, compounds **1** and **2** showed no antimicrobial activity against all test organisms. We also measured the ABTS radical scavenging activity of both compounds by using ABTS radical cation decolorization assay with minor modifications.[12] As a result, these compounds were found to exhibit moderate ABTS radical scavenging
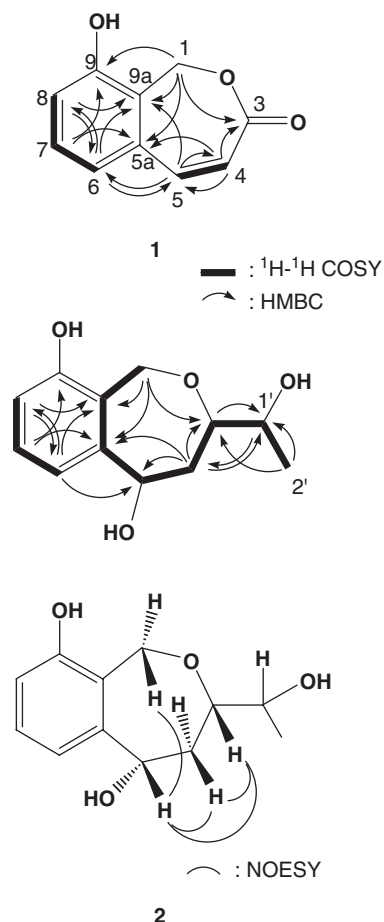
Figure 2 Structures of xylarinol A (**1**) and B (**2**) elucidated by 2-D NMR experiments.

activity with 40 and 45% inhibition, respectively, at 100 μM concentration. Compounds **1** and **2** were obtained in too small amounts for biological activity test, and so some synthetic effort is needed for further study.

ACKNOWLEDGEMENTS

1 Zaidman, B. Z., Tassin, M., Mahajna, J. & Wasser, S. P. Medicinal mushroom modulators of molecular targets as cancer therapeutics. *Appl. Microbiol. Biotechnol.* **67,** 453–468 (2005).
2 Jayasuriya, H. *et al.* Isolation structure of antagonists of chemokine receptor (CCR5). *J. Nat. Prod.* **67,** 1036–1038 (2004).
3 Boonphong, S., Kittakoop, P., Isaka, M., Pittayakhajonwut, D., Tanticharoen, M. & Thebtaranonth, Y. Multiplolides A and B, new antifungal 10-membered lactones from *Xylaria multiplex. J. Nat. Prod.* **64,** 965–967 (2001).
4 Davis, R. A. Isolation and structure elucidation of the new fungal metabolite (−)-xylariamide A. *J. Nat. Prod.* **68,** 769–772 (2005).
5 Smith, C. J. *et al.* Novel sesquiterpenoids from the fermentation of *Xylaria persicaria* are selective ligands for the NPY Y5 receptor. *J. Org. Chem.* **110,** 5001–5004 (2002).
6 Lin, Y. *et al.* Five unique compounds: xyloketals from mangrove fungus Xylaria sp. from the South China Sea coast. *J. Org. Chem.* **66,** 6252–6256 (2001).
7 Jang, Y. W. *et al.* Xylarinic acids A and B, new antifungal polypropionates from the fruiting body of *Xylaria polymorpha. J. Antibiot.* **60,** 696–699 (2007).
8 Turner, W. B. & Aldridge, D. C. *Fungal Metabolites II* 3–45 (Academic Press, London, 1983).
9 Wijnberg, J. P. A., Veldhuizen, A., Swart, H. J., Frankland, J. C. & Field, J. A. Novel monochlorinated metabolites with a 1-benzoxepin skeleton from *Mycena galopus. Tetrahedron Lett.* **40,** 5767–5770 (1999).
10 Engler, M., Anke, T., Sterner, O. & Brandt, U. Pterulinic acid and pterulone, two novel inhibitors of NADH: ubiquinone oxidoreductase (complex I) produced by a *Pterula* species. I. Production, isolation and biological activities. *J. Antibiot.* **50,** 325–329 (1997).
11 Engler, M., Anke, T. & Sterner, O. Pterulinic acid and pterulone, two novel inhibitors of NADH: ubiquinone oxidoreductase (complex I) produced by a *Pterula* species. II. Physico-chemical properties and structure elucidation. *J. Antibiot.* **50,** 330–333 (1997).
12 Jung, J. Y. *et al.* Antioxidant polyphenols from the mycelial culture of the medicinal fungi *Inonotus xeranticus* and *Phellinus linteus. J. Appl. Microbiol.* **104,** 1824–1832 (2008).

npg

NOTE

PM070747, a new cytotoxic angucyclinone from the marine-derived *Saccharopolyspora taberi* PEM-06-F23-019B

Marta Pérez[1], Carmen Schleissner[1], Pilar Rodríguez[1], Paz Zúñiga[1], Gonzalo Benedit[1], Francisco Sánchez-Sancho[2] and Fernando de la Calle[1]

The benz[α]anthraquinones are a class of compounds that have attracted a great deal of attention owing to their interesting biological properties.

As part of our on-going screening for new antitumor compounds from marine microorganisms, we have isolated a new angucyclinone, PM070747 (**1**) (Figure 1), produced by the actinomycete *Saccharopolyspora taberi* PEM-06-F23-019B, from a marine sponge collected from near the coast of Tanzania. Additionally, traces of the known angucyclinone, PD116740[1] (**2**), were also found.

Compound **1** is structurally closely related to **2** and TAN-1085[2] (**3**) (Figure 1). Compound **2** was first isolated from the unknown actinomycete, WP4669, and it was described as a compound with antitumor properties against leukemia and adenocarcinoma cell lines.[1] Recently, an epimer of **2** was isolated from a marine fungus, *Penicillium* sp.[3] Compound **3** and its aglycone were described as angiogenesis and aromatase inhibitors in the Japanese patent JP02289532.[2]

The microbial producer of **1**, *Saccharopolyspora taberi* PEM-06-F23-019B, was isolated by spreading the homogenized ectosome of the sponge on Bennett's agar medium[4] plates supplemented with nalidixic acid (0.02%) and cycloheximide (0.02%). The plates were incubated at 28 °C for 30 days.

The strain was subjected to a phylogenetic analysis based on 16S rRNA sequences analyzed by BLAST (Basic Local Alignment Search Tool) against the NCBI (National Center for Biotechnology Information) database,[5] and showed a high identity with that of *Saccharopolyspora*, such as *Saccharopolyspora taberi* DSM 43856 (956/968, 98.8%) (sequence AF002819).[6]

The seed culture was developed in two scale-up steps, first in 100-ml Erlenmeyer flasks containing 20 ml of seed medium, and then in 250-ml Erlenmeyer flasks with 50 ml of the same medium. The seed culture was grown on a medium containing dextrose (0.1%), soluble starch 2.4%, soy peptone 0.3%, yeast extract 0.5%, Tryptone 0.5%, soya flour 0.5%, NaCl 0.54%, KCl 0.02%, $MgCl_2$ 0.24%, Na_2SO_4 0.75% and $CaCO_3$ 0.4% in tap water, and cultured at 28 °C on an orbital shaker for 72 h. For production, 12.5 ml of the seed medium was transferred into 2000-ml Erlenmeyer flasks containing 250 ml of fermentation medium, comprising yeast extract 0.5%, soy peptone 0.1%, dextrose 0.5%, soya flour 0.3%, Glucidex 2.0%, NaCl 0.53%, KCl 0.02%, $MgCl_2 \cdot 6H_2O$ 0.24%, Na_2SO_4 0.75%, $MnSO_4 \cdot 4H_2O$ 0.00076%, $CoCl_2 \cdot 6H_2O$ 0.0001%, K_2HPO_4 0.05% and $CaCO_3$ 0.4%. The culture was grown at 28 °C using an orbital shaker (5-cm eccentricity, 220 r.p.m.) for 5 days.

The bioassay-guided isolation of **1** from the fermentation broth is depicted in Figure 2 and summarized below.

The fermentation broth (6 l) was subjected to centrifugation, and the clarified broth was extracted with ethyl acetate 1:1 (v/v). The extract was concentrated to give a broth extract (382 mg). It was subjected to reversed-phase vacuum chromatography by a filter funnel on Polygoprep 100-50 μm C18, using a H_2O–MeOH–CH_2Cl_2 mixture as the eluting solvent. The cytotoxic activity was detected in fractions eluted with H_2O:MeOH 3:1 (35 mg), 1:1 (100 mg) and 1:3 (50 mg). As these three fractions displayed similar HPLC profiles, they were combined and evaporated under reduced pressure, resulting in a crude extract (185 mg). This extract was then chromatographed on a reversed-phase (C-18) column eluted in a stepwise gradient with increasing ratios of MeOH in water, followed by CH_2Cl_2 in MeOH. Three out of the fourteen fractions eluted with H_2O–MeOH mixtures showed antitumor activity and similar HPLC profiles. Further purification of two of these active fractions by preparative HPLC was carried out at room temperature using a C-18 Atlantis column (19×150 mm, 5 μm, Waters). A gradient of CH_3CN/H_2O (15–60% in 20 min) was
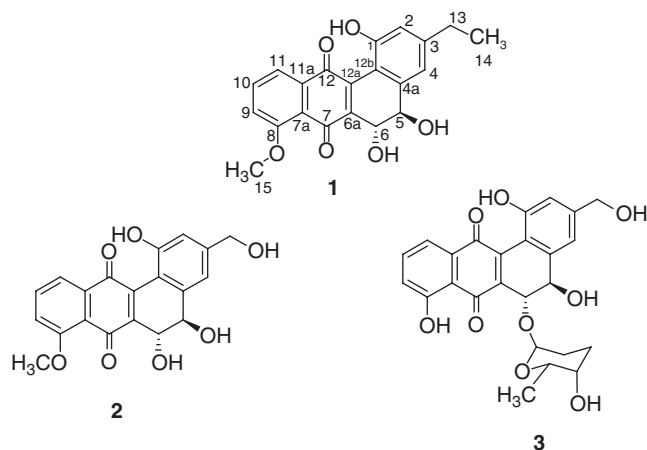
Figure 1 Structures of PM070747 (**1**), PD 116740 (**2**) and TAN-1085 (**3**).

employed as a mobile phase, with a flow rate of 13.65 ml min^{-1} with UV detection at 215 nm. Under these conditions, a total amount of 5 mg of pure **1** was isolated, along with traces of **2**.[1]

The structure of **1** was established as shown in Figure 1 on the basis of analysis of the physico-chemical properties (Table 1) and NMR data (Table 2), and by comparison with data reported for the related angucyclinone **2**.[1]

The physico-chemical properties of **1** are summarized in Table 1. Compound **1** was obtained as a reddish powder. Its molecular formula was determined as $C_{21}H_{18}O_6$, on the basis of high resolution electrospray ionization mass spectrum (HR-ESI-MS) and the NMR data (Table 2), indicating 13 degrees of unsaturation.

The ESI-MS experiments showed ions at *m/z* 367 (M+H) and 389 (M+Na), which confirmed the molecular mass. The UV spectrum of **1** in MeOH exhibited absorption maxima at 203 and 408 nm, indicating the presence of a substituted anthraquinone moiety. The IR indicated the presence of hydroxyl groups (3353 cm^{-1}). In addition, a strong absorption peak at 1639 cm^{-1} and the absence of a peak near 1670 cm^{-1} indicated that both carbonyls were involved in hydrogen bonding to neighbouring hydroxyls.[7,8] As described for **2**, the absence of an IR band at around 1700–1725 cm^{-1}, assigned to the C-1 carbonyl in related antibiotics, suggested the presence of a hydroxyl group, hydrogen bonded to the C-12 quinone carbonyl, attached to the C-1 position (see Table 1).

The ^1H NMR spectrum of **1** exhibited a signal at δ 4.00 for an aromatic methoxy group (Table 2). Moreover, a pair of coupled signals at δ 4.59 (H-5) and 5.12 (H-6) revealed the presence of a 5,6-diol moiety in **1**. Two more signals were observed as doublets with a small coupling constant at δ 6.76 (H-2) and 6.86 (H-4), each integrating for one proton, representing meta-coupled aromatic protons. In addition, an aromatic ABX system with a pattern very similar to that observed for **2**[1] was present in the ^1H NMR spectrum of **1**. However, no signals for a benzylic hydroxymethyl group were observed compared with **2**. Instead, coupled signals at δ 1.26 (H$_3$-14) and 2.64 (H$_2$-13) clearly indicated the presence of an ethyl group attached to the C-3 position. Assignment of the rest of the benz[α]anthraquinone signals was confirmed by 2-D NMR experiments. In the ^1H–^1H COSY, correlations of H-10 with H-9 and H-11, H-5 with H-6 and H-13 with H-14 revealed the linkages in these substructures. A correlation between the H-5 and H-6 protons in the COSY, together with the observed coupling constant for both protons (3 Hz), suggested the same *trans* stereochemistry as that of PD 116740, the X-ray diffraction analysis of
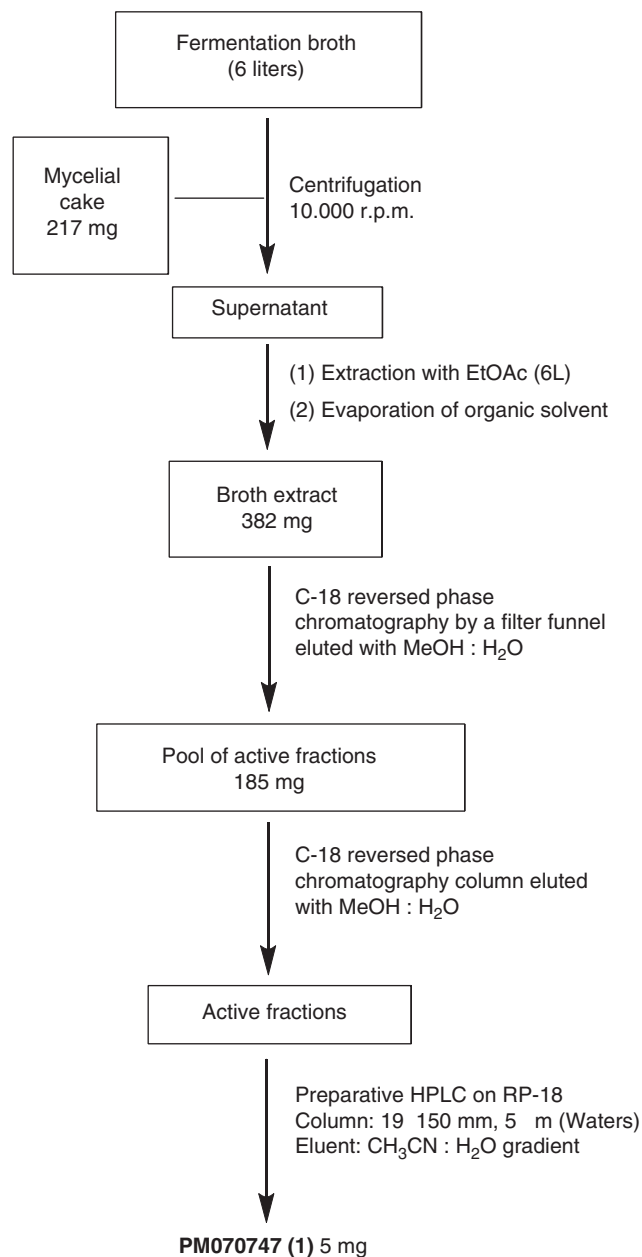

Figure 2 Isolation procedure for PM070747 (**1**) from the culture of *Saccharopolyspora taberi* PEM-06-F23-019B.

which has been described in the literature.[1] The rest of the correlations observed in the ROESY (that is, H-4 with H-5 and H-13; H-2 with H-13; H-9 with H-15) were consistent with the proposed structure (Figure 3). The relationship between these fragments was established through the heteronuclear multibond correlation (HMBC) NMR spectrum. The H$_3$-15 methoxy group at δ 4.00 was coupled to the aromatic carbon C-8, indicating its position. Moreover, long-range couplings observed between H-13 with C-2 and C-4 showed the position of the ethyl group (Figure 3). Long-range couplings observed between H-4 with C-2, C-12b and C-5, and between H-6 with C-4a, C-12a and the carbonyl group C-7 indicated two substructures fused through C-6–C-6a and C-12a—C-12b, which was further supported by cross peaks between H-5 with C-6a and between H-2 with C-12b in HMBC as complementary evidence (Figure 3). On the other hand,

Table 1 Physico-chemical properties of PM070747 (1)

Appearance	Reddish powder
Molecular formula	$C_{21}H_{18}O_6$
Molecular weight	366.364
HR-ESI-MS (pos) m/z	$(M+Na)^+$
Calculated	389.0995
Found	389.0988
UV λ_{max} (MeOH) nm	203, 408
IR ν_{max} (neat) cm^{-1}	3353, 2959, 1730, 1639, 1376, 1340, 860, 839, 801, 738, 663
$(\alpha)_D^{25}$ ($c=0.32$, MeOH)	+220

— ¹H–¹H COSY
→ HMBC
→ ROESY

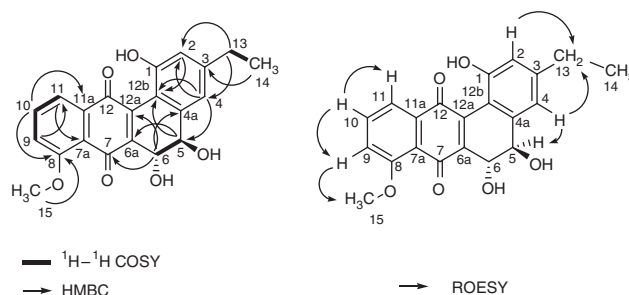**Figure 3** Summary of 1H-1H COSY, HMBC and ROESY correlations in PM070747 **(1)**.

Table 2 ¹H and ¹³C NMR (MeOD, 500 and 125 MHz) assignments of PM070747 (1)

Position C/H No.	¹H shifts[a,b,c]	¹³C shifts[a]	HMBC
1	—	157.34	—
2	6.76 d, 1H ($J=2$)	118.53	C-1, C-13, C-12b
3	—	150.40	—
4	6.86 d, 1H ($J=2$)	123.21	C-2, C-5, C-12b, C-13
4a	—	143.04	
5	4.59 d, 1H ($J=3$)	72.79	C-4, C-12b, C-6a
6	5.12 d, 1H ($J=3$)	64.69	C-7, C-4a, C-12a
6a	—	141.88	
7	—	184.32	—
7a	—	120.80	
8	—	160.70	—
9	7.50 d, 1H ($J=8$)	119.14	C-11
10	7.77 dd, 1H ($J=7.5, 8$)	136.22	C-8, C-11a
11	7.69 d, 1H ($J=7.5$)	120.18	C-9, C-7a
11a	—	137.58	
12	—	187.49	
12a	—	140.27	
12b	—	114.42	
13	2.64 q, 2H ($J=7.5$)	29.66	C-2, C-3, C-4
14-Me	1.26 t, 3H ($J=7.5$)	15.56	C-3
15-Me	4.00 s, 3H	56.83	C-8

[a]Chemical shifts (δ) are in ppm.
[b]Coupling constants (J) in hertz (Hz) are given in parentheses.
[c]s: singlet; d: doublet; t: triplet; q: quartet.

Table 3 Cell-survival values (μM) for three tumor cell lines treated with PM070747 (1)

	A549	HT29	MDA-MB-231
GI$_{50}$	3.28	1.42	0.71
TGI	4.64	1.97	1.06
LC$_{50}$	6.82	>2.73	1.72

GI$_{50}$, compound concentration that produces 50% inhibition on cell growth as compared with control cells; TGI, compound concentration that produces total growth inhibition as compared with control cells; and LC$_{50}$, compound concentration that produces 50% cell death as compared with control cells.

1 Wilton, J. H., Cheney, D. C., Hokanson, G. C., French, J. C., Cunheng, H. & Clardy, J. A new dihydrobenz[a]anthraquinone antitumor antibiotic (PD 116740). *J. Org. Chem.* **50**, 3936–3938 (1985).
2 Kanamaru, T., Nozaki, Y. & Muroi, M. TAN-1085 and its aglycon as angiogenesis and aromatase inhibitors and their manufacture with *Streptomyces* species Japanese patent 02289532 (1990). Takeda Chemical Industries, Ltd, Japan.
3 Li, X., Yao, Y., Sun, G., Zheng, Y., Lin, W. & Scattler, I. Studies on chemical structure of an anthraquinone derivative from marine fungus *Penicillium*. *Fenxi Ceshi Xuebao* **26**, 195–197 (2007) (in Chinese).
4 Atlas, R. M. (ed). In *Handbook of Microbiological Media* 3rd edn, 205–206 (CRC Press LLC, NW Corporate Blvd, Boca Raton, Florida, 2004).
5 Altschul, S. F. *et al.* Gapped BLAST and PSIBLAST: a new generation of protein database search programs. *Nucl. Acids Res.* **25**, 3389–3402 (1997).
6 Labeda, D. P. Transfer of the type strain of *Streptomyces erythraeus* (Waksman 1923) Waksman and Henrici 1948 to the genus *Saccharopolyspora Lacey* and Goodfellow 1975 as *Saccharopolyspora erythraea* sp. nov., and designation of a neotype strain for *Streptomyces erythraeus*. *Int. J. Syst. Bacteriol.* **37**, 19–22 (1987).
7 Sun, C. H. *et al.* Chemomicin A, a new angucyclinone antibiotic produced by *Nocardia mediterranei* subsp. *kanglensis* 1747–64. *J. Antibiot.* **60**, 211–215 (2007).
8 Bloom, H., Briggs, L. H. & Cleverley, B. Physical properties of anthroquinone and its derivatives. Part I. Infrared Spectra. *J. Chem. Soc.* 178–185 (1959).
9 Skehan, P. *et al.* New colorimetric cytotoxic assay for anticancer-drug screening. *J. Natl Cancer Inst.* **82**, 1107–1112 (1990).
10 Robert, H. S. The NCI60 human tumour cell line anticancer drug screen. *Nat. Rev. Cancer* **6**, 813–823 (2006).

C-7a was assigned by its correlation with H-11, and the C-11a position was revealed by a cross peak between H-10 and C-11a in HMBC (Figure 3).

The antitumor activity of **1** was evaluated against a panel of three tumor cell lines: human breast adenocarcinoma MDA-MB-231 cells, human colorectal adenocarcinoma HT-29 cells and human lung carcinoma A-549 cells (concentration of 50% inhibition on cell growth (GI$_{50}$) 0.71, 1.42 and 3.28 μM, respectively), according to the procedure described in the literature.[9] Cell survival was estimated using the National Cancer Institute algorithm.[10] Three dose–response parameters were calculated for **1** (Table 3).

NOTE

Aldgamycin I, an antibacterial 16-membered macrolide from the abandoned mine bacterium, *Streptomyces* sp. KMA-001

Jin-Soo Park, Hyun Ok Yang and Hak Cheol Kwon

Abandoned mines are often extremely contaminated by heavy metals and acid, creating a unique nutrient environment. Nonetheless, it has been recognized that microorganisms have adapted to life in this unique bioregion.[1] In the harsh conditions of an abandoned mine, microorganisms are likely to be subjected to substantial levels of competition, which could lead them to develop unique chemical arsenals, such as antibiotics.[2,3] In the course of our study on the production of secondary metabolites by the mine actinomycete, *Streptomyces* sp. KMA-001 was isolated from a heat-treated soil sample (55 °C, 5 min) collected at the Yeonhwa abandoned zinc mine in Korea. From a pure culture of this strain, we have isolated a new aldgamycin derivative, aldgamycin I (**1**), along with four earlier reported 16-membered macrolides, aldgamycin E (**2**),[4,5] aldgamycin F (**3**),[6] aldgamycin G (**4**)[7] and chalcomycin (**5**)[8] (Figure 1).

A stock culture of the strain KMA-001 was maintained on Yeast–Malt extract (YM) agar containing nystatin (50 µg ml^{-1}) to minimize fungal contamination. The YM agar medium consisted of a yeast extract (Difco, Detroit, MI, USA) 0.5%, a malt extract (Difco) 3.0% and agar 1.5%. The strain KMA-001 was grown on the YM agar medium for 7 days and was then cultured in 25 ml YM broth medium (0.5 g yeast extract (Difco) and 3 g malt extract (Difco) in 100 ml deionized water) in a 100-ml erlenmeyer flask for 3 days. The seed culture broth (25 ml) was transferred to a 1-l erlenmeyer flask containing 500 ml A1BFe broth (pH 6.4 before sterilization) consisting of starch (Difco, 10 g), yeast extract (Difco, 4 g), peptone (Difco, 2 g), FeSO$_4$·7H$_2$O (0.08 g) and KBr (0.1 g) in 1 l of deionized water for the second culture step. After 3 days, each 25 ml broth from the second culture was inoculated into 25 erlenmeyer flasks of 1 l, each containing 500 ml A1BFe medium, and was cultured at 28 °C with shaking at 200 r.p.m. for 7 days.

Total genomic DNA preparation of the KMA-001 strain was carried out according to the G-spin Genomic DNA Extraction Kit (iNtRON Biotechnology, Seongnam, Korea). PCR amplification of the 16S rDNA was performed using two universal primers 27f (5′-AGA GTT TGA TCM TGG CTC AG-3′) and 1492R (5′-TAC GGH TAC CTT GTT ACG ACT T-3′).[9] The PCR mixture consisted of 30 picomoles of each primer, 100 ng of chromosomal DNA, 200 µM dNTPs and 2.5 U of *Taq* polymerase in 50 µl of total volume. The amplification was carried out for 35 cycles at 94 °C for 30 s, annealing at 54 °C for 30 s and extension at 72 °C for 1.5 min. The PCR product was analyzed by agarose gel eletrophoresis and the remaining mixture was purified using a PCR purification kit (Solgent Co., Ltd, Daejeon, Korea). The 16S rDNA PCR product was sequenced by Solgent Co., Ltd. BLAST (http://blast.ncbi.nlm.nih.gov/Blast.cgi) was used to access the DNA similarities. The 16S rDNA sequence of KMA-001 strain showed a homology of 99.3% with *Streptomyces goshikiensis* NBRC 12868, *S. citricolor* NBRC 13005 and *S. sporoverrucosus* NBRC 15458. The cultured strain, KMA-001, was deposited with the Korean Culture Center of Microorganisms (KCCM42921).

The secondary metabolites of this bacterium were analyzed by HPLC-MS using a gradient solvent system, 10–100% CH$_3$CN/water, for 30 min (flow rate 0.7 ml min^{-1}, column agilent eclipse XDB-C18, 4.6×150 mm, 5 µm) daily for 7 days to observe temporal production. Five chromatographic peaks were selected for purification after comparison analysis with our in-house HPLC-MS-UV database. After 7 days of fermentation, 20 g l^{-1} Amberlite XAD-7 adsorbent resin (Supelco, Bellefonte, PA, USA) was added into each 1-l culture flask (the volume of broth 500 ml×25), and the mixture was shaken for an additional hour. The resin was then collected by filtration through cheesecloth, washed with deionized water and eluted twice with Me$_2$CO. The crude extract was fractionated by C18 flash column chromatography using mixtures of MeOH–water (20, 40, 60, 80 and 100% MeOH in water, each 200 ml, flow rate 20 ml min^{-1}) as elution solvents. The 60% MeOH fraction contained all the HPLC peaks of interest and was repurified by prep-HPLC with a Luna C18 (2) column (21.2×250 mm, 15 µm, Phenomenex Inc., Torrance, CA, USA)

Natural Products Research Center, Korea Institute of Science and Technology, Gangneung, Gangwon-do, Republic of Korea
Correspondence: Dr HC Kwon, Natural Products Research Center, Korea Institute of Science and Technology, Gangneung, Gangwon-do 210-340, Republic of Korea.
E-mail: hkwon@kist.re.kr

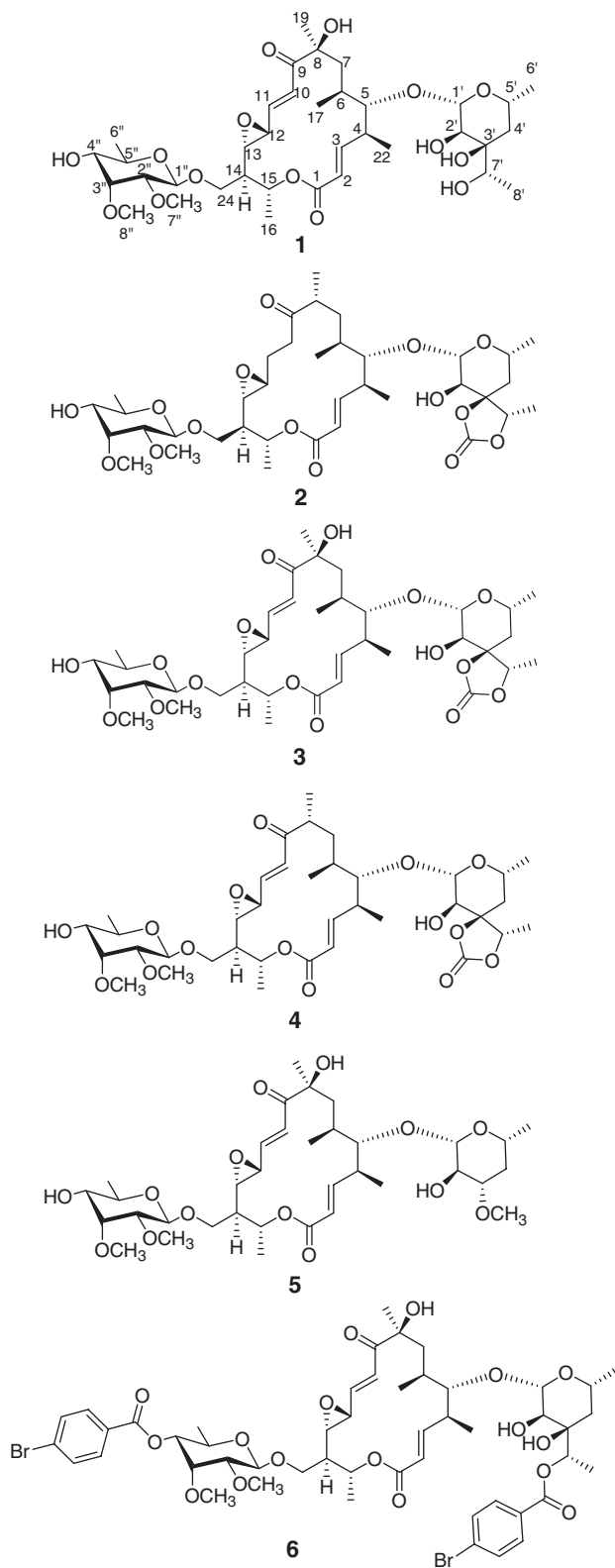Aldgamycin I from Streptomyces sp. KMA-001
J-S Park et al

172

Figure 1 Structures of compounds 1–6.

using an acetonitrile–water (1.6:1 v/v) isocratic condition (flow rate 10 ml min^{-1}) to yield five 16-membered macrolides, aldgamycin I (1, 16.0 mg), aldgamycin E (2, 5.4 mg), aldgamycin F (3, 4.0 mg), aldgamycin G (4, 3.5 mg) and chalcomycin (5, 12.0 mg).

Aldgamycin I (1) was obtained as a white amorphous powder. The molecular formula was assigned to be $C_{36}H_{58}O_{15}$ by HR-FAB-MS ((M+Na)$^+$=753.3668), ^{1}H and ^{13}C NMR data (Table 1). The observed IR absorptions at 1709 and 1235 cm^{-1} showed the presence of α,β-unsaturated carbonyl and epoxide functionalities (Table 2), which were confirmed by the presence of an ester carbonyl carbon at δ_C 165.6 and oxygenated carbons at δ_C 58.7 and 59.1 in the ^{13}C NMR spectrum. Comparison of ^{13}C NMR spectra of 1 and 3 was essentially identical except for C-3′, C-4′, C-7′ and C-8′ (1: δ 74.8, 37.1, 70.0, and 16.7, aldgamycin F: δ 85.0, 40.7, 81.5 and 13.0). Comprehensive NMR analysis, using data from HSQC, HMBC, ^{1}H-^{1}H COSY and ^{1}H-^{1}H TOCSY experiments allowed us to assign the structure of 1, which contained a decarboxylated D-aldgaroside, 4,6-dideoxy-3-C-(1-hydroxyethyl)-β-D-ribo-hexopyranose, instead of the D-aldgarose in earlier reported aldgamycin F (3). Aldgamycin I (1) was so named because aldgamycin H, an 8-dehydroxy derivative of 1, was described in an earlier French patent.[10]

The absolute configuration of 1 was determined mainly by comparison of the CD spectral data of aldgamycin I (1) and aldgamycin F (3). Treatment of 1 and 3 (each 0.5 mg) in dry pyridine (1 ml) with dimethylaminopyridine (0.5 mg) and 4-bromo benzoyl chloride (2 mg) at room temperature for 12 h, in separate experiments, yielded the reaction mixture including, 7′,4″-di-O-p-bromobenzoyl-aldgamycin I (6; Figure 1). Compound 6 was purified by normal phase HPLC (Gilson 321 system; Luna 10 μ silica (2) 250×10 mm column, Phenomenex Inc.; 4 ml min^{-1}) using isocratic elution with hexane-EtOAc (2:1). Both products showed identical ^{1}H NMR and CD spectra (Figure 2), as well as similar quasi-molecular ion peaks and retention times in LC-MS data. These data suggested that the absolute configuration of 1 was the same as that of 3.

Compound 2 was also obtained as a white amorphous powder that analyzed for the molecular formula $C_{37}H_{58}O_{15}$ by HR-FAB-MS ((M+H)$^+$=743.3860) in combination with ^{1}H and ^{13}C NMR data. The IR absorption bands at 1800 and 1709 cm^{-1} suggested the presence of a ketone and an α,β-unsaturated carbonyl group. Analyses of the 2D NMR spectra of 2 allowed us to assign the structure of 2 as aldgamycin E, which was reported earlier.[5] The ^{1}H NMR spectrum of 2 is very similar to that of aldgamycin E, although the reported structure of aldgamycin E was defined incompletely and its sugar linkage position was not determined. Two sugar units and an aglycone of 2, as well as the optical rotation (2 −50.4° (CHCl₃); aldgamycin E −56° (CH₃OH)) are the same as those of aldgamycin E. We, thus, proposed that the structure of 2 was identical to aldgamycin E. In addition to the ^{1}H NMR spectrum described earlier, the NMR data and the structure of compound 2 (Tables 1 and 2) need to be further described.

The absolute configurations of two sugar units of aldgamycin E were already described in an earlier literature.[5,6] However, the aglycone of aldgamycin E was reported as a planar structure. In an earlier literature, the absolute configuration of GERI-155, a relative of chalcomycin, was assigned to be identical to that of chalcomycin on the similarities of their optical rotation values (GERI-155 [α]$_D$ −75.5°; chalcomycin [α]$_D$ −43.5°) and NMR data.[11] Similarly, compound 2 has a very similar optical rotation value as that of 4 (2, −50.4°; 4, −29.0°). This comparison is further strengthened when biosynthetic origins are considered. As these compounds were isolated from the same microbial culture, it is likely that compound 2 is produced through the same biosynthetic pathway as aldgamycin G, and is then reduced by an enoylreductase.[12] On the basis of the spectroscopic data and biosynthetic considerations, the absolute configuration of 2 is proposed to be identical to that of aldgamycin G (4).

Aldgamycin I from Streptomyces sp. KMA-001
J-S Park *et al*

173

Table 1 ^{1}H (500 MHz) and ^{13}C (125 MHz) NMR data of compounds 1 and 2 in CD$_3$CN

Position	Compound 1		Compound 2	
	$\delta_H{}^a$, mult (J in Hz)	δ_C^a	$\delta_H{}^a$, mult (J in Hz)	δ_C^a
1		165.6		165.7
2	6.01 d (15.5)	121.2	6.01 d (15.5)	121.2
3	6.65 dd (15.5, 10.5)	152.0	6.77 dd (15.5, 10.5)	151.6
4	2.75 ddq (10.5, 10.0, 7.0)	41.4	2.82 ddq (10.5, 10.0, 7.0)	40.6
5	3.26 d (10.0)	87.5	3.53 d (10.0)	85.4
6	1.17 m^b	34.3	1.50 m	34.8
7	2.00 dd (15.0, 3.0)	36.8	1.80 m	32.2
	1.76 dd (15.0, 12.5)		1.33 m^b	
8		78.6	2.52 m	45.5
9		201.1		208.1
10	6.92 d (15.0)	126.5	2.71 m	33.0
			2.05 m	
11	6.51 dd (15.0, 9.0)	145.4	1.97 m	26.5
			1.33 m	
12	3.42 dd (9.0, 2.0)	58.7	2.81 m	59.7
13	3.11 dd (9.0, 2.0)	59.1	2.67 m	57.5
14	1.43 br m	49.3	1.36 m	48.2
15	5.33 dq (10.5, 6.5)	68.4	5.28 dq (10.0, 6.0)	69.3
16 (15-CH$_3$)	1.34 d (6.5)	17.6	1.33 d (6.0)	17.8
17 (6-CH$_3$)	0.99 d (6.5)	18.7	0.96 d (6.5)	16.0
19 (8-CH$_3$)	1.38 s	27.3	1.12 d (6.5)	17.3
22 (4-CH$_3$)	1.20 d (7.0)	18.1	1.21 d (7.0)	17.7
24	4.08 dd (10.0, 2.5)	66.8	4.03 dd (10.0, 2.5)	67.0
	3.66 dd (10.0, 3.0)		3.60 dd (10.0, 3.0)	
1′	4.49 d (7.5)	102.6	4.58 d (8.0)	101.9
2′	3.52 m^b	71.1	3.43 dd (8.0, 4.5)	70.8
3′		74.8		85.6
4′	1.51 dd (14.0, 2.0)	37.1	1.91 dd (14.5, 2.0)	40.6
	1.38 m^b		1.60 dd (14.5, 11.0)	
5′	3.84 (11.0, 6.5, 2.0)	66.6	3.84 (11.0, 6.5, 2.0)	66.9
6′ (5′-CH$_3$)	1.16 d (6.5)	20.6	1.19 d (6.0)	20.3
7′	3.72 br m	70.0	4.47 q (6.0)	81.4
8′ (7′-CH$_3$)	1.15 d (6.5)	16.7	1.52 d (6.5)	12.8
O(C=O)O				154.3
1″	4.57 d (8.0)	101.1	4.53 d (8.0)	100.9
2″	3.06 dd (8.0, 2.5)	81.8	3.05 dd (8.0, 2.5)	81.7
3″	3.77 t (2.5)	80.1	3.76 t (2.5)	79.9
4″	3.15 td (9.5, 2.5)	73.1	3.13 td (9.5, 2.5)	73.0
5″	3.56 m^b	70.3	3.55 m^b	70.2
6″ (5″-CH$_3$)	1.21 d (6.5)	17.4	1.20 d (6.5)	17.7
7″ (2″-OCH$_3$)	3.52 s	58.6	3.51 s	58.4
8″ (3″-OCH$_3$)	3.56 s	61.3	3.56 s	61.1
8-OH	3.75 br s		—	
2′-OH	2.22^b		ND^c	
3′-OH	3.00 br s		—	
7′-OH	3.09 br s		—	
4″-OH	2.99 br d (9.5)		2.96 d (9.5)	

^{a}Varian unity: 500; reference standard: acetonitrile (δ_H: 1.96 p.p.m., δ_C: 1.79 p.p.m.).
^{b}The multiplicity of signal was unresolved by peak overlapping and the chemical shift was assigned by the analysis of HSQC and TOCSY spectra.
^{c}The signal was not detected.

The antimicrobial activities of aldgamycin I (**1**), aldgamycin E (**2**), aldgamycin F (**3**), aldgamycin G (**4**) and chalcomycin (**5**) were measured using a MIC assay against *Micrococcus luteus*, *Bacillus subtilis*, *Proteus vulgaris*, *Salmonella typhimurium*, *Aspergillus fumigatus*, *Trichophyton rubrum* and methicillin resistant *Staphylococcus aureus* (Table 3). Ampicillin and amphotericin B were used as positive controls in each assay. Interestingly, all compounds showed selective antibacterial activ-

ities against *M. luteus* and *S. typhimurium*. These compounds exhibited weak or no antimicrobial activities against *B. subtilis*, *P. vulgaris*, *A. fumigatus*, *T. rubrum* and MRSA as shown in Table 3.
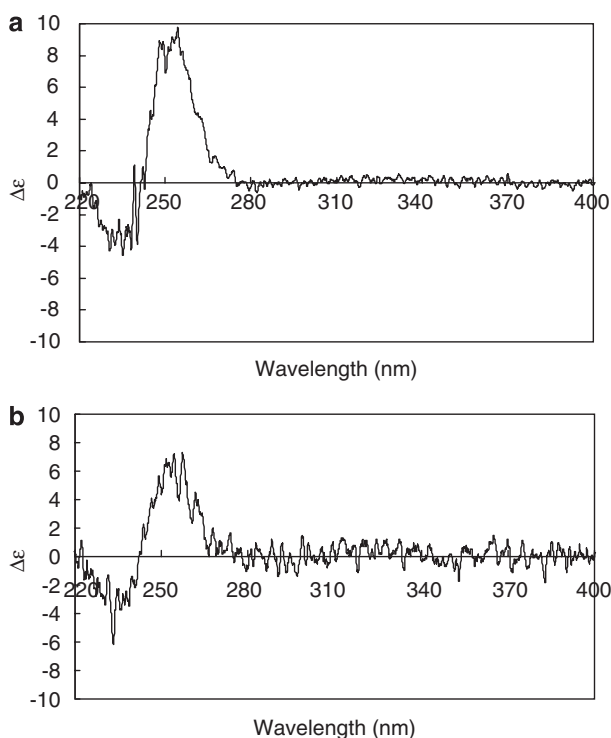
7′, 4″-DI-*O*-*P*-BROMOBENZOYL-ALDGAMYCIN I
^{1}H NMR (500 MHz, acetonitrile-d_3) δ 7.98 (4H, m, Bz^a 3-H and 3′-H), 7.74 (4H, m, Bz^a 4-H and 4′-H), 6.91 (1H, d, *J*=15.5 Hz, 10-H),

npg

Aldgamycin I from *Streptomyces* sp. KMA-001
J-S Park *et al*

174

Table 2 Physicochemical properties of aldgamycins I (1) and E (2)

	1	*2*
Appearance	Colorless amorphous powder	Colorless amorphous powder
Molecular weight	730.8	742.8
Molecular fomular	$C_{36}H_{58}O_{15}$	$C_{37}H_{58}O_{15}$
$[\alpha]_D$	$-19.1°$ (*c* 0.15, CHCl$_3$)	$-50.4°$ (*c* 0.28, CHCl$_3$)
HR FAB MS (m/z)		
Found:	753.3668 (M+Na)$^+$	743.3860 (M+H)$^+$
Calculated:	753.3673	743.3854
UV λ_{max} nm (ϵ) (MeCN)	218 (22 500)	216 (12 900)
IR (KBr) v_{max}	3467, 2975, 2933, 1709, 1655, 1629, 1235, 1083	3457, 2972, 2934, 1800, 1709, 1652, 1083
Solubility	Soluble: MeOH, MeCN, CDCl$_3$	Soluble: MeOH, MeCN, CHCl$_3$
	Insoluble: Hexane, H$_2$O	Insoluble: Hexane, H$_2$O
HPLC, Rt (min)^a	14.2 min	19.7 min

^{a}Luna C18 (2) (4.6×150 mm, 5 μm, Phenomenex) 10–100% acetonitrile/water for 30 min, 1.0 ml min^{-1}.

Table 3 Antimicrobial activities of compounds 1–5 (MIC, μg ml^{-1})

	Micrococcus luteus IFC12708	*Bacillus subtilis ATCC6633*	*Proteus vulgaris ATCC3851*	*Salmonella typhimurium ATCC14028*	*Aspergillus fumigatus HIC 6094*	*Trichophyton rubrum IFO 9185*	*MRSA ATCC 43300*
1	3.13	>50	>50	6.25	>100	>100	>100
2	0.78	12.50	50.00	1.56	>100	>100	>100
3	0.78	25.00	>50	1.56	>100	>100	>100
4	1.56	50.00	>50	1.56	>100	>100	>100
5	0.78	12.50	12.50	1.56	>100	>100	>100
A	0.78	3.13	1.56	12.50	—	—	12.5
B	—	—	—	—	1.56	1.56	—

Abbreviations: A, ampicillin; B, amphotericin B.

$J=6.0$ Hz, 7′-CH$_3$), 1.22 (3H, d, $J=6.0$ Hz, 5′-CH$_3$), 1.21 (3H, d, $J=6.5$ Hz, 5″-CH$_3$), 1.18 (3H, d, $J=7.0$ Hz, 4-CH$_3$), 1.17 (1H, m, 6-H), 0.99 (3H, d, $J=6.5$ Hz, 6-CH$_3$). Carbon chemical shift in HSQC and HMBC spectra (125 MHz, acetonitrile-d_3) δ 200.8 (C-9), 165.3 (C-1), 164.8 (Bz^a 1 and 1′), 151.7 (C-3), 145.3 (C-11), 132 (Bz^a 4 and 4′), 128.0 (Bz^a 2 and 2′), 127.7 (Bz^a 5 and 5′), 131.5 (Bz^a 3 and 3′), 126.2 (C-10), 121.0 (C-2), 102.4 (C-1′), 100.9 (C-1″), 87.8 (C-5), 80.4 (C-2″), 78.2 (C-8) 77.5 (C-3″), 75.3 (C-4″), 74.1 (C-3′), 71.4 (C-7′), 70.5 (C-2′), 68.2 (C-15), 67.8 (C-5″), 66.9 (C-24), 66.5 (C-5′), 60.9 (C-7″), 58.7 (C-13), 58.5 (C-12), 58.3 (C-8″), 49.0 (C-14), 41.1 (C-4), 36.7 (C-4′), 36. (C-7), 27.2 (C-18′), 20.5 (C-6′), 18.6 (C-17), 17.8 (C-22), 17.6 (C-16), 17.1 (C-6), 17.1 (C-6″), 12.8 (C-19). ^{a}Bz: *p*-bromobenzoyl group. ESI-MS *m/z* 1095 (M+H)$^+$.

Figure 2 CD spectra of 7′,4″-di-*O*-*p*-bromobenzoates of **1** (**a**) and aldgamycin F (**b**).

6.64 (1H, dd, $J=15.5$, 10.5 Hz, 3-H), 6.52 (1H, dd, $J=15.5$, 9.0 Hz, 11-H), 6.01 (1H, d, $J=15.5$ Hz, 2-H), 5.33 (1H, dq, $J=10.5$, 6.5 Hz, 15-H), 5.20 (1H, m, 7′-H), 4.73 (1H, d, $J=10.0$, 2.5 Hz, 4″-H), 4.69 (1H, d, $J=8.0$ Hz, 1″-H), 4.52 (1H, d, $J=8.0$ Hz, 1′-H), 4.11 (1H, dd, $J=10.0$, 3.0 Hz, 24a-H), 4.07(2H, m, 3″-H and 5″-H), 3.91 (1H, m, 5′-H), 3.75(1H, s, 8-OH), 3.71 (1H, dd, $J=10.0$, 3.0 Hz, 24b-H), 3.52 (3H, s, 3″-OCH$_3$), 3.48 (3H, s, 2″-OCH$_3$), 3.42 (1H, dd, $J=9.0$, 2.0 Hz, 12-H), 3.30 (1H, m, 2′-H), 3.26 (1H, d, $J=10.0$ Hz, 5-H), 3.22 (1H, dd, $J=8.0$, 3.0 Hz, 2″-H), 3.12 (1H, dd, $J=9.0$, 2.0 Hz, 13-H), 3.08 (1H, br s, 3′-OH), 2.71 (1H, m, H-4), 2.22 (1H, br s, 2′-OH), 1.93 (1H, m, 7a-H), 1.82 (1H, dd, $J=14.0$, 2.0 Hz, 4′a-H), 1.71 (1H, dd, $J=15.0$, 12.0 Hz, 7b-H), 1.59 (1H, dd, $J=14.0$, 10.0 Hz, 4′b-H), 1.44 (1H, m, 14-H), 1.34 (3H, d, $J=6.5$ Hz, 15-CH$_3$), 1.33 (3H, s, 8-CH$_3$), 1.31 (3H, d,

1 Haferburg, G. & Kothe, E. Microbes and metals: interactions in the environment. *J. Basic Microbiol.* **47**, 453–467 (2007).
2 Stierle, D. B., Stierle, A. A., Hobbs, J. D., Stokken, J. & Clardy, J. Berkeleydione and berkeleytrione, new bioactive metabolites from an acid mine organism. *Org. Lett.* **6**, 1049–1052 (2004).

Aldgamycin I from Streptomyces sp. KMA-001
J-S Park *et al*

npg

175

3 Stierle, D. B., Stierle, A. A. & Patacini, B. The berkeleyacetals, three meroterpenes from a deep water acid mine waste Penicillium. *J. Nat. Prod.* **70,** 1820–1823 (2007).

4 Kunstmann, M. P., Mitscher, L. A. & Patterson, E. L. Aldgamycin E, a new neutral macrolide antibiotic. *Antimicrob. Agents Chemother.* **10,** 87–90 (1964).

5 Achenbach, H. & Karl, W. Investigations on metabolites of microorganisms, VI. On the structure of the antibiotic aldgamycin E. *Chem. Ber.* **108,** 759–771 (1975).

6 Achenbach, H. & Karl, W. Metabolites of microorganisms. VIII. Aldgamycin F, in a new antibiotic from *Streptomyces lavendulae. Chem. Ber.* **108,** 780–789 (1975).

7 Mizobuchi, S., Mochizuki, J., Soga, H., Tanba, H. & Inoue, H. Aldgamycin G, a new macrolide antibiotic. *J. Antibiot.* **39,** 1776–1778 (1986).

8 Frohardt, R. P., Pitillo, R. F. & Ehrlich, J. (Parke, Davis & Co.) Chalcomycin and its fermentative production. U.S. 3,065,137 (1962).

9 Gurtler, V. & Stanisich, V. A. New approaches to typing and identification of bacteria using the 16S–23S rDNA spacer region. *Microbiology* **142,** 3–16 (1996).

10 Zitouni, A., Mathieu, F., Lebrihi, A., Sabaou, N. (National Polytechnic Institute of Toulouse) New Saccharothrix strain and its antibiotic derivatives, in particular mutactimycin and aldgamycin. Fr. 2870853 (2005).

11 Kim, S. D. *et al.* GERI-155, a new macrolide antibiotic related to chalcomycin. *J. Antibiot.* **49,** 955–957 (1996).

12 Donadio, S., McAlpine, J. B., Sheldon, P. J., Jackson, M. & Katz, L. An erythromycin analog produced by reprogramming of polyketide synthesis. *Proc. Natl Acad. Sci.* **90,** 7119–7123 (1993).